Development of bioelectrochemical system based constructed wetland technology for efficient wastewater treatment and resource recovery

By

Pratiksha Srivastava

BTech. + MTech. (Biotechnology)

Submitted in fulfilment of the requirements for the degree of

Doctor of Philosophy

National Centre for Maritime Engineering and Hydrodynamics

Australian Maritime College

University of Tasmania

July 2021

[Page intentionally left blank]

Dedicated to:

My father Dr. Harendra Prasad Srivastav, My mother Lalita Devi

For their sacrifices, support, love, and care.

Thanks for making me the person who I am today.

My brother Arpit, who has been a good friend and always beside me.

&

My husband Asheesh, for his precious companionship and endless support.

[Page intentionally left blank]

Declarations

Declaration of originality and authority of access

I declare that this thesis is my own work and contains no material which has been submitted for any other degree or diploma at any university or other institution of tertiary education. Information derived from the published or unpublished work of others has been duly acknowledge in the text and list of references of the thesis. The thesis does not contain any material that infringes copyright.

This thesis may be made available for loan and limited copying and communication in accordance with the Copyright Act 1968.

Signature: Date: 20-07-2021

Pratiksha Srivastava

[Page intentionally left blank]

Statement of Published work contained in Thesis

The following three published and three under review journal articles constitute the content of this thesis. The publishers of the papers comprising Chapters 1, 2, 3, 4, 5 and 6 hold the copyright of that content, and access to the materials should be sought from the respective journals.

Statement of Co-Authorship

The following people and institutions contributed to the publications of work undertaken as a part of this thesis:

Candidate- Pratiksha Srivastava, National Centre for Maritime Engineering and Hydrodynamics, Australian Maritime College, University of Tasmania

Author 1- Associate Prof. Rouzbeh Abbassi, School of Engineering, Faculty of Science and Engineering, Macquarie University

Author 2- Dr. Vikram Garaniya, National Centre for Maritime Engineering and Hydrodynamics, Australian Maritime College, University of Tasmania

Author 3- Associate Prof. Trevor Lewis, School of Natural Sciences, University of Tasmania

Author 4- Dr. Asheesh K Yadav, Environment and Sustainability Department, CSIR-Institute of Minerals and Materials Technology

Author 5- Prof. Stuart Khan, Civil & Environmental Engineering, University of New South Wales

Author 6- Prof. Yaqian Zhao, School of Civil Engineering, University college Dublin, Xi'an University of Technology

Author 7- Dr. Naresh Kumar, Environmental Geosciences, University of Vienna

Author 8- Dr. Mohsen Asadnia, School of Engineering, Faculty of Science and Engineering, Macquarie University

Author 9- Andrew Belford, School of Engineering, Faculty of Science and Engineering, Macquarie University

Contribution of work by co-authors for each paper:

Paper 1: Located in Chapter 1. This chapter is a slightly modified version of published book chapter "Constructed wetland coupled microbial fuel cell technology: development and potential applications" in the book **Microbial Electrochemical Technology** published by **Elsevier** https://doi.org/10.1016/B978-0-444-64052-9.00042-X

Author contributions:

- *Conception of the idea, designing the studies: Candidate, Author 1, Author 2, Author 4*
- *Manuscript writing: Candidate*
- *Manuscript evaluation and submission: Candidate, Author 1, Author 2, Author 4*

Paper 2: Located in Chapter 2. Electrode dependent anaerobic ammonium oxidation in microbial fuel cell integrated hybrid constructed wetlands: A new process." Science of The Total Environment 698 (2020): 134248. (IF=7.9) https://doi.org/10.1016/j.scitotenv.2019.134248

Author contributions:

- *Conception of the idea, designing the studies: Candidate, Author 1, Author 2, Author 4*
- *Performing the experiments and data analysis: Candidate*
- *Manuscript writing: Candidate*
- *Manuscript evaluation and submission: Candidate, Author 1, Author 2, Author 3, Author 4, Author 5*

Paper 3: Located in Chapter 3. Enhanced chromium (VI) treatment in electroactive constructed wetlands: influence of conductive material. Journal of Hazardous Materials 387 (2020): 121722. (IF=10.5) https://doi.org/10.1016/j.jhazmat.2019.121722

Author contributions:

- *Conception of the idea, designing the studies: Candidate, Author 1, Author 2, Author 4*
- *Performing the experiments and data analysis: Candidate*
- *Manuscript writing: Candidate*
- *Manuscript evaluation and submission: Candidate, Author 1, Author 2, Author 3, Author 4, Author 5, Author 7*

Paper 4: Located in Chapter 4. Interrelation between sulphur and conductive materials and its impact on ammonium and organic pollutants removal in constructed wetlands-microbial fuel cells. (IF=10.5) https://doi.org/10.1016/j.jhazmat.2021.126417

Author contributions:

- *Conception of the idea, designing the studies: Candidate, Author 1, Author 2, Author 4*
- *Performing the experiments and data analysis: Candidate*
- *Manuscript writing: Candidate*
- *Manuscript evaluation and submission: Candidate, Author 1, Author 2, Author 3, Author 4, Author 6*

Paper 5: Located in Chapter 5. Influence of applied potential on treatment performance and clogging behaviour of hybrid constructed wetland-microbial electrochemical technologies. (IF=7.0) https://doi.org/10.1016/j.chemosphere.2021.131296

Author contributions:

- *Conception of the idea, designing the studies: Candidate, Author 1, Author 2*
- *Performing the experiments and data analysis: Candidate*
- *Manuscript writing: Candidate*
- *Manuscript evaluation and submission: Candidate, Author 1, Author 2, Author 3, Author 4, Author 5, Author 8*

Paper 6: Located in Chapter 6. Low-power energy harvester from constructed wetland-microbial fuel cells for initiating a self-sustainable treatment process. (IF=5.3) https://doi.org/10.1016/j.seta.2021.101282

Author contributions:

- *Conception of the idea, designing the studies: Candidate, Author 1, Author 2*
- *Performing the experiments and data analysis: Candidate*
- *Manuscript writing: Candidate*
- *Manuscript evaluation and submission: Candidate, Author 1, Author 2, Author 4, Author 8, Author 9*

We, the undersigned, endorse the above stated contribution of work undertaken for each of the published (for submitted) peer-reviewed contributing to this thesis:

Signed:

Pratiksha Srivastava	Dr. Vikram Garaniya	Dr. Prashant Bhaskar
Candidate	Primary Supervisor	Director
Australian Maritime College	Australian Maritime College	Australian Maritime College
University of Tasmania	University of Tasmania	University of Tasmania

[Page intentionally left blank]

Acknowledgements

This is hard to believe that the journey I always wanted to accomplish is coming to an end. I am very thankful to all the people who are part of this journey; each one of them had an important role to play. I believe that whatever I learned in the past few years will open a new opportunity for my future. Thus, I would like to express my gratitude to few people who had a special role in this journey.

My first gratitude goes to my supervisory committee, Dr. Vikram Garaniya, Associate Prof. Rouzbeh Abbassi, and Associate Prof. Trevor Lewis. Without their support and guidance throughout my research, this journey would not be that easy.

I would like to thank Associate Prof. Rouzbeh Abbassi for not just being a great mentor but also for his generosity in sharing his knowledge and experience. His continuous support and encouragement throughout my research journey always inspired me to continue my research efficiently. In the last few years, I learned a lot from him; a few major things that I learned were dedication and hard work, which I would like to follow in my future. I am also thankful to Dr. Vikram Garaniya for his endless support not only as a mentor but also as a family. I want to extend my thanks to Associate Prof. Trevor Lewis for sharing his valuable knowledge and for his encouragement and support.

I would like to extend my thanks to the technical staff at Australian Maritime College, Darren Young, Jock Ferguson, and Michael Underhill. I appreciate them for all the help during my research, particularly for fixing my leaking reactors, and sometimes support beyond their capacity. Thanks for sharing good and bad times with me; our countless laughter, food, and my first birthday surprise in Australia is unforgettable. I am thankful that I got a chance to work with you guys, you were a family far from family to me, and you will always be missed.

I am also thankful to all my colleagues at the University of Tasmania for their help and support. My special thanks to a few special friends Upul Inoka, Christelle Auguste, Manoja Herath, Mariam Tanveer, Sanaz Jahangiri, Mathieu Couridier, and Doug Potts, for sharing friendship and lifetime memories with me.

I would like to acknowledge my long-time friend Supriya Gupta for her friendship and love.

I would also like to acknowledge AMC's Tasmanian Graduate Research Scholarship-RTP base stipend to support my study and living expenses.

Lastly, my special thanks to my father, mother, brother, sister-in-law (Anamika), and my in-laws, for their love, care and support throughout my research journey.

[Page intentionally left blank]

Abstract

Bioelectrochemical systems (BES), also known as microbial electrochemical technology (MET), has emerged as a potential sustainable technology for wastewater treatment and complimentary electricity generation. BES consists of a set of technologies focused on the interaction between microbes and conductive materials/electrodes, which leads to a high catalytic rate at the microbe-electrode interface. The primary benefit of the favourable interaction between microbes and conductive materials is that it can boost microbial metabolism in an electron acceptor deficient anaerobic environment. This pioneering technology has shown great potential for wastewater treatment with simultaneous electricity generation along with other environmental applications.

In the last decades, BES has been incorporated into constructed wetland (CW) technology to form an integrated hybrid technology, i.e., CW-BES. The CW-BES is the most innovative scalable development so far in the field of BES for wastewater treatment and other environmental applications. The CW-BES merger assists in overcoming the challenges associated with both technologies at an individual level. An anaerobic environment mainly dominates CW, leading to slow treatment performance and requiring a larger land footprint; nevertheless, BES integration assists in improving its treatment efficiency and additional functionalities.

The CW-BES merger is still in its infancy stage. It requires a better understanding of many aspects of microbe-electrode interaction to remove various types of pollutants, such as organic/inorganic, recalcitrant, etc. It also needs further comprehensive investigation on electricity generation enhancement and practical application of generated electricity along with its applications.

This PhD thesis aims to establish a deeper understanding of anaerobic microbe-electrode interaction in CW-BES to remove various pollutants from wastewater such as carbon, nitrogen, sulphate, toxic heavy metals and dyes, as well as operational problems like clogging, hydraulic retention time, and organic loading rates. The study also focussed on determining a way of harvesting energy, its storage and practical application of bioenergy generated from CW-BES. Thus, this study is divided into five stages to explore a different set of CW-BES technology for achieving sustainability in wastewater treatment.

In the first stage, this study has focused on treating carbonaceous and nitrogenous (ammonium nitrogen) wastes, both high energy and cost demanding pollutants, from wastewater using CW-BES. CW removal of carbon and ammonium nitrogen is a challenge due to the anaerobic environment and slow treatment rate. Oxidation of both carbon and ammonium nitrogen requires sufficient electron acceptors in an anaerobic environment. Hence, in the first stage, CW was incorporated into one of the BES technologies, a microbial fuel cell (MFC). The presence of electrodes in the anaerobic environment of CW-MFC acted as an artificial electron acceptor and assisted efficient electron transfer resulting in high treatment performance. Further, in the same study for anaerobic ammonium nitrogen removal, the study developed a new process where the electrode at the anode (anaerobic environment) of CW-MFC acts as an artificial electron acceptor. Based on electrode dependent anaerobic ammonium oxidation, the process was named the electroanammox process. This process provided a new pathway for ammonium nitrogen removal from wastewater in an anaerobic environment. The study was conducted in open and closed circuit conditions in a CW-MFC to better understand the electron flow role. This was further compared with the traditional CW. Based on the higher performance of open-circuit CW-MFC over the traditional CW, a CW filled only with conductive materials without electrical connections (electroactive CW) was then assessed to treat chromium, a typical heavy metal pollutant. The performance of electroactive CW was constant throughout,

with chromium removal of 99.9%. The study exhibited a strong link between microbes and conductive material for this removal. In contrast, the presence of the conductive material decreased toxicity build up in the system and allowed microbial activity at a higher loading of chromium. The redox gradient developed in electroactive wetland assisted the system's electron flow, leading to better microbial metabolism.

As sulphur is a very well-known redox metabolite in BES, a further study was conducted in CW-MFC to emphasise the interrelation between sulphate and a conductive material in electron transfer and treatment performance. CW-MFC performance was examined in the presence and absence of sulphate in wastewater. This indicated that sulphate acts as a redox coupling that significantly influences other CW-MFC treatment processes compared to the CW-MFC with no sulphate in the wastewater. The redox metabolites of sulphur improved the electron transfer mechanism and influenced treatment performance.

Based on the outcome of previous stages, more complex wastewater consisting of various common pollutants and other, more recalcitrant pollutants was employed for the next stage. This was to examine the CW-BES technology's versatility to resist clogging at different loads, toxicity tolerance, and treatment performance. A variety of BES technologies integrated with CW were tested in this stage, such as CW-microbial electrolysis cell (MEC), CW-MFC, and electroactive wetland. The result indicated that the redox coupling of CW-BES has a significant influence on its treatment performance. Based on the favourable redox potential, the treatment performance increased, decreasing the toxicity build-up in the system with low sludge generation. The other significant outcome of the study was even at higher loading of recalcitrant pollutants, microbiology in terms of diversity and communities was not affected.

Hence, CW-BES was found to be a versatile technology even at higher loading with recalcitrant pollutants. In the final stage, storage and the practical application of generated electricity from

CW-MFC was explored. Since CW-MFC generates low power, scaling up the generated energy for real applications is a challenge. Therefore, the generated electricity from CW-MFC was stored using a power management system (PMS), mainly designed to store low power from CW-MFC. Further, the stored energy was used to operate an air-pump to provide aeration at the cathode of CW-MFC. The result showed significant improvement in treatment performance after aerating the cathode while decreasing the system's internal resistance. Thus, the study overall demonstrated practical application of bioenergy generated from the CW-MFC system.

Economically, this study's advanced technology can provide a sustainable method for wastewater treatment while addressing the water-energy nexus, a prime focus in the current era. Overall, the study attempted to provide a low-cost sustainable, innovative approach for wastewater treatment to keep a greener and cleaner environment.

[Page intentionally left blank]

Table of Contents

Table of Figures

Table of Tables

Abbreviations

CW	Constructed Wetland
FWS	Free Water Surface
SSF	Sub Surface Flow
HSSF	Horizontal Sub-Surface Flow
VF	Vertical flow
HR	Horizontal flow
BOD	Biological oxygen demand
MFC	Microbial Fuel Cell
MEC	Microbial electrolysis cell
EAB	Electroactive bacteria
DIET/DET	Direct Electron Transfer
IET	Indirect electron transfer
PEM	Proton Exchange Membrane
ORR	Oxygen Reduction Reaction
DIET/DET	Direct Electron Transfer
SMFC	Sediment Microbial Fuel Cell
CW-MFC	Constructed Wetland-Microbial Fuel Cell
COD	Chemical Oxygen Demand
BES	Bioelectrochemical System
HF	Horizontal Flow
VUF	Vertical upflow
CL	Closed Circuit
OP	Open Circuit
TN	Total nitrogen
TOC	Total Organic Carbon
HF-CW	Horizontal Flow-Constructed Wetland
mm	millimetre
CW-HF	Constructed Wetland-Horizontal Flow
mg/L or mg/l	Milligram per litre

v/v	Volume by volume
g/L or g/l	Gram per litre
HRT	Hydraulic retention time
VSS	Volatile suspended solid
APHA	American Public health association
Iw	Initial weight of the sample
Fw	Final weight of the sample
mg	Milligram
DNA	Deoxyribose nucleic acid
W	Watt
P	Power
E	Cell Potential
V	Volt
I	Current
A	Ampere
R	Resistance
D	Dilution rate
X	Mass of Cell
μ	Specific Growth Rate
CE	Coulombic Efficiency
Ce	Experimental Coulombic Efficiency
Ct	Theoretical Coulombic Efficiency
F	Faraday's Constant
b	Number of electrons exchanged per mole of substrate
v	Anodic volume
l	litre
S	Substrate concentration
M	Molecular weight of the substrate
ANOVA	Analysis of Variance
DO	Dissolved oxygen
mV	Millivolt

SEM	Scanning Electron Microscopy
EDX	Energy Dispersive X-ray
PVC	Polyvinyl Chloride
EDTA	Ethylenediamine tetra acetic acid
h	Hour
AGRF	Australian Genome Research Facility
PZC	Point of Zero Charge
GOx	Glucose Oxidase
S-replete	Sulphate Replete
S-deplete	Sulphate Deplete
SRB	Sulphate Reducing Bacteria
SOB	Sulphate Oxidizing Bacteria
SHE	Standard Hydrogen Electrode
E_{cell}	Cell Potential/Cell Voltage
M	Molecular Weight
XPS	X-ray Photon Spectroscopy
XRD	X-ray Diffraction Spectroscopy
MET	Microbial Electrochemical Technology
ICP-MS	Inductively coupled Plasma Mass Spectroscopy
OLR	Organic Loading Rate
DC	Direct Current
Eq	Equation
ppb	Part Per Billion
PMS	Power Management System
CDC	Capacitor Engaged Duty Cycling
IA	Intermittently Aerated
OCV	Open Circuit Voltage
MPPT	Maximum Power Point Tracking
F	Farad
d	Days
μW	Micro Watt

s	Seconds

[Page intentionally left blank]

Chapter 1 has been removed for copyright or proprietary reasons.

It is the following published book chapter: Srivastava, P., Yadav, A. K., Garaniya, V., Abbassi, R., 2019. Chapter 6.3 - Constructed wetland coupled microbial fuel cell technology: development and potential applications, in, Mohan, S. V., Varjani, S., Pandey, A., (eds.), Microbial electrochemical technology : sustainable platform for fuels, chemicals and remediation, Radarweg, Netherlands, Elsevier, pp. 1021-1036.

Chapter 2: Electrode dependent anaerobic ammonium oxidation in microbial fuel cell integrated hybrid constructed wetlands: A New Process

Graphical abstract

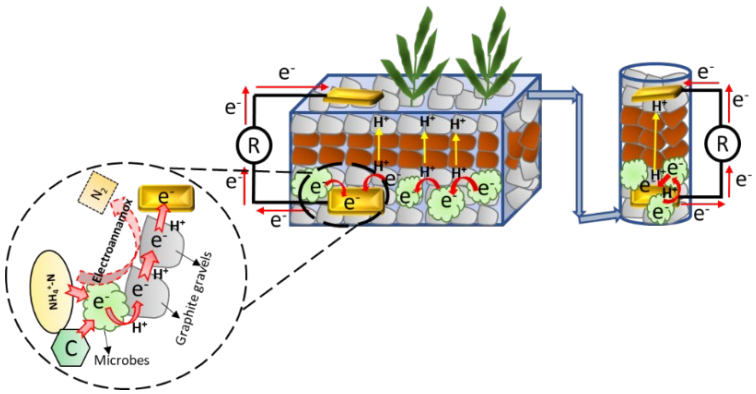

Abstract

This study provides a new approach of electrode dependent anaerobic ammonium oxidation (electroanammox) in a microbial fuel cell (MFC) integrated hybrid constructed wetlands (CWs). The study was carried out in three CWs, each with a horizontal flow (HF) followed by a vertical upflow (VUF). Two of the CWs were integrated with MFC; one was operated in closed circuit (CL) mode and the other in open circuit (OP) mode to determine the influence of electron transfer through an external electrical circuit. The initial nitrogen and carbon concentrations were 40 mg/l and 880 mg/l, respectively. The total nitrogen (TN), NH_4^+-N, TOC and COD removal achieved in CW-MFC-CL were 90.0 ± 1.15%, 94.4 ± 0.75%, 64.8 ± 3.0% and up to 99.5 ±3.4%, respectively. The TN and NH_4^+-N removal in CW-MFC-CL was 20.0% and 13.6% higher than the normal CW. The maximum current density achieved in CW-MFC-HF was of 75 mA/m^3 and in CW-MFC-VUF was 156 mA/m^3. Furthermore, the study revealed that even at low microbiological biomass, an MFC integrated CW operating in a closed circuit

gave higher removal of NH_4^+-N and COD than the normal CW and open circuit CW-MFC. The microbiological analysis shows the presence of already known nitrifiers and denitrifiers, indicating their role in electrode dependent nitrogen removal.

2.1. Introduction

Nitrogen removal involves two significant steps, nitrification and denitrification, making it a costly and complex process in wastewater treatment. The nitrification step requires an electron acceptor (such as oxygen) for the conversion of ammonium to the nitrite and nitrate, whereas for the conversion of nitrate to nitrogen gas in denitrification, an electron donor (such as carbon) is needed [66]. Constructed wetlands (CWs) are a natural treatment technology for wastewater. The conventional CW consists of a gradient of oxic, anoxic and anaerobic zones. The bottom portion of the CW is considered as an anaerobic portion and the uppermost layer as an aerobic portion [67]. The anaerobic zones of a CW limit the removal of the pollutants such as NH_4^+ and organics.

On the other hand, the aerobic zone of a CW prevents the removal of pollutants such as NO_3^-. Hybrid CWs were developed to overcome the problem of anaerobic and aerobic conditions for such pollutants. The possible designs of a hybrid CW consist of horizontal flow, vertical flow, combined vertical flow-horizontal flow and several other combinations Vymazal [68]. The general estimation of total nitrogen from municipal wastewater in HF-CW is around 40%, and in VF-CW, it is around 75% [20, 31, 69, 70]. Moreover, complete nitrogen removal in a CW needs aerobic conditions for ammonium oxidation and anaerobic conditions for denitrification. However, providing external aeration to a CW for ammonium oxidation is not economically viable and sustainable [69].

Similarly, the addition of extra carbon to the CW for denitrification is also not economical viable [71].On the other hand, an MFC has been reported as an efficient potential technology for wastewater treatment, including nitrogen and carbon removal [72, 73]. However, several shortcomings, such as challenges related to the cathode, scale-up, and low energy production, that have not been implemented in field-level applications [74]. A typical MFC needs an anaerobic zone and an aerobic zone. These zones provide a redox gradient for flowing electrons and protons from anaerobic to aerobic zones. Similar, redox gradients are naturally present in CWs, which can integrate an MFC into a CW. In recent years attempts were made to merge MFC and CWs to make an integrated CW-MFC technology [32, 62, 75]. The integration of MFC technology with CW is gaining interest among researchers due to improved treatment performance and other benefits [33, 63, 76]. It has been reported that integrating MFC technology into a CW can increase treatment efficiency by 27-49% compared to normal CW [77]. Corbella and Puigagut [78] reported that the treatment efficiency of CW-MFC closed-circuit mode was 18% better for COD, 15% better for TOC, 31% better for PO_4^{3-} and 25% better for NH_4^+ removal in comparison to CW-MFC operated in open circuit mode. The open-circuit mode operation of MFC is the situation when the electric circuit is disconnected, which ultimately hinder the flow of electron from the anode (anaerobic zone) to the cathode (aerobic zone). Such reported enhancements are due to the presence of electrodes in the anaerobic portion of a CW-MFC, which act as a temporary electron acceptor in oxidation and transfer the accepted electron to the cathode through an external wire or other routes [79]. The said process of electron acceptance and transfer gives the possibility of electricity generation and enhancement of oxidation of pollutants in an anaerobic environment where electron acceptor is present in a limited amount [63, 80]. Externally provided anode or conductive material can act as an artificial electron acceptor in anaerobic zones of CWs for promoting the oxidation of

pollutants such as NH_4^+-N and organic materials. On the other hand, externally provided cathode can act as an electron donor for the reduction of pollutants such as NO_2^--N and NO_3^--N [71, 81, 82].

This study was conducted to develop electrode dependent anaerobic ammonium oxidation (electroanammox), and overall total nitrogen (efficient nitrification and denitrification) from the wastewater in MFC integrated CWs. A hybrid CW consisting of a horizontal flow path followed by a vertical flow path has been used. This configuration was adopted under the assumption that a horizontal bed will provide larger surface area of conductive materials (act as an electron acceptor) for ammonium oxidation, and denitrification would occur in CW-MFC-VUF as wastewater will come in contact of anaerobic zone first.

2.2. Materials and methods

2.2.1. Experimental setup

Three laboratory-scale hybrid HF-VUF-CW microcosms were set up. Two of these were integrated with an MFC, one operated in closed circuit (CW-MFC-CL) mode and the other in open circuit (CW-MFC-OP) mode. The third microcosm was a normal CW (CW-Normal). All three microcosms were identical in shape, dimension and planted with common sedges. The HF-CW dimension was 254 mm X 181 mm X 140 mm (length X width X depth) and the VUF-CW was 300 mm X 90 mm (length X diameter). The HF-CW was equipped with three ports-one port was located 10 mm from the bottom while the other two ports were 30 mm below the surface at the opposite end to the first port. Of the two ports near the surface, one was for sample collection, and the other was to connect to the VUF-CW (*Figure 2-1*). The VUF-CW also had three ports, one 10 mm from the bottom, the second 150 mm from the bottom, and the third 10 mm from the surface. The CW-Normal-HF microcosm and CW-Normal-VUF microcosm were filled with normal stone pebbles of Ø = 5.0 -8.0 mm. Both CW-MFC-HF

microcosms were filled with graphite granules (Ø = 5.0 -8.0 mm) to a depth of 40 mm overlayed by a 60 mm layer of normal pebbles (Ø = 5.0 -8.0 mm) and a 30 mm layer of graphite granules (Ø = 5.0 -8.0 mm). A few large stones were placed at the ports of the CW-HF microcosm to avoid clogging. A graphite plate of 100 mm x100 mm (length x width) and 9 mm thickness was inserted in the bottom graphite layer (anode zone) as an electron collector. A hole was provided in graphite plate to wrap copper wire around the plate tightly to make maximum contact between wire and plate. The exposed area of wire was then covered with water-proof non-conductive epoxy to insulate it. A second graphite plate of the exact dimensions was inserted in the upper layer of graphite (cathode zone) as an electron donor. The free end of copper wire of both the graphite plates were connected to make a circuit. The CW-MFC-VUF microcosms were filled to a depth of 100 mm with graphite granules (Ø = 5.0 -8.0 mm), overlayed by 150 mm of regular pebbles (Ø = 5.0 – 8.0 mm) which was followed by a 50 mm layer of graphite granules (Ø = 5.0 – 8.0 mm). A graphite plate of 100 mm x 51mm (length x width) with a thickness of 9 mm was inserted in the anode zone as an electron collector. This was connected by a copper wire to a second graphite plate of the same dimensions inserted in the upper layer of graphite (cathode zone) as an electron donor.

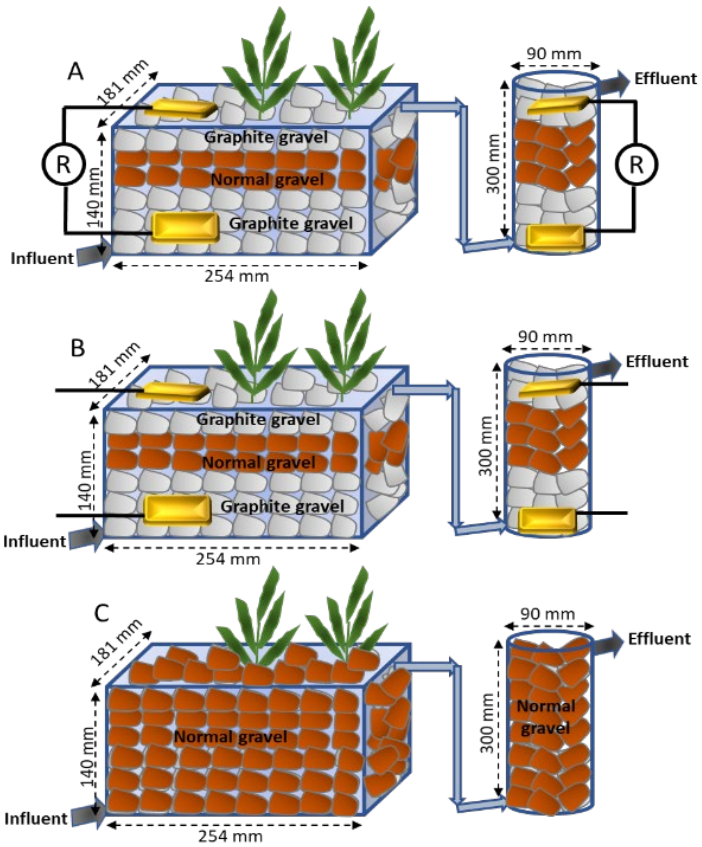

Figure 2-1. Laboratory scale three sets of HFs followed by VUF microcosms namely: A) CW-MFC-CL, B) CW-MFC-OP and C) CW-Normal.

2.2.2. Inoculation and operating conditions

The inoculum sludge was taken from a conventional activated sludge-based municipal wastewater treatment facility in Tasmania, Australia. The microcosms were inoculated with the 2.0 % v/v sludge with dilution by synthetic wastewater in a 1:1 ratio. The synthetic wastewater instead of real wastewater was used in this study to control ammonium concentration in the wastewater. Since this study was to optimise the technology, the varying concentration of ammonium would not have provided proper information. The composition was adopted from Yang, et al. [83]. The composition of wastewater was modified to vary the amount of carbon sources. The composition of the wastewater used was (in g/l): sodium acetate, 0.5; sodium citrate, 3.0; NH_4Cl, 0.8; KH_2PO_4, 0.5; $Na_2HPO_4.7H_2O$, 1.0; $FeSO_4.7H_2O$,

0.1; $MgSO_4$, 0.2; trace element solution, 2.0 ml. The trace element solution was the same as the composition described in the previous literature [83]. All the chemicals were bought from the company Chem supply, Adelaide, Australia. The initial carbon and ammonium concentration of the wastewater was 880.0 mg/l and 40.0 mg/l, respectively.

The experiment was commenced in summer with an average room temperature of 23±3°C. The inoculum was mixed with synthetic wastewater and added to all three microcosms in equal amounts. Freshly prepared synthetic wastewater was mixed (1:1) with the effluent flowing from the microcosm on a daily basis for one month. After this time, continuous feeding of microcosms continued for a further month for stabilization and to achieve a steady-state condition before analysis commenced. The void volumes of CW-Normal-HF and CW-Normal-VUF were 2.0l and 0.6l, respectively. The void volumes of CW-MFC-HF and CW-MFC-VUF were 2.2l and 0.65l, respectively. Hydraulic retention time (HRT) of 15.0 h was maintained. The wastewater was prepared daily and added to the reservoir bucket after proper cleaning of the bucket to avoid any biomass growth. The wastewater was pumped into the HF-CW and then flowed into the bottom of the VUF-CW. Effluent samples were taken once a week from the HF-CW as well as VUF-CW of all the microcosms. The volatile suspended solids (VSS) of all three sets of microcosms were measured at the beginning of the experimental period (two months after microcosm setup) and again after four months.

2.2.3. Chemical analysis

All samples were filtered through a cellulose syringe filter (0.45µm, Ø=25mm, MicroScience) before analysis. The concentration of total organic carbon (TOC) and total nitrogen (TN) was analysed with a Shimadzu TOC-TN analyser (Model TNM-L ROHS). The chemical oxygen demand (COD) was estimated using the APHA Standard Methods5220D method [84]. The nitrate, nitrite and ammonium were analysed by ion chromatography (Eco IC, MEP

instruments, Metrohm). The pH was measured with an Ohaus ST series pen meter (Model ST20, Australia). The voltage was recorded daily with Nova PC^{LINK} multimeter (PC20, Australia). The percentage removal of COD, TN, TOC, NH_4^+-N, NO_3^--N and NO_2^- in HF and VUF was calculated from Equation (Eq.) 1,

$$Removal\ \% = \frac{Influent - Effluent}{Influent}\ X\ 100 \qquad Eq.1$$

The overall removal efficiency of the microcosm was calculated based on final effluent from the VUF microcosm and calculated from Eq. 2:

$$Overall\ removal\ (\%) = \frac{Influent - Effluent\ from\ VUF}{Influent}\ X\ 100 \qquad Eq.2$$

The VSS of each microcosm was calculated using Eq. 3.

$$VSS\ (mg/l) = \frac{\mathrm{I_w} - F_w}{sample\ volume(ml)}\ X\ 100 \qquad Eq.3$$

Where F_w = final weight of the sample (mg), I_w = initial weight of the sample (mg).

2.2.4. Microbial Community Analysis

The phylogenetic analysis of CW-MFC-CL-HF, CW-MFC-CL-VUF, CW-MFC-OP-HF, CW-MFC-OP-VUF, CW-Normal-HF and CW-Normal-VUF was conducted using 16s rRNA gene pyrosequencing. The samples, including granules and pebbles and charge collector, were collected from each microcosm's anode and cathode and vortexed for 15 min at 1000 rpm before DNA extraction. The FavorPrep soil DNA kit from Favorgen, Fischer Biotech, was used for extracting genomic DNA by following standard prescribed procedures provided with the DNA kit. The target sequence, with a forward primer (27F) AGAGTTTGATCMTGGCTCAG and reverse primer (519R) GWATTACCGCGGCKGCTG was used for diversity profiling [85].

2.2.5. Electrochemical and other calculations

The electrochemical parameters were calculated using Ohm's law from Eq. 4 to 7,

$$Power\ (P) = E\ (V)\ X\ I\ (A) \qquad Eq.4$$

$$Power\ density\ \left(\frac{mW}{m^3}\right) = \frac{P}{Anodic\ volume\ (m^3)} \qquad Eq.5$$

$$Current, I(A) = E\ (V)\ X\ R(A) \qquad Eq.6$$

$$Current\ density\ \left(\frac{mA}{m^3}\right) = \frac{I}{Anodic\ volume\ (m^3)} \qquad Eq.7$$

Polarization studies were done on closed-circuit microcosms (CW-MFC-CL-HF and CW-MFC-CL-VUF) after they had reached a steady-state by varying the external resistance from higher to lower between 1MΩ to 22Ω. Each resistance was maintained for 15 minutes, and after every 15 minutes, the voltage was recorded.

The microbes' specific growth rate was calculated according to Maier and Pepper [86] for a continuous system by taking the conversion factor of VSS per gram of biomass from the present study. As this was a continuous system with wastewater continuously flowing through the microcosm, the dilution factor was also included in the calculation to determine the system's exact biomass. Eqs. 8 and 9 were used for the calculation:

$$D = \frac{Flowrate\ (ml/h)}{total\ volume\ of\ the\ reactor\ (ml)} \qquad Eq.8$$

$$\frac{dX}{dt} = \mu X - DX \qquad Eq.9$$

Where X is the mass of cell, μ is the specific growth rate ($time^{-1}$), and D is the dilution rate ($time^{-1}$).Further, coulombic efficiency (CE) and energy recovery were calculated using formula adopted from Liu, et al. [87] Eq. 10:

$$CE = \frac{C_e}{C_t} \qquad Eq.10$$

C_e = Experimental coulomb efficiency, determined by integrating the current with respect to time, C_t = theoretical coulomb obtained from Eq. 11:

$$C_t = \frac{FbSv}{M} \qquad Eq.11$$

F= faraday's constant, b= number of electrons exchanged per mole of substrate, v = anodic volume (l), S= substrate concentration, M = molecular weight of the substrate (g/mol).

2.2.6. Statistical analysis

The statistical analysis such as mean, standard deviation and standard error were calculated using Microsoft Excel. The significance level taken for calculation was 95% ($\alpha = 0.05$). The ANOVA (analysis of variance) test was performed to compare the results of CW-MFC and CW-Normal.

2.3. Results and discussion

2.3.1. Nitrogen removal

The average influent TN and NH_4^+-N concentrations were 50.1 ± 8.3 mg/l and 43.8 ± 5.0 mg/l, respectively. The overall TN and NH_4^+-N in CW-MFC-CL were at almost 90.0 ± 1.1% and up to 94.4 ± 0.7%, respectively (*Figure 2-2*). The range of TN and NH_4^+-N removal of HF and VUF regions are also shown in *Figure 2-2*. Furthermore, the overall TN and NH_4^+-N removal was approximately 70.0 ± 1.75% and 85.1 ± 2.7% in CW-Normal and 80.0 ± 1.2% and 89.1± 1.9 % in CW-MFC-OP. The overall TN and NH_4^+-N removal were found to be high, particularly in CW-MFC-CL in comparison to CW-MFC-OP and CW-Normal. Moreover, CW-MFC-OP removal efficiency was still higher than the CW-Normal. In the anaerobic conditions, the high removal of NH_4^+-N was found to be interesting. The microcosms'

anaerobic condition was further justified with the microcosm's DO concentration at the surface and the bottom. The DO concentration in all the microcosms was low, shown in *Table 2-1*, which indicates the microcosms' anaerobic situation. The low DO concentration also shows the limited availability of an electron acceptor in the deeper or bottom zones. The average pH and DO concentration of deeper/bottom zones and all the microcosms' surfaces are given in *Table 2-1*. Though the cathode was exposed to air the measured DO value was not significantly different from the microcosm's bottom. A similar DO situation for the anaerobic condition is already reported by [88, 89]. In the low DO situation, with conductive material equipped, microcosm NH_4^+-N removal was found to be high. The higher removal of NH_4^+-N in CW-MFC-CL and CW-MFC-OP indicates that the electrode was acting as an electron acceptor for NH_4^+-oxidation in the absence or deficiency of oxygen. Due to the presence of conductive material, particularly in the close circuit (CW-MFC-CL), the electron transport mechanism was favourable for the microbes [90]. Whereas in CW-MFC-OP, due to the lack of electron transfer or electron build-up, the mechanism was not that faster, which causes lower treatment efficiency than CW-MFC-CL. The higher removal in CW-MFC-OP than in the CW-Normal indicates that electrons' transfer was not completely ruled out in the open circuit system. Similar findings were also reported by Srivastava, et al. [91]. The conclusion about the role of conductive material for NH_4^+-N oxidation was arrived at due to the higher removal efficiency of CW-MFC-CL than the other microcosms under the same conditions. The electron dependent anaerobic NH_4^+-N oxidation has also been reported by a number of researchers [66, 71, 92].

Table 2-1. Average pH and DO at the surface and bottom of all microcosms.

	Surface DO (mg/l)	Bottom DO (mg/l)	Surface pH	Bottom pH
CW-Normal-HF	0.51±0.24	0.40±0.26	7.2±0.28	7.20±0.18
CW-Normal-VUF	0.39±0.26	0.35±0.30	7.34±0.22	7.20±0.14
CW-MFC-CL-HF	0.42±0.24	0.38±0.18	7.16±0.12	7.30±0.20
CW-MFC-CL-VUF	0.58±0.23	0.40±0.22	7.20±0.09	7.20±0.12
CW-MFC-OP-HF	0.42±0.25	0.37±0.21	7.25±0.18	7.33±0.13
CW-MFC-OP-VUF	0.50±0.41	0.23±0.24	7.34±0.23	7.19±0.13

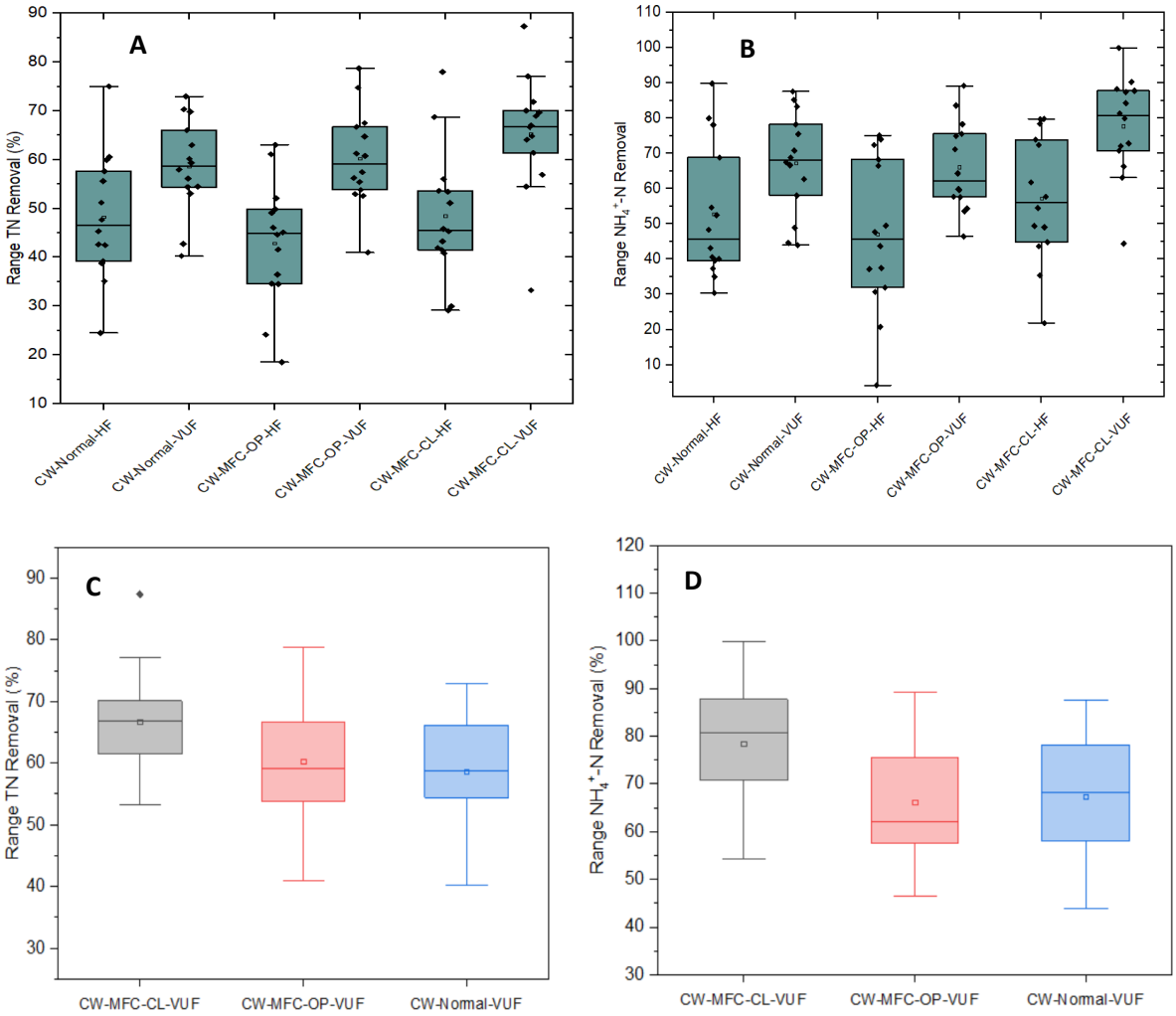

Figure 2-2. Percentage removal range of TN and NH_4^+-N in the microcosms of CW-MFC-CL, CW-MFC-OP and CW-Normal. A) TN in HF and VUF, B) NH_4^+-N in HF and VUF, C) Overall TN removal, D) Overall NH_4^+-N removal.

Furthermore, for the first three months of the experiment the average concentration of NO_3^--N was found to be 2.9 mg/l in the CW-MFC-CL-HF, 2.4 mg/l in the CW-MFC-CL-VUF; 3.4 mg/l in the CW-MFC-OP-HF, 1.33 mg/l in CW-MFC-OP-VUF; 1, 4.9 mg/l in CW-Normal-HF and 3.23 mg/l in CW-Normal-VUF. The average concentration of NO_2^- was found to be 0.17 mg/l in the CW-MFC-CL-HF, 0.025 mg/l in the CW-MFC-CL-VUF, 0.125 mg/l in the CW-MFC-OP-HF, 0.08 mg/l in the CW-MFC-OP-VUF, 0.125 mg/l in the CW-Normal-HF, and 0.15 mg/l in the CW-Normal-VUF. The results indicate that NH_4^+-N was removed with no

accumulation of NO_2^--N and NO_3^--N. This result also indicates that there would be some shortcut for electrode dependent anaerobic ammonium oxidation, through which no intermediate product formation occurs. Interestingly, even with low VSS, NH_4^+-N removal capacity of the CW-MFC-CL was high. It also indicates that the biomass of CW-MFC-CL was more efficient at NH_4^+-N removal than in the CW-MFC-OP and CW-Normal. The higher removal efficiency of CW-MFC-CL was due to the efficient microbe electron transfer to the conductive materials in that system. On the other hand, the CW-MFC-OP removal efficiency was low due to the limited electron transfer as the MFC's electrical circuit was not connected; hence, the transfer of the electron was limited. Conversely, in the normal CW, there was limited availability of electron acceptors in the anaerobic zone; hence the removal was low.

Further, to help elucidate all the microcosms' biomass, the VSS in all reactors was measured. The VSS analysed at the beginning of the experiment (after two months of inoculation) was very low, with only minor differences between all microcosms (*Table 2-2*). After 120 days, it increased in all microcosms, though not to the same extent in the CW-MFC-CL as in the CW-Normal and CW-MFC-OP. The VSS of CW-Normal-HF and CW-Normal-VUF were higher than in the CW-MFC-OP-HF and CW-MFC-OP-VUF and these were in turn higher than in the CW-MFC-CL-HF and CW-MFC-CL-VUF. As depicted in *Table 2-2*, it was found that the VSS of the CW-MFC-CL was lower than the CW-MFC-OP and CW-Normal. Surprisingly, even with higher VSS, CW-Normal could not compete with the removal efficiency of either CW-MFC. The CW-Normal and the CW-MFC-OP's removal efficiencies were lower even though the VSS concentrations were higher than the CW-MFC-CL. The removal performance of CW-MFC-CL indicates that the micro-organisms present in the CW-MFC-CL were electrode dependent and more efficient for the removal of NH_4^+-N in the wastewater than in the CW-Normal. The microbiological details later in *Section 2.3.4.* will give more insight into

it. The VSS of CW-MFC-OP was higher than the CW-MFC-CL, but the removal was still less because of the open circuit and limitation for the electron transfer from anaerobic zones to aerobic zones. The differences in VSS in different microcosms and their treatment performances clearly indicate their respective efficiencies. The microcosm with electrodes/conductive materials produces less biomass, but the said biomass efficiencies are higher than the biomass produced in normal microcosms. The results also revealed that efficient electron transfer from anaerobic zones to aerobic zones also influences microcosms' treatment performance. The lesser biomass generation may further help avoid clogging in the system. Such a system may also tolerate higher loads of pollutants without being adversely affected.

Table 2-2. VSS of the three microcosms at the beginning and in the middle of the experiment.

Duration	CW-MFC-CL-HF (mg/l)	CW-MFC-CL-VUF (mg/l)	CW-MFC-OP-HF (mg/l)	CW-MFC-OP-VUF (mg/l)	CW-Normal-HF (mg/l)	CW-Normal-VUF (mg/l)
60 days after inoculation	101	107	90	88	115	70
120 days after inoculation	940	466	1900	1120	2200	5466

2.3.2. COD and TOC removal

The average influent TOC and COD were 840 ± 20 mg/l and 1014 ± 10 mg/l, respectively. The variation in TOC and COD concentration is due to the presence of other chemical constituents in influent wastewater, which themselves contains COD. The three microcosms' overall removal efficiency was based on the TOC and COD in the final effluent from the VUF. The final TOC removal in the CW-MFC-CL was as high as 64.8 ± 3.0%, while COD removal was 99.5 ± 3.54%. The performance of the CW-MFC-OP was close to that of the CW-MFC-CL at

62.4 ± 1.5% for TOC removal and 97.7 ± 1.1% for COD, whereas the TOC removal in the CW-Normal-VUF was 55.9 ± 1.7% and 95.5 ± 2.5% for COD removal.

Figure 2-3 show the range of percentage removal of COD and TOC in the HF and VUF of all the microcosms. The overall removal efficiency of all the microcosms is present in *Appendix 1, Figure A1*. From the initial influent concentration, the HF microcosm had removed the bulk of COD and TOC, and then the remainder had been removed in the VUF microcosm. The reason behind the difference in total TOC and COD removal was the possibility of the presence of autotrophic bacteria, which was dependent on NH_4^+-N instead of carbon. That could also be a reason for the almost complete removal of COD compared to the much lower removal of TOC. The microbiological analysis presented later also indicates the presence of autotrophic bacteria in the anode of microcosms. Overall the removal performance of CW-MFC-CL was high in comparison to CW-MFC-OP and CW-Normal due to the presence of an electrode that was acting as an artificial electron acceptor in the anaerobic conditions [63, 79].

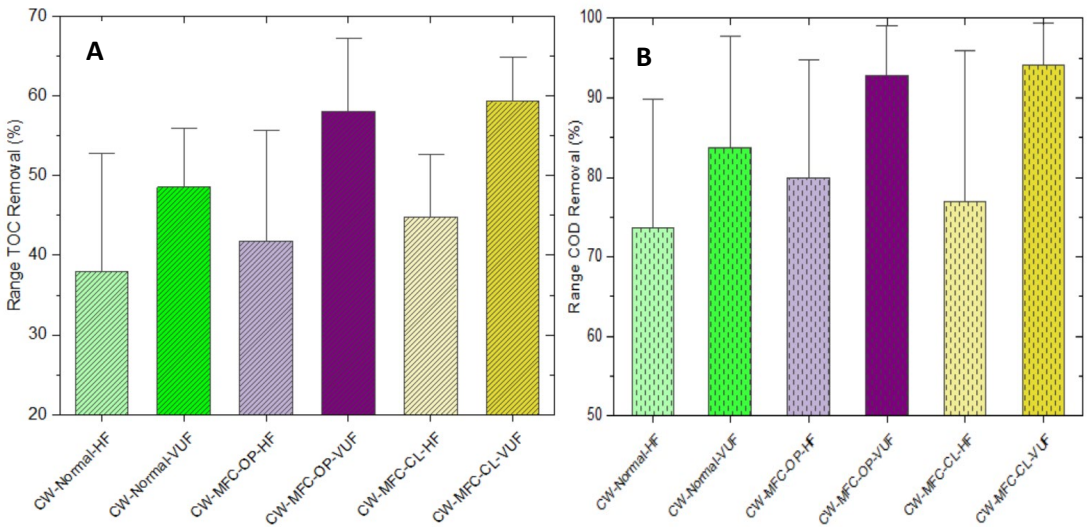

Figure 2-3. Percentage removal in the various microcosms of the CW-MFC-CL, CW-MFC-OP and CW-Normal systems. A) TOC in HF and VUF, B) COD in HF and VUF.

2.3.3. Bioelectricity generation

The voltage output of the CW-MFC-CL along with the open-circuit voltage of the CW-MFC-OP was assessed during the whole experimental period. The maximum voltage achieved from the CW-MFC-CL-HF was on an average 80 mV, whereas in CW-MFC-CL-VUF, it was almost 95 mV (*Figure 2-4*). The voltage output was very low in comparison to other CW-MFC closed-circuit systems studies, such as Oon, et al. [93] reported 421.7 mV, Liu, et al. [94] with 598-713 mV, Zhao, et al. [62] 371.14 ± 78.97 mV to 495 mV Shen, et al. [95] with 558.50 mV, 399.80 mV, 358.00 mV and 336.00 mV. Moreover, the open-circuit voltage of the CW-MFC-OP-HF and the CW-MFC-OP-VUF was higher than the closed-circuit in the present study. In the closed-circuit system, the voltage was restricted by the internal resistance, such as ohmic resistance and the electrode over-potential [69]. The voltage achieved could also be affected by COD concentration at the anode, pH, temperature and substrate conversion frequency [79]. The low DO condition at the cathode of CW-MFC could also be the reason for low voltage performance. Liu, et al. [96] has also reported that DO within the present study range could also hinder the electron transfer at the cathode, due to which electricity generation could be affected. The maximum power density achieved in the CW-MFC-CL-HF was 12.4 mW/m^3 while in CW-MFC-CL-VUF, it was 25 mW/m^3 (*Figure 2-4*). It was also found that increasing COD normally decreased the electricity generation in CW-MFCs [63]. The reason behind low electricity generation could be due to the consumption of all the dissolved oxygen by an elevated amount of COD which could lead to the anaerobic situation throughout (reduction or elimination of redox gradient) filter bed of CW. The redox gradient is required for generating electricity. Furthermore, the current density achieved in the CW-MFC-CL-HF and the CW-MFC-CL-VUF was 75.09 mA/m^3 and 156 mA/m^3, respectively (*Figure 2-4*).

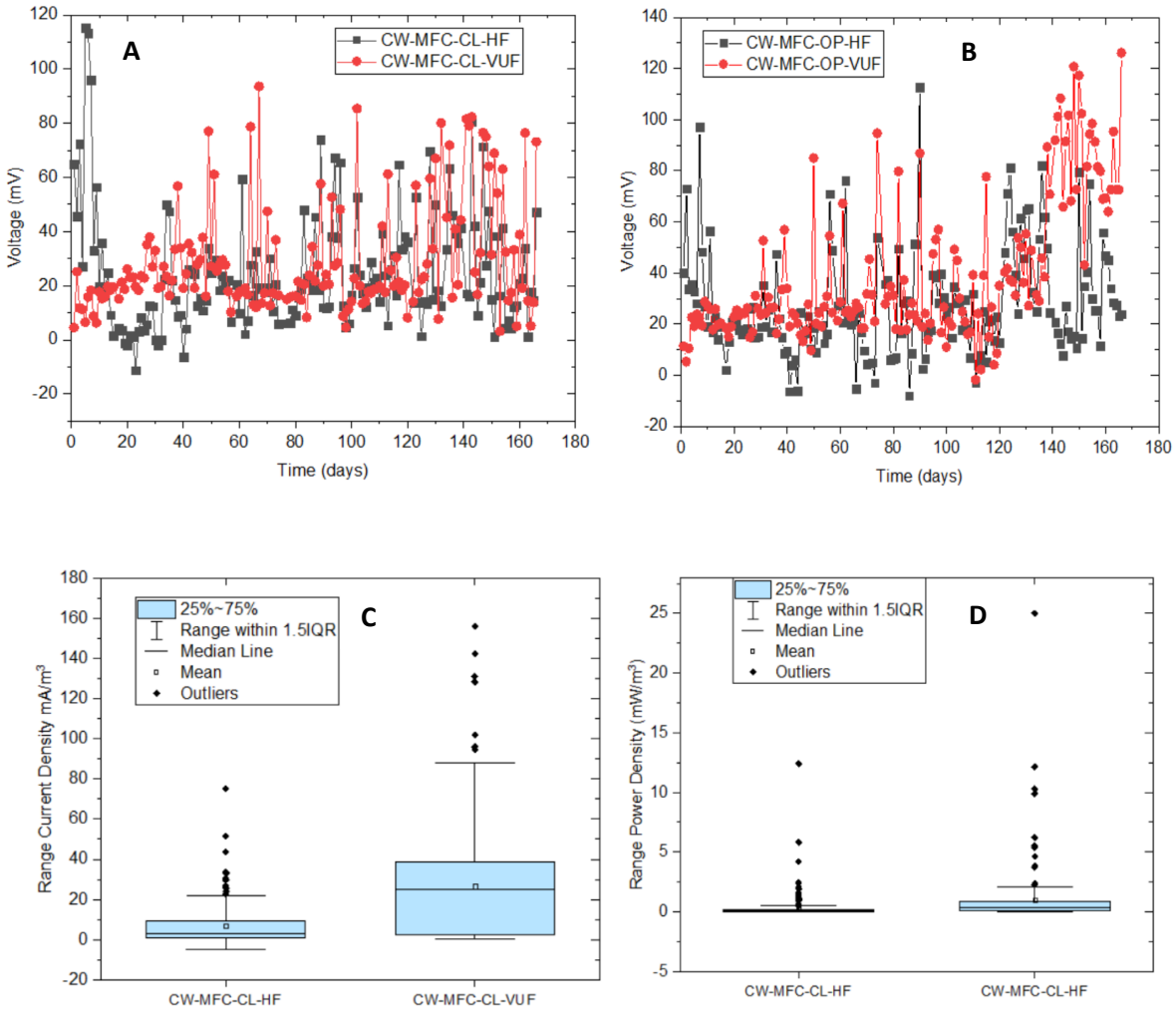

Figure 2-4. Voltage performance of HF and VUF regions of: A) CW-MFC-CL and B) CW-MFC-OP; C) Current density of CW-MFC-CL; D) Power density of CW-MFC-CL

The polarization study was performed to gain an understanding of the internal resistance in closed circuit microcosms. The CW-MFC-CL-HF voltage was in the range of 34.0 to 27.2mV, whereas in CW-MFC-CL-VUF, it was 41.0 to 42.0mV. The polarization curves of CW-MFC-CL-HF and CW-MFC-CL-VUF are shown in *Figure 2-5*. The maximum power density and current density achieved was 224 mW/m^3 and 1706 mA/m^3, respectively. In a typical MFC treating kitchen wastewater, Mohamed, et al. [97] achieved a power density of 41.5 ± 1.2 mW/m^{-2} and a current density up to 135 mA/m^{-2}. Similarly, in a dual-chambered MFC treating nitrogen rich wastewater achieved 0.54 W/m-3 of power density and 6.51 A/m^{-3} of current

density. The achieved power and current density in CW-MFC are significantly lower than MFC; however, there are several factors that creates electron losses in CW-MFC. The major loss was found to be due to ohmic loss [98]. Logan [99], Corbella, et al. [100] have also stated that insufficient mass transfer to and from the electrode can hinder the reaction rate, as well as electricity generation.

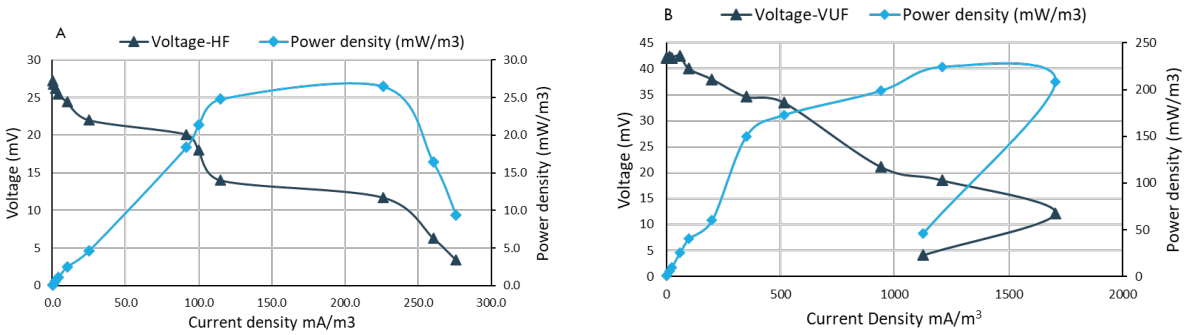

Figure 2-5. Polarization curve of A) CW-MFC-CL-HF and B) CW-MFC-CL-VUF, with varying resistance.

The achieved Columbic efficiency (CE) was 0.97% in the CW-MFC-CL-HF and 6.67% in the CW-MFC-CL-VUF. The reason for low CE could be due to the use of electrons for purposes other than electricity generation, such as denitrification. Lower CE may also be due to electrons bypassing the external electrical circuit and transferring via other routes due to the microcosm design (membrane-less system with no sharp compartmentalisation of anodic and cathodic zones) and operation (flowthrough of water). Many studies have reported that CE could be lower due to several other factors, such as anaerobic bacteria, which dominate the anode portion using the electrons [101, 102].

2.3.4. Microbial Community Analysis

The microbiology of the HF and VUF microcosms was characterised based on 16S rDNA sequencing. This showed a higher diversity of micro-organisms in all the microcosms than in the original inoculum. *Figure 2-6* illustrate the microbiological diversity based on phylum for

the HF and VUF of all microcosms and the inoculum. The result of all microbiological analyses indicates that the microbiological diversity/distribution and the population were high in the CW-Normal microcosm. The result is complementary to the result of VSS for the CW-Normal microcosm. The VSS of CW-Normal microcosm was higher than for the CW-MFC-OP, which was in turn higher than the CW-MFC-CL, and the same trend was followed for the microbiological population. The most abundant bacteria found in the anaerobic region of the CW-Normal microcosm was from the phylum *Proteobacteria (77%),* followed by *Firmicutes (9.5%)*, *Fusobacteria (4.6%)*, and then *Bacteroidetes (4.6%).*On the other hand, in the anode region of the CW-MFC-CL the phylum *Lentispaerae (33.7%)* predominates*,* followed by *Proteobacteria (12.3%), Bacteroidetes (11.9%)*, *Firmicutes (11.8%)*, and *Tenericutes (11.8%),* and the remainder of organisms from another phylum was less than 1%. A similar trend was found in CW-MFC-OP. The main micro-organisms that dominate the CW-Normal-HF were from the phylum Proteobacteria. The largest population was from class *ß-Proteobacteria,* which accounts for 38.7%. Further details about microbiology at the surface and at the bottom of all the microcosm based on *Class* are given in *Appendix 1 (Figure A2).*

On the other hand, *ß-Proteobacteria* accounted for12.3% in the CW-MFC-CL-HF,22% in the CW-MFC-CL-VUF, 8.4% in the CW-MFC-OP-HF and22.2% in the CW-MFC-OP-VUF. Furthermore, bacteria from class *Lentisphaeria* and phylum *Lentispaerae*, reported as nitrogen fixation bacteria [103], dominated the CW-MFC-CL. In addition, Yilmaz, et al. [103] also reported *Proteobacteria, Bacteroidetes,* and *Firmicutes* as denitrification and nitrogen fixation bacteria (*Figure 2-6*). *Tenericutes* has been reported as abundant in a reducing environment [104]. Furthermore, bacteria from the phylum *Planctomycetes* were found highest in the population in the CW-Normal microcosm than the other microcosms. Interestingly, *Anammox*, also belongs to phylum *Planctomycetes*, which was completely

absent in all the microcosms. Only micro-organisms from the genera Phycisphaerae (0.5%) and Pirellulales (0.1%) were present in the CW-MFC. The presence of different genus of *Planctomycetes* indicates that there could be a possibility of some other bacteria than the annamox from genus of *Planctomycetes* playing a role in ammonium oxidation. Furthermore, the presence of *Geobacter* was only 0.1% in the CW-MFC-CL and 0.4% in the CW-Normal. However, in sludge it accounts for 0.3%. The absence of *Geobacter* has also been reported in electrode dependent anaerobic ammonium oxidation in a MEC (microbial electrolysis cell) [92, 105-107]. In addition, they reported that *Pseudomonas* species were responsible for transferring electrons to the electrode and worked as an electron shuttle. Furthermore, the bacteria from class *ß-proteobacteria,* genus *Rhodocyclaceae,* which is known as an autotrophic denitrification bacteria [108], was present in all the microcosms. However, the highest population was in the CW-Normal microcosm. Other autotrophic denitrification bacteria from class *ß-proteobacteria,* genus *Thiobacillus*, were absent in the CW-Normal though present in CW-MFC-CL (0.4%) and CW-MFC-OP (0.3%) [109, 110]. Additionally, some other bacteria from genus *Hydrogenophaga*, a heterotrophic denitrification bacterium, were present in the CW-MFC-CL and CW-MFC-OP; however, they were absent in the CW-Normal.

Microbiological analysis indicates that traditional nitrification/denitrification bacteria and other bacteria, even in the low population, were able to remove total nitrogen in MFC integrated CW. Many bacteria that participate in the denitrification process were abundantly present in all the microcosms [109]. That could be the one reason for no trace of NO_2^--N and NO_3^--N at the later stage. Another reason could be the microbes in the presence of the electrode were using other pathways or shortcut pathways to convert it into gaseous forms. Moreover, further exploration is required to prove the above-said statement.

Furthermore, all the bacteria which take on the role of an electrode in CW-MFC for TN removal have been categorised as electrode (*Electro*) dependent anaerobic (*an*) ammonium (*amm*) oxidation (ox) and the process was termed as *Electroanammox*. However, this study only indicates that, in the presence of electrode, microbes were efficient for TN removal than the CW-Normal. This shows that there was a role of the electrode for ammonium oxidation. Still, further study is needed to understand the dominant bacteria for the *Electroanammox* process and ammonium oxidation pathway while using an electrode as an electron acceptor in anaerobic conditions.

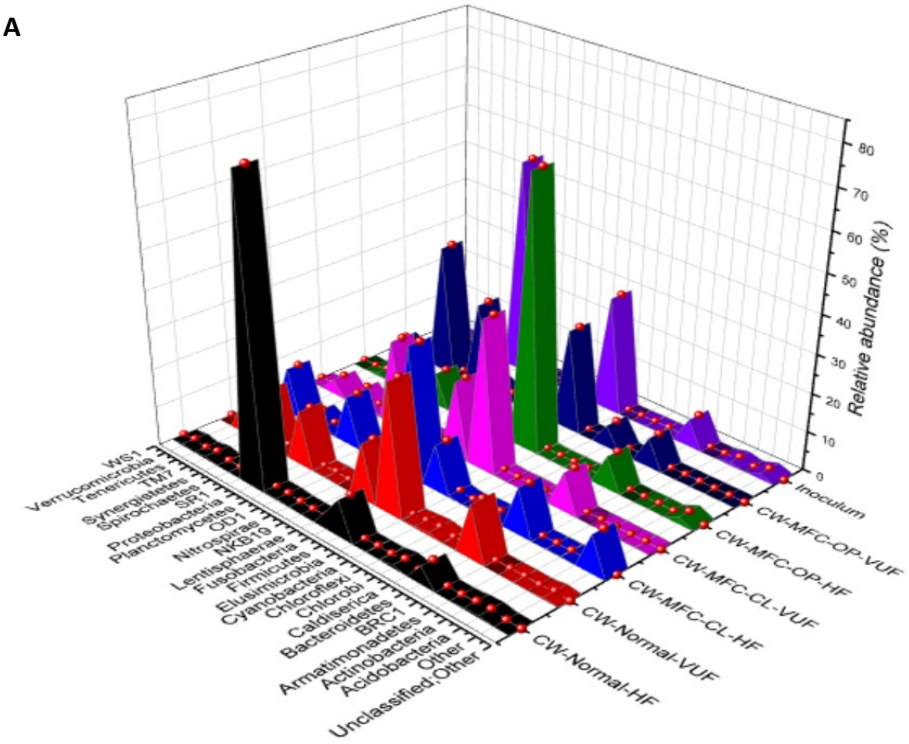

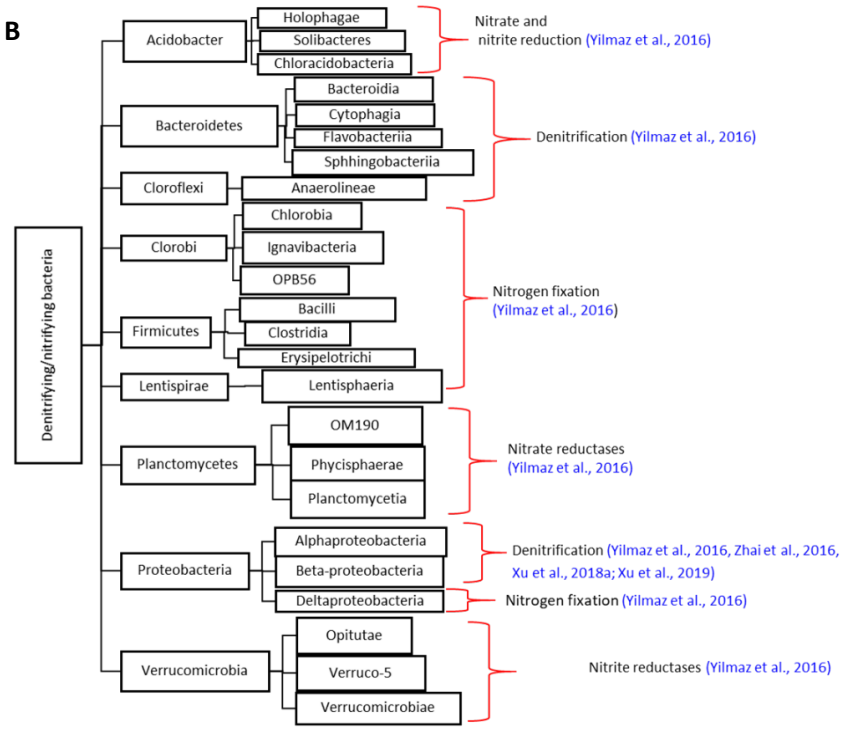

Figure 2-6. A) Microbiological analysis based on Phylum in: CW-MFC-OP, HF and VUF; CW-MFC-CL, HF and VUF; CW-Normal, HF and VUF; Sludge; B) Phylogenetic tree based on nitrifying and denitrifying species present in CW-MFC-CL.

Furthermore, the specific growth rate of biomass in the CW-Normal was calculated to be higher than in the other microcosms. The D and μ of CW-MFC-CL and CW-MFC-OP were found to be 0.066 ml/h and 1.066, respectively. On the other hand, in CW-Normal, D and μ were found to be 0.072 ml/h and 1.072, respectively. Moreover, even with a higher biomass generation, the removal efficiency was low in CW-Normal. Additionally, high biomass generation signifies that the chances for clogging in CW-Normal is higher than the CW-MFC. The positive characteristic of CW-MFC is that it had a low biomass generation rate while maintaining a high removal efficiency capacity, which also could be a solution to preventing clogging in CW.

2.4. Conclusions

A microbial fuel cell integrated into an HF-VUF-CW has been proven to be an efficient technology for organics and nitrogen removal from wastewater. The study also showed that a conductive material-based CW produced low biomass (low VSS) while retaining high-performance capabilities. This signifies that electro-active microbes are more efficient at TN removal than normal microbes, even at a low population number. Additionally, low biomass generation in MFC integrated CW could be a solution for preventing CW from clogging for a long-term operation. The most important finding was that anaerobic ammonium oxidation could be possible with a solid electron acceptor. The finding of this study indicates that there is a possibility of other pathways for anaerobic ammonium oxidation. Further understanding of anaerobic ammonium oxidation with a solid electron acceptor may also change the nitrogen cycle's existing understanding.

Acknowledgement

The authors would like to acknowledge the financial support received from the University of Tasmania, and the Grant received from the Tasmanian Community Fund (31Medium00171).

Chapter 3: Enhanced Chromium (VI) Treatment in Electroactive Constructed Wetlands: Influence of Conductive Material

Graphical abstract

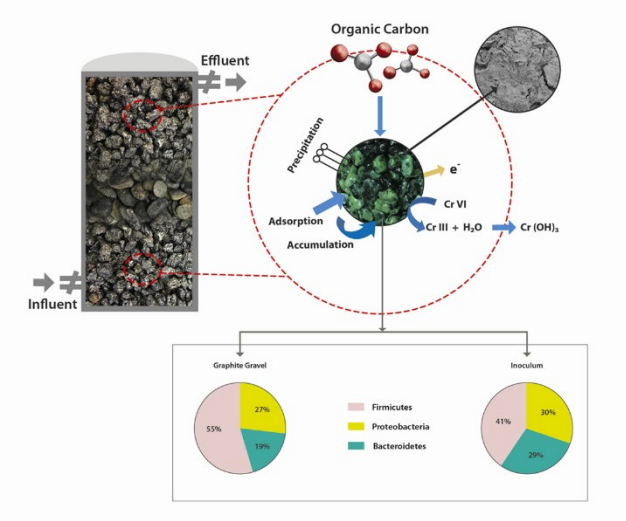

Abstract

A constructed wetland (CW) microcosm based on conductive graphite gravel was investigated for hexavalent chromium (Cr(VI)) treatment from synthetic wastewater. Its performance was evaluated and compared with a traditional gravel-based CW microcosm. The microcosms were operated at varying initial Cr(VI) concentrations (5-20 mg/L) and hydraulic retention times (HRT) (3-7.5 h). Near-complete treatment (99.9±0.06%) was achieved in the graphite-based microcosm throughout the experiment. The performance was consistently high throughout, with 42.9% improvement in Cr(VI) treatment compared to a traditional gravel microcosm. Scanning electron microscopy with energy-dispersive X-ray spectroscopy (SEM-EDX) analysis indicated that chromium was adsorbed to microbial biofilms. Moreover, microbial diversity profiling suggested that the microbial population in both microcosms differed in diversity and communities. The results suggest that the use of conductive materials in CW

significantly enhances the treatment of Cr(VI) and, more importantly, allows microbial activity even at high levels of Cr(VI) in the CW.

3.1. Introduction

Constructed wetlands (CWs) with an integrated microbial fuel cell (MFC) or another bio-electrochemical system such as microbial electrolysis cells (MEC) are gaining considerable attention owing to their enhanced wastewater treatment efficiency as well as their electricity generation potential [63, 71, 80]. The various forms of bioelectrochemical systems (BESs), such as MFCs [32] and MEC [71] have been successfully integrated into CWs and shown to enhance pollutant removal efficiency. So far, CW-MFC has been examined for different wastewater such as municipal wastewater [111], dye-containing wastewater [33, 76], and industrial wastewaters [80]. CW technologies are also used to treat (heavy) metal-contaminated wastewater as it involves multiple mechanisms of treatment such as adsorption on the substrate, biosorption and uptake by plants and microbes, co-precipitation, sedimentation, *etc*. In the CW, co-precipitation occurs mainly in the presence of other metals. For example, Maine, et al. [112] have reported that heavy metals such as Cr can be co-precipitated with iron in CW. On the other hand, according to Sheoran and Sheoran [113], sedimentation is another efficient process for the removal of heavy metals in natural or constructed wetlands. Prior to the sedimentation, precipitation and co-precipitation should occur to make larger flocs settle down in wetlands to remove the heavy metals from wastewater [113]. However, the main mechanism for the removal of heavy metals in CWs is believed to be adsorption on various surfaces. Therefore, as the available sorption sites become exhausted, a drop in the removal efficiency is often observed [114]. Industrial wastewater, in particular, may contain considerable amounts of heavy metals, *e.g.* mercury, cadmium, chromium, selenium and lead [115]. Chromium (Cr), owing to its wide range of industrial applications, is one of the major toxic heavy metals of concern [116]. The maximum permissible limits of total Cr in drinking water is established as

0.1 mg/l by the United States Environmental Protection Agency [117, 118]. When released into the waterways, it poses a threat to ecological entities and human health, including an elevated risk of stomach and skin tumours, liver and kidney damage. It has the potential to interfere with DNA transcription process [115, 119]. Cr(VI) is known to be a more hazardous form of Cr [120]; its toxicity persists in the environment due to its slow rate of conversion [115, 121]. There are some treatment technologies that convert toxic Cr(VI) to the less toxic Cr(III) form [122], as described in Reaction 1 [123]:

$$\mathrm{Cr_2O_7^{2-}} + 14\mathrm{H^+} \rightarrow 2Cr^{3+} + 7H_2O \qquad Reaction\ 1$$

Cr(III) is a less-toxic form of Cr, which is commonly found in groundwater. At low concentration, it is an essential element for metabolism in various organisms, including humans [115, 119]. Microbially catalysed reduction reactions are well known, and various aerobic and anaerobic bacteria have already been reported for the reduction of Cr(VI) to Cr(III) [124]. According to Wu, et al. [125], microbially catalysed reactions are a safe and sustainable process. Reaction 2 [122] and 3 [125] are examples of microbial mediated reduction reactions:

$$CrO_4^{2-} + 8H^+ + 3e^- \rightarrow Cr^{3+} + 4H_2O \qquad Reaction\ 2$$

$$CrO_7^{2-} + 6Fe^{2+} + 14H^+ \rightarrow 2Cr^{3+} + 6Fe^{3+} + 7H_2O \qquad Reaction\ 3$$

In recent years, a wide range of electroactive microbes (or electrogens) such as *Bacillus, Sulphovibro*, *Ochrobacterium, Pseudomonas* and other bacterial species have been reported for the reduction of metals [119]. Electro-active bacteria in the bioelectrochemical systems use conductive materials for electron transport and have been studied for metal removal and recovery at lab scale MFCs [126]. Conductive materials such as graphite gravels are low-cost materials that have been used previously for CW-MFCs in lab-scale studies for wastewater treatment and electricity generation [91, 127]. Graphite is a crystalline form of elemental carbon with a hexagonal structure of atom arrangement [32]. The graphite electrodes are

proven to be a conducive and stable conductive material. The CW-MFC study showed higher chemical oxygen demand (COD) removal than the traditional (normal gravel-based) CW. In the CW-MFC, the conductive material functioned as either an artificial electron acceptor in the anaerobic environment, which promoted high oxidation or an electron donor for reduction reactions [71, 91]. In the present study, a CW incorporated with conductive material was investigated without any external electrical connection. A CW incorporating a conductive material system is quite similar to any BES, except for the absence of an electrical connection. As mentioned earlier, CW-BES have received a lot of attention to enhance the pollutant treatment from wastewater. However, these systems have been mainly examined for open and closed circuit operation [75, 128]. Studies without an electrical circuit in snorkel mode (throughout filled with conductive materials) are minimal [128].

The present study aimed to investigate a conductive material-based CW performance for treating Cr(VI) containing wastewater. The conductive material used in the present study was graphite granules, which had 99.5% carbon, 0.5% ash, and volatile matter. Different Cr(VI) concentrations were investigated to evaluate a conductive material-based CW's performance compared to normal gravel-based (traditional) CW. Adsorption behaviour of conductive material (graphite granules) and regular river gravel were studied in order to establish their role in the treatment. Further, the microbial analysis was carried out to identify various microbial communities and potential mechanisms. Finally, solid-phase characterization by scanning electron microscopy (SEM) equipped with energy-dispersive X-ray spectroscopy (EDX) was also performed to decipher the role of surface processes in the treatment. This is the first study of conductive material-based CWs for Cr(VI) treatment to the best of our knowledge.

3.2. Materials and methods

3.2.1. Microcosm fabrication and installation

Two single-chamber vertical CWs were fabricated using polyvinyl chloride (PVC) rigid pipe (height - 34.5 cm; diameter - 9.0 cm). One of the microcosms was filled with graphite gravel (0.4 - 0.8 cm diameter) to the height of 32 cm (*Figure 3-1*). The second microcosm was filled only with normal river gravel to the same height (0.4 - 0.8 cm diameter). Both microcosms were fed with synthetic wastewater in continuous up-flow mode with the help of a peristaltic pump (Masterflex). The void volume of each of the microcosms was 550 ml. A reservoir bucket filled with synthetic wastewater was used for regular feeding of the microcosms. The reservoir bucket was washed thoroughly daily to remove any biomass growth on the walls and re-filled with freshly prepared synthetic wastewater. Effluents from the microcosms were collected into effluent buckets, provided separately for each microcosm.

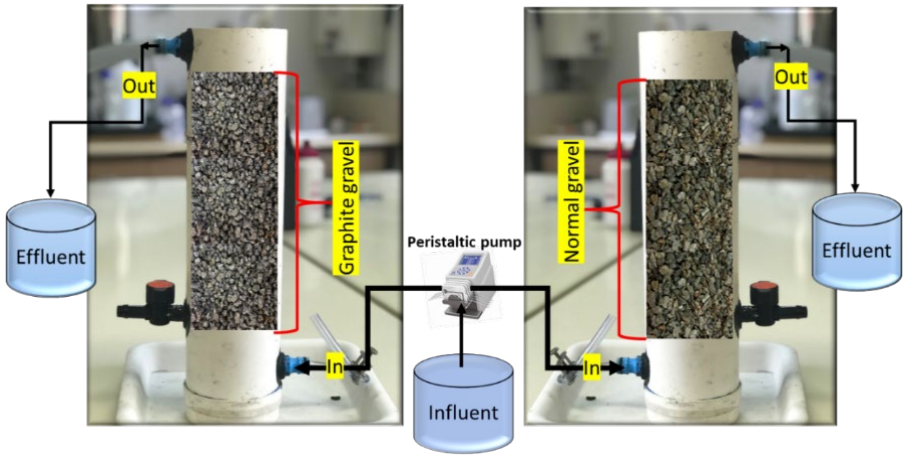

Figure 3-1. Schematic of the microcosm setup in the laboratory, graphite based (left) and normal gravel-based microcosms (right). Graphite gravel was used as a conductive material to enhance the microbe-based reactions, whereas normal gravel was used to replicate a traditional CW.

3.1.1. Wastewater preparation and inoculum source

The synthetic wastewater used in this study contained: 0.1 g/l CH_3COONa, 3.0 g/l $Na_3C_6H_5O_7$, 0.8 g/l NH_4Cl, 0.5 g/l KH_2PO_4, 1.0 g/l $Na_2HPO_4.7H_2O$, 0.1 g/l $FeSO_4.7H_2O$, 0.2 g/l $MgSO_4$, and 2 ml/l trace element solution. Trace element solution contained: 3.0 g/l $FeSO_4.7H_2O$, 0.01

g/l H_3BO_3, 0.01g/L $Na_2MoO_4.2H_2O$, 0.02g/l $MnSO_4.H_2O$, 0.01g/l $CuSO_4.5H_2O$, 0.01 g/l $ZnSO_4$, and 0.5 g/l ethylenediaminetetraacetic acid (EDTA). The wastewater was designed to mimic general wastewater and not to represent any specific industry type. The desired amount of $K_2Cr_2O_7$ as a Cr(VI) source was also added to the wastewater. Three different concentrations of Cr(VI) (5 mg/l, 10 mg/l, 20 mg/l) were studied. Both microcosms were inoculated with sludge inoculum (2.0% *v/v*) collected from a local sewage wastewater treatment plant in Launceston, Tasmania, Australia (TasWater).

3.1.2. Experimental design, operation, and analytical methods

After the addition of inoculum, the microcosms were acclimatized for a four-week period in recirculation mode with periodic changes of synthetic wastewater. The microcosms were then switched to the continuous flow mode at an HRT of 7.5 h. For the next 60 days, the feeding concentration of Cr(VI) was held at 5 mg/l at an HRT of 7.5 h, providing a Cr(VI) loading rate of 0.6 mg Cr(VI)/l/d. To estimate the treatment efficiency at higher concentration of Cr(VI), the concentration was then further increased to 10 mg/l (corresponding loading rate 1.0 mg Cr(VI)/l/d) for 30 days and further to 20 mg/l for the next 30 days at the same HRT (corresponding loading rate 2.0 mg Cr(VI)/l/d). Following this, the HRT of microcosms was decreased to 5 h and subsequently to 3 h at the Cr(VI) concentration of 20 mg/l, and the loading rate was 4.0 mg Cr(VI)/l/d and 6.0 mg Cr(VI)/l/d, respectively.

The total carbon concentration in the influent was kept constant throughout the experiment. However, with the change in HRT, the organic loading rate of the microcosms increased from 30 mg COD/l/d for the 7.5-h HRT, to 50 mg COD/l/d for 5-h HRT, and 80 mg COD/l/d for 3-h HRT, respectively. The effluent from both the microcosms was collected into a separate bucket, from which the sample was taken. The experiments were run in continuous mode. After achieving a steady-state, samples were collected in triplicate each week and all analysis was done in triplicate. Total organic carbon (TOC) was analysed with a Shimadzu TOC-L analyser

(Model TNM-L ROHS). COD was analysed using the spectrophotometric method as described in the APHA Standard Methods 5220 D [84]. The conversion of Cr(VI) to Cr(III) was also followed using the spectrophotometric method [129, 130]. Iron was analysed using the APHA spectrophotometric method [84]. Volatile suspended solids (VSS) were analysed using the method described in APHA Standard Methods at the beginning of the experiment (after 20 days of inoculation), in the middle (after 3 months) and at the end of the experiment (after 6 months). The VSS was done on the basis of free-floating biomass from the microcosms to avoid any disturbance in the microcosm setup during the experiment.

Regression analysis was performed using the Microsoft Excel 2016 data analysis tool to determine the significance of data and to statistically validate the trend of treatment efficiencies of Cr(VI) along with other parameters.

3.1.3. Microbial analysis

The initial microbial population was identified from the fresh inoculum collected from the wastewater treatment plant. At the end of the experiment, the second set of samples were taken from the top (at the height of 28 cm) and bottom (at 4 cm from the bottom) of both microcosms. A representative amount of gravel (~150.0 grams wet weight) and ~ 150.0 ml wastewater were taken from each microcosm and thoroughly vortexed before DNA extraction using a soil DNA kit (Favorgen, Fischer Biotech). Extracted DNA was then sent to the Australian Genome Research Facility (AGRF) for diversity profiling. The amplicon sequencing was performed with the target 27F-519R, reverse primer (GWATTACCGCGGCKGCTG) and forward primer (AGAGTTTGATCMTGGCTCAG).

3.1.4. Surface Morphology Analysis

The surface morphology, precipitate covering and microbial biofilm on the gravels were investigated with Scanning Electron Microscopy analysis (SEM), Hitachi SU-70 field emission

SEM. The elemental composition was determined by the attached Energy Dispersive X-ray (EDX) spectroscopy, Oxford AZtec XMax80 EDX system.

3.1.5. Adsorption study

For the adsorption properties analysis of both types of gravel, batch experiments were performed by adding 5.0 g of each gravel type (normal gravel and graphite gravel) into two separate glass beakers filled with 100 ml of 20 mg/l Cr(VI) containing the same wastewater at room temperature (21±3.0℃) with intermittent manual shaking. Samples for Cr(VI) analysis were collected from these solutions at time intervals of 0, 12, 24, 48 and 72 h. The percentage of Cr(VI) treatment was determined by comparing initial and final Cr(VI) concentrations, as shown in Equation 1:

$$\%\ of\ Cr(VI) removal = \frac{Initial\ concentration - Final\ concentration}{Initial\ concentration}\ X\ 100 \qquad \text{Eq. 1}$$

3.2. Results

3.2.1. Organic matter removal and Cr(VI) treatment

Figure 3-2 depicts TOC and COD removal in graphite-based and normal gravel-based CW microcosms. The TOC concentrations in the influent wastewater were found to range between 230±3.0 to 267±3.0 mg/l at an organic loading rate of 30 mg/COD/l/d. At this organic loading rate, the highest percentage of TOC removal observed in the graphite gravel-based microcosm was 64.7±2.8%, and in the normal gravel-based microcosm, it was 63.8±3.1%. At the same HRT, the highest percentage COD removal observed in the graphite gravel-based microcosm was 93.8±3.0%, and for the normal gravel-based microcosm, it was 86.9±4.0%. *Figure 3-2* shows that when the organic loading rate increased, the percentage removal of TOC and COD decreased. The TOC and COD removal was also found to be dependent on the loading rate of Cr(VI). *Table 3-1* shows the relationship between TOC and COD removal with a loading rate of Cr(VI) at different HRTs. The results show that the TOC and COD removal was dependent

on the Cr(VI) loading rate for both the microcosms. As shown in *Table 3-1*, even on the same organic loading rate with the change in Cr(VI) loading, the removal rate of TOC and COD has decreased subsequently. The difference in TOC and COD removal from the microcosm indicates that the removal was dependent on both autotrophic and heterotrophic types of bacteria. COD removal was always higher than TOC removal. Higher COD removal than TOC removal has also been reported by Srivastava, et al. [131]. Furthermore, various researchers have reported that Cr (VI) microbial treatment always remains low in carbon deficient conditions [125, 132, 133].

Srivastava, et al. [127] has estimated the carbon balance for their electroactive constructed wetlands. The microcosm setup was similar to this study and found that out of total removed carbon, 5.48 % of carbon was utilized in biomass synthesis, 0.34 % was used in electricity generation, while 33.99 % of carbon was used for other purposes such as conversion to gases, or mineralized etc.

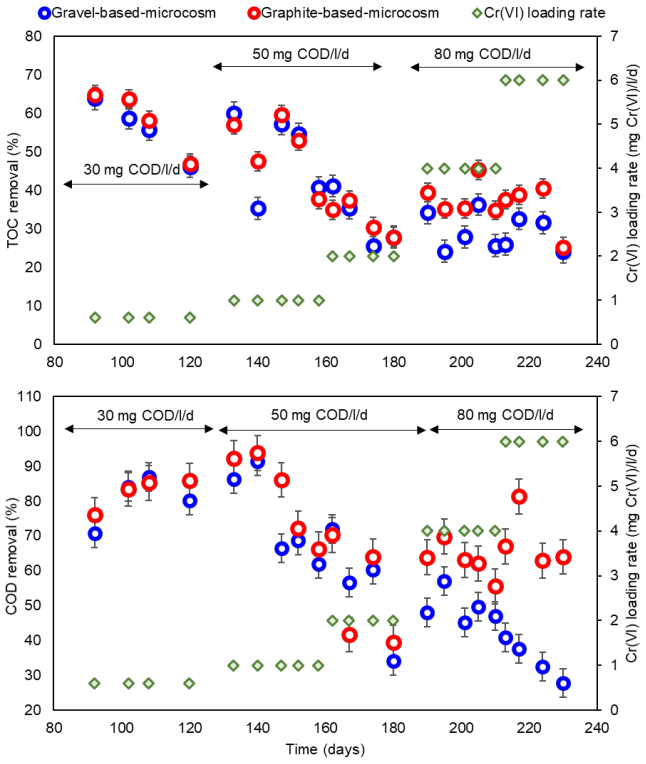

Figure 3-2. The percentage removal of TOC (top) and COD (bottom) in graphite-based and normal gravel-based microcosms.

Table 3-1. TOC and COD removal in graphite-based and normal gravel-based microcosms at various Cr(VI) loadings and HRTs.

Cr(VI) Concentration (mg/l)	HRT (h)	Organic loading rate (mg COD/l/d)	Cr(VI) loading rate (mg Cr(VI)/l/d)	Graphite-based-microcosm		Gravel-based-microcosm	
				COD (%)	TOC (%)	COD (%)	TOC (%)
5.0	7.5	30.0	0.6	83.5 - 92.3	46.1 - 64.7	83.5 - 86.3	46.1 - 63.8
10.0	7.5	30.0	1.0	72.2 - 93.8	57 - 59.6	68.7 - 91.4	57.2 - 60.0
20.0	7.5	30.0	2.0	64.1 - 66.1	37.4 - 52.9	60.3 - 62.0	35.4 - 54.6
20.0	5.0	50.0	4.0	39.4 - 63.1	30.4 - 35.3	34.2 - 45.2	24.1 - 25.6
20.0	3.0	80.0	6.0	62.1 - 62.9	25.2 - 35.3	27.8 - 49.7	24.0 - 27.9

Volatile suspended solids (VSS) were used in this study to estimate the suspended biomass present in the microcosms. The VSS result shows that when Cr(VI) loading rate was increased from 0.6 mg Cr(VI)/l/d to 2.0 mg Cr(VI)/l/d, VSS decreased from 4888 mg/l to 1350 mg/l (a 72% decrease) in the graphite gravel microcosm. Additionally, in a normal gravel-based microcosm it decreased from 20,894 mg/l to 2,690 mg/l (an 87% decrease). By the end of the experiment, the VSS values had increased to 12,893 mg/l in the graphite gravel-based microcosm and to 7,560 mg/l in the normal gravel-based microcosm. These results indicate that biomass concentration was less affected at an elevated Cr(VI) concentration in the graphite-based microcosm. Based on the general principle of MFC, an anode (conductive material) acts as an electron acceptor in the anaerobic zone. The conductive materials at the anode act as an electron acceptor that assists microbes in oxidising substrates/pollutants, which subsequently produces electrons and protons. These electrons are transferred from anaerobic

to the aerobic region (cathode), where they work as an electron donor and assist abiotic or microbial reduction reactions. The presence of conductive materials in two different redox conditions promotes oxidation and reduction. Therefore, any biocompatible conductive material should be able to perform redox reactions in bioelectrochemical systems. Based on a few published literatures on BES, conductive materials have a positive impact on the treatment efficiency of industrial wastewater treatment [134, 135].

Bhatnagar, et al. [136] have also reported graphite as a conductive material for electrochemical degradation of COD and colour from the textile industry wastewater. Furthermore, they have also mentioned that in recent years bioelectrochemical technologies are gaining a lot of attention for industrial wastewater treatment. Graphite is a crystalline form of carbon; in most of the bioelectrochemical systems, it has been used in the form of electrodes/conductive material. In most of the bioelectrochemical systems, it has been used either in the form of pure carbon or graphite; for example, Tandukar madan [133] has used graphite plates as an anode and cathode whereas Li, et al. [137] has used carbon felt as an anode and graphite as a cathode. Based on Bhatnagar, et al. [136], a significant perspective of using conductive materials in industrial wastewater eliminates the redox chemicals that further avoid subsequent treatment. Further, the use of such systems could run in a controlled manner with close control on reactions by providing applied potential or current.

Additionally, it can also provide on-site treatment, and due to the efficient reaction rate in the presence of conductive material, it would not require a large space. BES still has a few challenges, mainly because oxygen is used as a main oxidant at a cathode due to its abundance and high reduction potential. However, the oxygen reduction reaction (ORR) at carbon or graphite electrode (low-cost cathode material) is still one of the challenges due to its high over-potential and low kinetics [131].

Furthermore, the increase in Cr(VI) loading from 0.6 mg Cr(VI)/l/d to 6.0 mg Cr(VI)/l/d, had very different effects on the graphite gravel-based microcosm and the normal gravel-based microcosm. The graphite gravel-based microcosm showed continuous Cr(VI) treatment of 99.9±0.06% throughout the experiment, regardless of the Cr(VI) loading in the influent. On the other hand, while the percentage treatment of Cr(VI) was also observed to be up to 99.9±3.25% in the normal gravel-based microcosm up to a loading rate of 2.0 mg Cr(VI)/l/d, it decreased to 57±3.25% at a loading of 6.0 mg Cr(VI)/l/d (*Figure 3-3*). The treatment rate in both microcosms was compared statistically and the P-value was found to be less than 0.05. This suggests that the null hypothesis was true, and the microcosms were significantly different in terms of treatment with an increase in the Cr loading rate.

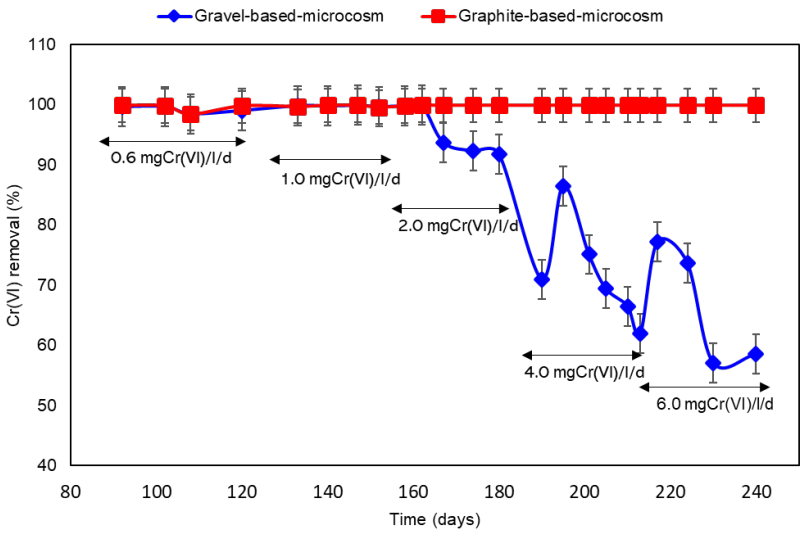

Figure 3-3. Cr(VI) treatment in graphite-based and normal gravel-based microcosms with time. These results clearly indicate that when Cr(VI) loading rate increased the treatment efficiency of normal gravel-based microcosm decreased. In contrast, graphite gravel-based microcosm performance was stable throughout the experimental period.

Cr(III) concentrations were also measured in effluent samples of both the microcosms. The concentration of Cr(III) varied with changing Cr(VI) concentration. With initial Cr(VI) concentrations of 5, 10 and 20 mg/l, the average Cr(III) concentration in the effluent of the graphite gravel microcosm varied between 0.02 ± 0.006 and 0.05 ± 0.006 mg/l, whereas in the

normal gravel-based microcosm, it varied between 0.04 ± 0.01 and 0.09 ± 0.01 mg/l with varied loading rate. The average measured concentration of Cr(III) in the effluent of the graphite-based and normal gravel-based microcosms is shown in *Figure 3-4*. The green precipitates observed in the microcosm was most likely due to the precipitation of $Cr(OH)_3$, which has low solubility in water at pH observed in this study. As pH fluctuation was not significant in the microcosms, the precipitation of $Cr(OH)_3$ was more likely, as solubility is low, between pH 6.5 ~11. The low solubility of Cr(III) in the water at neutral or basic pH might also be a reason for low concentration in the effluent wastewater. However, a thick layer of green precipitate was observed on the substrate in both graphite-based and normal gravel-based microcosms (*Figure 3-4*). Precipitates of equal mass were collected from two randomly picked gravels from each of the microcosms with the help of a spatula and were dissolved in 25ml of 0.3 M HCl. In *Figure 3-4* the light green (Left) solution was from graphite gravel-based microcosm precipitate and the darker green solution (Right) was from the precipitate of a normal gravel-based microcosm. After dissolution in HCl solution, Cr(VI) and Cr(III) levels were estimated. The estimated concentration of Cr(VI) was 0.1 mg/l and 0.5 mg/l in graphite and normal gravels-based microcosm, respectively, whereas Cr(III) concentration was 0.04 mg/l in graphite-based and 0.44 mg/l in normal gravel-based microcosm. These are only indicative results as a precise measurement of the amount of total precipitate was difficult. SEM-EDX also confirmed the presence of Cr on the gravels (please refer to section 3.4 below).

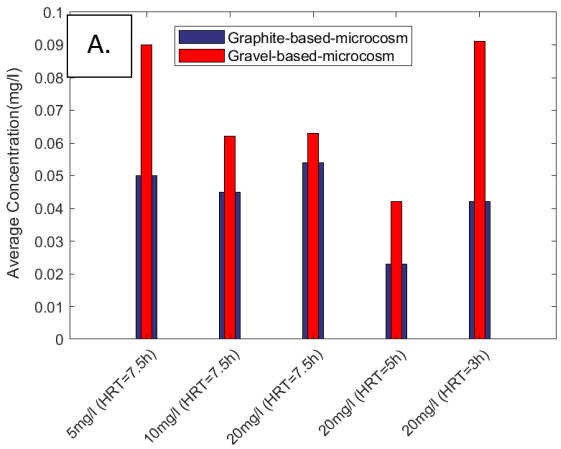

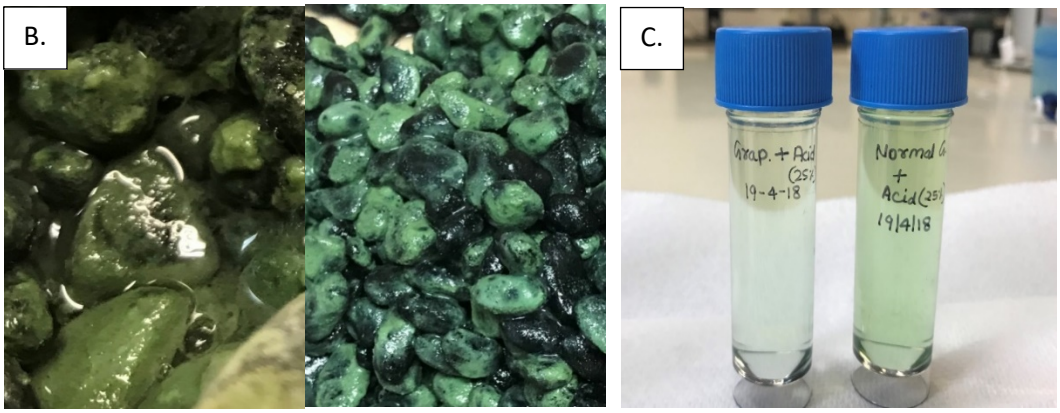

Figure 3-4. A) Average Cr(III) concentration in influent and effluent samples, B) Green precipitates on the gravels, C) The dissolved green precipitates from the Graphite gravel (Left), and Normal gravel (Right).

pH and dissolved oxygen (DO) values in both microcosms were also measured in the surface and bottom zones of the microcosms throughout the experimental period. The measured pH at the surface of the graphite gravel microcosm was in the range of 6.8 to 7.1, whereas at the bottom, it was 6.5 to 6.9. In the normal gravel-based microcosm, the pH was 6.8 to 7.5 at the surface and 6.6 to 6.9 at the bottom. No significant difference was observed in the pH of the microcosms, and it remained close to neutral in both microcosms. DO values in the surface and bottom zones of the microcosms were also measured. These were found to be 0.28 to 0.74 mg/l and 0.14 to 1.1 mg/l, at the surface of the graphite gravel and normal gravel-based microcosms, respectively, whereas DO values in the bottom zones were 0 to 0.65 mg/l and 0 to 0.89 mg/l, in graphite gravel and normal gravel-based microcosms respectively (*Table 3-2*).

Table 3-2. DO profile of graphite-based and normal gravel-based microcosms at the surface and the bottom.

Time (days)	Graphite-based-microcosm (mg/l)		Gravel-based-microcosm (mg/l)	
	Surface	Bottom	Surface	Bottom
92	0.28	0.00	0.14	0.00
108	0.43	0.28	0.62	0.53
133	0.42	0.25	0.58	0.28

174	0.62	0.48	0.69	0.58
195	0.74	0.65	1.11	0.89
217	0.68	0.53	0.70	0.60
240	0.66	0.63	1.16	0.86

3.2.2. Influence of other chemical constituents

The graphite and normal gravels and microcosms were analysed to identify the influence of other dissolved or undissolved elements/compounds in the system that may have influenced the Cr(VI) treatment. As $FeSO_4$ was a component of the wastewater, dissolved Fe concentrations were measured in the effluent to determine if it had any effect on Cr(VI) treatment. The concentration of Fe measured in wastewater was ~ 1.0 g/l, with the theoretically calculated value of 0.8 g/l. In the effluent of graphite gravel-based microcosm, the average Fe concentration was found to be 0.6 g/l. In the normal gravel-based microcosm, the average Fe concentration was found to be 0.5 g/l. The chemical composition of both types of unused gravel was determined using SEM-EDX after grinding the gravels into a powder and coating them with a thin platinum layer (*Figure 3-5*, top). From the EDX analysis, the graphite gravels are largely carbon, whereas normal gravels contained a variety of elements. The various elements present on the normal gravel surface could also play a role in Cr(VI) treatment, particularly the Fe and Al phases, supported by higher Si, Mg and Ca ions on the surface. These ions on the surface can influence the electric double layer on the hydrated surface and consequently the sorption behaviour (*Figure 3-5*, bottom). The presence of various ionic species and trace metals in wastewater might have played a role in the reaction mechanism of different Cr treatment systems. The ionic species in contaminated water would not only impart ionic strength that would also affect the sorption/adsorption processes of the systems. Further, ionic species can also exert control on the microbial population and by virtue of that the dominant microbial processes that govern the redox cycling *e.g.,* sulphate reduction where sulphate is dominant

and nitrate reduction where nitrate is dominant. In order to develop a basic understanding of the initial concept, the present study tried to make this experimental setup simple to understand the importance of these ions and follow up studies will include these complexities.

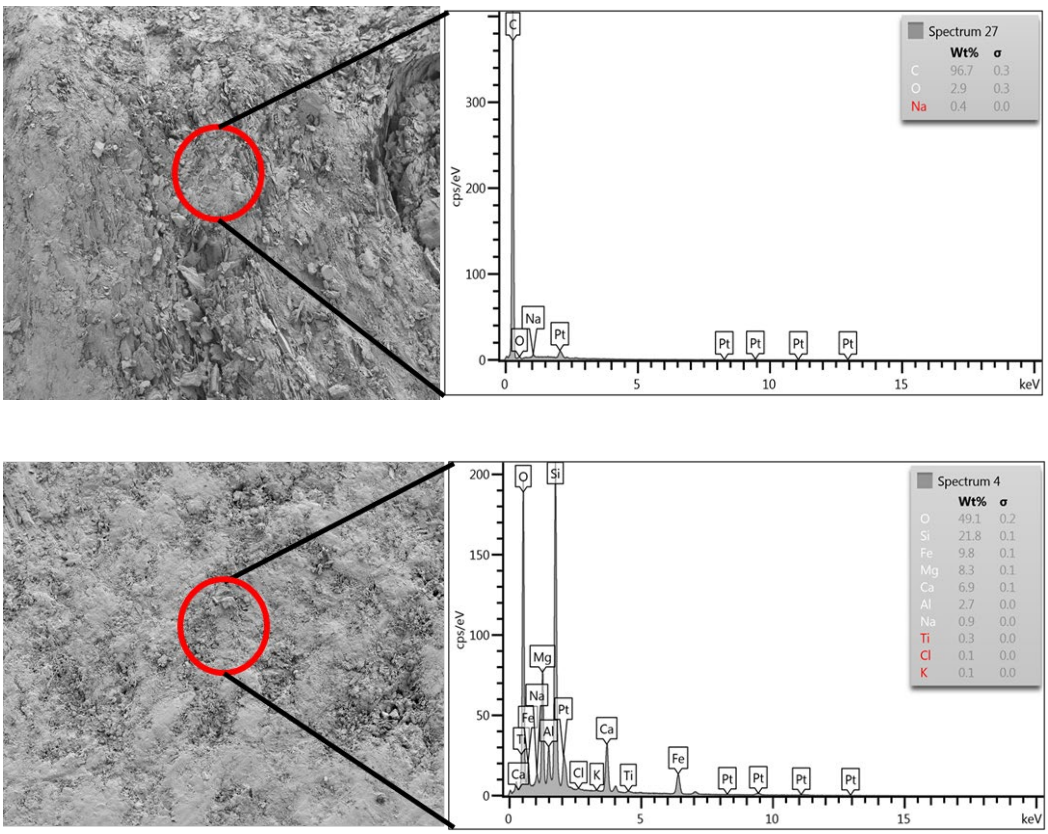

Figure 3-5. SEM-EDX analysis of graphite gravel (above) and normal gravel (below).

3.2.3. Microbial diversity analysis

The microbial diversity profiling was carried out to determine the microbial diversity in the initial inoculum and both microcosms at the end of the experiment. *Figure 3-6* shows the microbial diversity based on the Phylum and Class of both microcosms in compassion with the inoculum. The results showed significant differences in the number and diversity of microbes in the initial inoculum and the microbial population in the graphite gravel-based microcosm. Furthermore, the relative abundance of microbes increased in the graphite gravel-based microcosm compared to the normal gravel-based microcosm and the initially inoculated sludge. The dominant microbial species at the bottom of the graphite gravel microcosm was

from the Phylum *Firmicutes* and class *Bacilli* (60.5%), while at the surface, this made up 36.6% of species present.

On the other hand, this species' normal gravel-based microcosm was 10.4% at the bottom and 20.5% at the surface. The second most abundant species were from the Phylum *Proteobacteria,* primarily from class *Deltaproteobacteria.* The role of microbes from Phylum *Firmicutes* and *Proteobacteria* for Cr(VI) treatment has also been reported in other literature [138]. The third most dominant microbes were from the Phylum *Bacteroidetes,* representing 9.3% of the microbial species identified at the bottom of the graphite gravel-based microcosm and 6.2% at the surface. They represented 6.6% of the species at the bottom and 2.5% at the surface in the normal gravel-based microcosm. In the inoculum, it was 6.9%. A similar range and composition of phyla have also been reported in other studies on CW-BES [75, 139]. From the results reported in the current work, it is reasonable to state that the microbial population was always higher in the graphite gravel-based microcosm than the normal gravel-based microcosm inoculum. Moreover, many additional species were found in the graphite gravel-based microcosm including those from the phyla *Armatimonadete (2%), Elusimicrobia (4%), NKB19 (1%), OD1 (3%), Planctomycetes (8%), WS1 (1%)* and *WWE1 (2%).* All of these were absent in the initial inoculum. *Agrobacterium* from the class *Proteobacteria* was only found in the graphite-based microcosm. Other bacteria from the class *Bacilli* and *Clostridia* have also been reported for Cr(VI) reduction [133, 140, 141]. Furthermore, Chardin, et al. [141] have compared *D. vulgaris* and *De. norvegicum*, for Cr(VI) treatment and found that, *D. vulgaris* was more sensitive to the higher Cr(VI) concentration, whereas *De. norvegicum* were more reductant for the adsorption of Cr(VI) on its surface. On the other hand, Tandukar madan [133] have reported that, though bioelectrochemical systems can efficiently reduce Cr(VI), the mixed consortium works better than the single microbial consortium. Moreover, Chen and Hao [140] have also reported that biological reduction is a better option for Cr(VI) reduction to Cr(III),

Cr(VI) reduces to Cr(III) by co-precipitation with some other biosolids. They have also highlighted the factors that affect the microbial Cr(VI) reduction, including biomass concentration, initial Cr(VI) level, carbon source, pH and temperature, oxidation-reduction potential, other oxyanions, and metal cations.

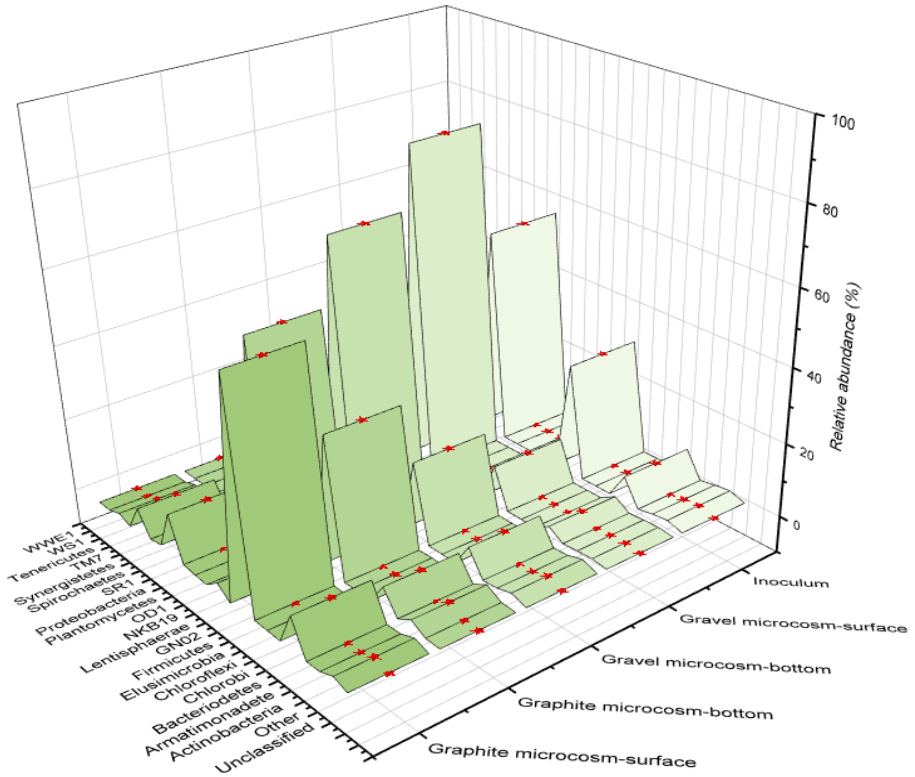

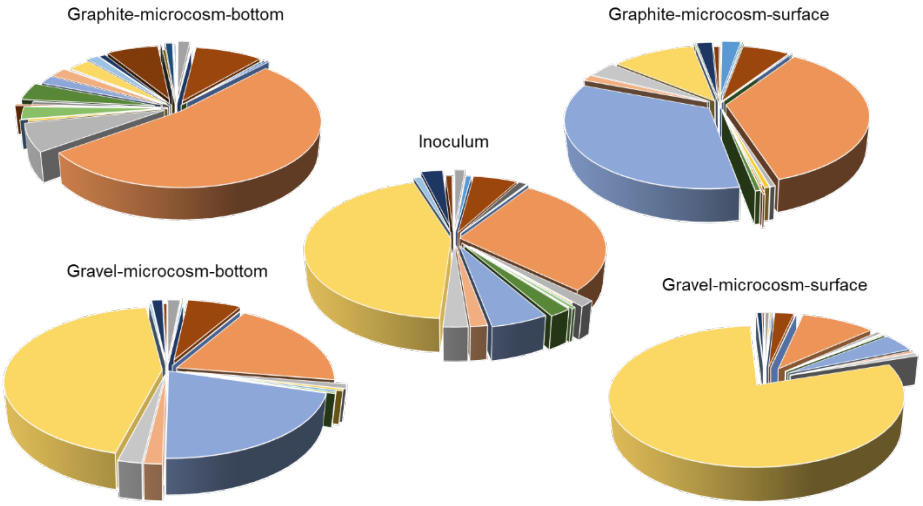

Figure 3-6. Microbial diversity profiling of the initial inoculum, surface and bottom of graphite and gravel-based microcosm. [Phylum-based classification (top panel), Class-based classification (bottom)], Phylum results show the relative abundance of microbes in both types of microcosms, Class result shows the diversification of microbes which was higher in graphite gravel microcosm than in the normal gravel microcosm and the initial inoculum.

3.2.4. Surface morphology and elemental composition study

Scanning electron microscopy was used to study graphite and normal gravels' surface morphology after the biofilm and green precipitate appeared. This was compared with unused normal gravels and graphite gravels. The SEM results of the used gravels show that the normal gravels were covered with a thick powdery substance with no clear bacterial attachment. However, at an elevated concentration of Cr(VI) in wastewater, biomass concentration was less affected in the graphite-based microcosm, which is also evident from VSS concentration in the effluent. This may be due to the fact that at our experimental pH values were very close to the point of zero charge (PZC) values of graphite and hence created weaker surface charges at these pH values. The other reason could be that the level of chromium on the graphite gravels was so high that it was killing the biofilm-forming micro-organisms. The assumption here is that in graphite-based microcosm, the process was driven by suspended growth of microbes leading to indirect transfer of electrons. EDX analysis was used to confirm that Cr, along with other elemental constituents, was bound to the biofilm of the normal gravel (*Figure 3-7*).

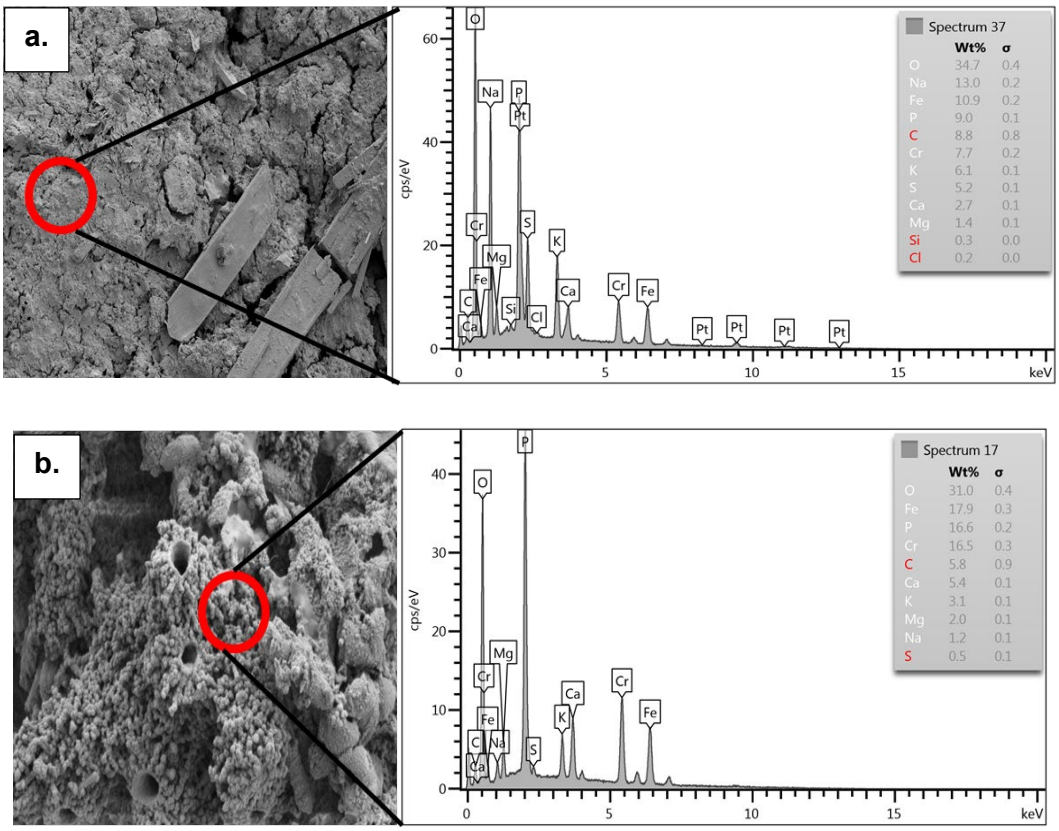

Figure 3-7. SEM imaging of gravels coated with biofilm / green precipitate. Graphite (a), with EDX analysis of graphite surface, b., with EDX analysis of normal gravel. Figure a. shows precipitation on the graphite gravels, along with the elemental composition of the precipitate, including the presence of Cr. Similarly, Figure b shows biofilm deposition on the normal gravel along with elemental composition and Cr on the surface of the biofilm.

3.2.5. Adsorption study with gravels

The adsorption properties of both gravel types were tested with different contact times using the same wastewater as used in the experiment. The pH of initial Cr(VI) containing wastewater (6.7) did not change significantly after adding graphite gravel (6.8) or normal gravel (6.8). However, a slight pH increase was observed after 72 h when the pH values were 7.0 for graphite gravels and 6.9 for normal gravels. The percentage treatment for graphite and normal gravels after 12 h were 3.3% and 2.8%, respectively and after 24 h they were 18.8%, 7.6%, respectively. Subsequently, both gravels' adsorption capability decreased with time and adsorption of Cr(VI) on both types of gravels after 72 h was not found to be significant, 0.6%

in graphite gravels and 0.9% in normal gravels. In the further cycle of adsorption study used graphite and normal gravels; there was negligible adsorption of Cr(VI) recorded.

3.3. Discussion

The present study's main aim was to investigate Cr(VI) treatment in a graphite-based microcosm and its comparison with the normal gravel-based microcosm. The results confirm the higher treatment of Cr(VI) in graphite-based microcosms than the normal gravel-based microcosm. The treatment of Cr(VI) in the graphite gravel-based microcosm was almost complete (99.9±0.06%) throughout the experiment. In contrast, the normal gravel-based microcosm treatment efficiency decreased to 57±3.25% with an increase in Cr(VI) loading rate. Furthermore, the maximum TOC and COD removal in a graphite gravel-based microcosm was higher than the normal gravel-based microcosm for each loading rate. The increase in Cr(VI) loading can cause toxicity to the microbes, which could also be a potential reason for the decrement in the removal of COD and TOC from the microcosm. Nevertheless, the TOC and COD removal efficiency of the graphite gravel-based microcosm was still higher than the normal gravel-based microcosm. This observation suggests that even in a potentially toxic environment, higher performance is due to the presence of conductive material (graphite gravels) in the microcosm. The presence of conductive materials accommodates the growth of microbes that was efficient enough to oxidize the organics. This evidently high microbes performance was essentially related to the electron transfer mechanism in the conductive bed as previously observed [128]. However, it can be observed that the COD loading rate in the present study was low in comparison to other CW-MFCs studies such as, Wang, et al. [142] has used 75.3 g COD/m^3/d^{-1} and has achieved 27.4 ± 3.5 to 57.4 ± 4.6% of COD removal. Similarly, Liu, et al. [94] has used 100 g/m^2/d of COD and has achieved up to 79.65% of removal, Doherty, et al. [143] has used 240 g/m^2/d COD and achieved removal of 79 to 81%. Whereas in the present study, COD loading rate was 30 mg COD/l/d, 50 mg COD/l/d, 80 mg

COD/l/d and has achieved up to 64.1 to 92.3%, 39.4 to 63.1%, 62.1 to 62.9% COD removal. The reason behind the low COD loading rate in the present study was to observe the role of conductive material Instead, high COD loading rate Cr(VI) would have been reduced with the influence of organics. Further, the adsorption studies of both gravels indicate that the gravels on their own did not contribute significantly to the Cr(VI) treatment over the longer term. It is also important to note that even though graphite gravels had a lower adsorption capacity than normal gravels, greater Cr treatment was achieved in a graphite gravel-based microcosm than a normal gravel-based microcosm. These results indicate that the graphite-based system was more dependent on mechanisms other than simple adsorption for Cr(VI) treatment. Adsorption of Cr(VI) onto gravels was only effective in the initial few hours of the experiment. After that, there was almost negligible adsorption as all adsorption sites were saturated. This observation strongly supports our assumption that the main Cr(VI) treatment mechanism was likely to be microbially mediated in both microcosms, either by adsorption or microbial uptake. Microbial conversion of Cr(VI) to Cr(III) may also be responsible in Cr(VI) treatment but to a lesser extent. The pH range also boosts the conversion of Cr(VI) to Cr(III), as, according to Xafenias, et al. [122], a pH between 6 and 9 allows the dominance of Cr(III). Xafenias, et al. [122] also reported the reduction of Cr(VI) to Cr(III) at neutral to slightly alkaline pH in dual-chamber electrochemical reactors with graphite felt electrodes. However, in the present study, Cr(III) was mainly in the precipitate form instead of a dissolved form. In other MFC studies Kim, et al. [144] studied bipolar membrane MFC for treating Cr(VI) wastewater and achieved 100% of Cr(VI) removal with achieved power density of 150 mW/m^2.

Regardless, the graphite gravel-based microcosm was more efficient than the normal gravel-based microcosm for Cr(VI) treatment as the conductive material played a role in the microbial assisted electron exchange/transfer. Electron exchange with electrodes in the anaerobic region is mainly ruled by three different mechanisms: (i) by electron shuttle, (ii) by direct physical

contact with the electrode, and (iii) through the pili, which develop on the cell wall of microbes (*Figure 3-8*) [145-147]. The electrode dependent anaerobic electron transfer is either dependent on living microorganisms or isolated enzymes [147]. The isolated enzymes play a critical role in transferring electrons across the membrane of a microbial cell. Several enzymes play a crucial role in the electron transfer mechanism. For example, Cytochrome P450, is a well-known enzymes for electron transfer mechanism [148] and Glucose oxidase (GOx) is an efficient redox enzyme [149].

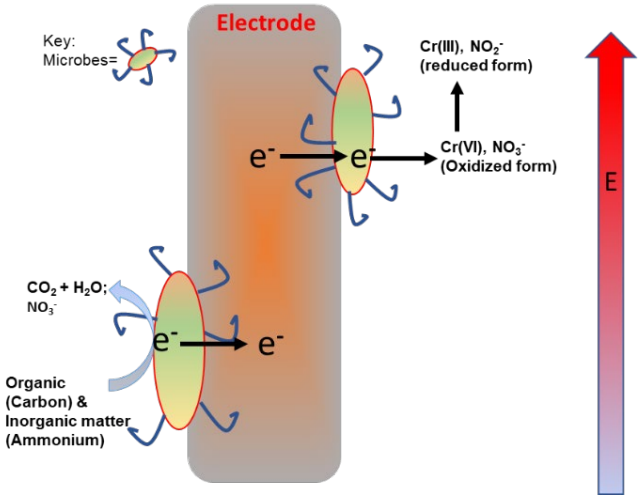

Figure 3-8. Scheme of the potential mechanisms of microbial electron transfer/exchange with electrode (conductive material).

In the present study, it was assumed that, by using these three-electron exchange/transfer mechanisms, the microbes were able to perform these functions more effectively than microbes in a normal gravel-based microcosm. Additionally, the presence of conductive materials may have assisted the microbes in the oxidation or reduction of metal ions and organic matter, as indicated by the higher microbial population in graphite-based microcosms. The microbial diversity profiling and VSS also indicate the presence of higher numbers of microbes on the graphite gravel microcosm, even at a high loading of Cr(VI). Tang, et al. [150] reported that due to biological activity, more than 90% of Cr(VI) was removed from solutions of 1-100 mg/l Cr(VI). The results of microbial diversity studies in our experiments are consistent with the

study conducted by Corbella, et al. [151];Sierra [139] using a graphite-based CW, although that study did not consider Cr(VI). Furthermore, microbe numbers were found to be high in the bottom region of a graphite gravel-based microcosm compared to a normal gravel-based microcosm. This also signifies that even in a potentially toxic environment (with high Cr loading), conductive material supported higher biomass than the normal non-conductive gravel-based microcosm. Though high levels of Cr(VI) cause toxicity to microbes [115], the treatment efficiency in the present study remained high in the conductive gravel-based microcosm, even at high loading. This is most likely due to the graphite acting as an artificial electron acceptor in the anaerobic zone. This, in turn, may have increased the amount of microbial oxidation of the substrate to extract more energy, making their survival possible in the presence of a higher Cr(VI) loading. Moreover, the presence of microbes from genus *Desulfobulbus, Desulfovibrio, Geobacter* which comes under *Deltaproteobacteria* was most likely. In anaerobic environments, *Deltaproteobacteria* are the primary microbes that breakdown fatty acids to low energy molecules such as acetate and can compete with methanogenic bacteria. The presence of *Desulfobulbus* (2% in graphite-based and 1% in normal gravel-based microcosms, though absent in the inoculum) is relevant in the present study as it has the capacity to produce electrically conductive filaments [139, 152, 153]. In addition, the participation of *Desulfovibrio* in metal treatment is also reported by Heidelberg, et al. [154], Pradhan, et al. [155]. The other microbes from genus *Agrobacterium* are also capable of adsorbing Cr(VI) concentration of more than 100 mg/l from an aqueous solution in a 24h period [156]. The other bacterial species able to promote Cr(VI) reduction to Cr(III) could be from the phylum Firmicutes, Proteobacteria, such as Pseudomonas, Shewanella, and *Enterobacter,* which were present in both the microcosms. These microbes' presence indicates that the treatment was mainly dominated by these microbes more efficiently by using a conductive material.

Based on all the arguments above, it can be reasonably concluded that the dominant Cr(VI) treatment mechanism in a graphite gravel-based microcosm was microbial activity assisted by improved electron transfer made possible by the presence of conductive support. A graphite-based microcosm has a more remarkable ability to tolerate higher levels of Cr(VI) compared to a normal gavel-based microcosm. The conductive material directly influences the microbial diversity and total biomass of a microcosm. The presence of Cr in the precipitate was also established with EDX analysis. Furthermore, SEM-EDX analysis also indicates the presence of Cr on the microbial biofilm, which means that some of the Cr were absorbed on the surface of the biofilm. A similar result was previously reported by Tandukar madan [133].

3.4. Conclusions

This study demonstrated the role of conductive material in the treatment of Cr(VI) in anaerobic conditions, and a comparison was made with a normal gravel-based microcosm. Even at a higher loading of Cr(VI), which could affect micro-organisms' growth, the conductive gravel-based microcosm performed more efficiently than the normal gravel-based microcosm. The treatment of Cr(VI) in a graphite gravel-based microcosm was constant at 99.9% throughout the experiment (over almost 240 days), whereas in a normal gravel-based microcosm Cr(VI) treatment decreased to 57% under the same conditions. The results also indicate that microbes can perform well on a conductive material even in toxic environments (such as a high Cr(VI) level). It is concluded that conductive materials directly influence microbial diversity and total microbial biomass in the microcosm. Conclusively, this study established that the conductive material-based CW could be an efficient technology for the treatment of a toxic metal even at a high loading rate.

Acknowledgment

The authors would like to acknowledge the financial support received from the University of Tasmania and a Grant received from the Tasmanian Community Fund (31Medium00171). The authors would also like to acknowledge facilities provided by the Central Science Laboratory (CSL), the University of Tasmania for analysing the samples.

Chapter 4: Interrelation between sulphur and conductive materials and its impact on ammonium and organic pollutants removal in electroactive wetlands

Graphical Abstract

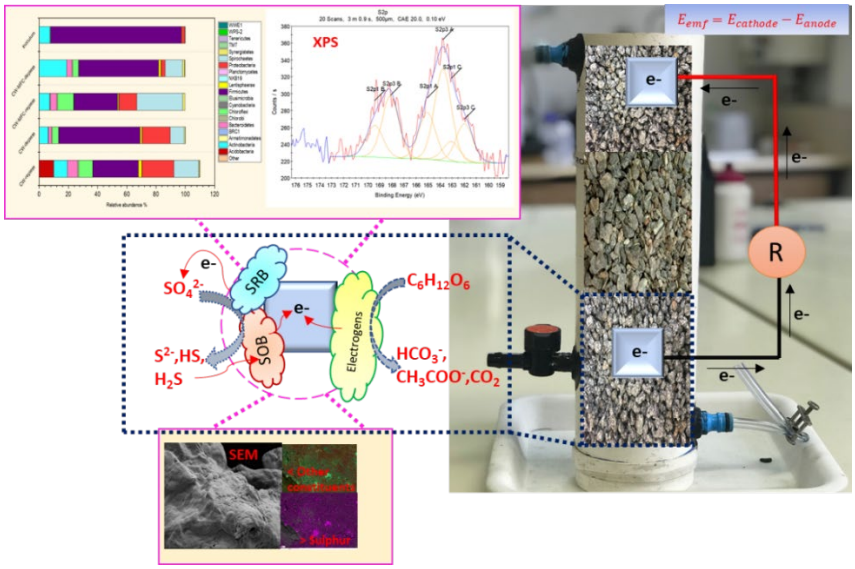

Abstract

This investigation is the first of its kind to evaluate the interrelation of sulphate (SO_4^{2-}) with conductive materials as well as their individual and synergetic effects on the removal of ammonium and organic pollutants in the constructed wetland (CW) microbial fuel cell (MFC). The role of MFC components in CW was investigated to treat the sulphate containing wastewater under a long-term operation without any toxicity build-up in the system. A comparative study was also performed between CW-MFC and CW, where sulphate containing wastewater (*S-replete*) and without sulphate wastewater (*S-deplete*) was assessed. The *S-replete* showed high NH_4^+ removal than the *S-deplete,* and the requesnce of removal was: *CW-MFC-replete>CW-MFC-deplete>CW-replete>CW-deplete.* The chemical oxygen demand

(COD) removal was high in case of *CW-MFC-replete,* and the sequence of removal was *CW-MFC-replete>CW-MFC-deplete>CW-deplete>CW-replete.* X-ray photon spectroscopic study indicates 0.84% sulphur accumulation in *CW-MFC-replete* and 2.49% in *CW-replete,* indicating high sulphur precipitation in CW without the MFC component. The high relative abundance of class *Deltaproteobacteria (7.3%)* in *CW-MFC-replete* along with increased microbial diversity (Shannon index=3.5) that rationalize the symbiosis of sulphate reducing/oxidizing microbes and its impact on the treatment performance and electrochemical activity.

4.1. Introduction

Various wastewaters including several industries such as edible oil processing, tannery, food processing, pulp and paper that can frequently contain a high level of sulphate which can reduce to form excessive hydrogen sulphide (H_2S) or HS^- [114]. Excess production of H_2S or HS^- adversely affects the aquatic environment due to its toxicity. The constructed wetland (CW) was designed to treat wastewaters using natural processes to recover the water quality [114]. The use of CW for wastewater treatment is due to its capacity as a cost-effective treatment process for long-term operation and involved natural eco-friendly processes. Despite its potential to remove sulphate-contaminated wastewater, highly contaminated precipitate deposition due to reduced sulphur compounds over the longer operation time are considered hazardous. Moreover, reduced sulphur compounds, on the other hand, reduce sulphate (SO_4^{2-}) and convert into the precipitate form of sulphur intervenes the sulphur cycle of CW [157] and impact microbiology and treatment performance. Whereas, sulphur cycle is intertwined with other elements present in wastewater, such as carbon and nitrogen [158]. The presence of sulphate (SO_4^{2-}) can act as an electron acceptor for pollutants oxidation. Its reduced sulphide (S^{2-}) acts as an electron donor, which further requires an electron acceptor for the conversion into its oxidized form. In CW due to limited electron acceptor, oxidation of S^{2-} may not occur,

which can start to accumulate. Subsequent reduction and deposition of sulphur compounds in CW could thus hinder the treatment performance as well as the microbiology of CW.

In the past decade, CW has been integrated with microbial fuel cell (MFC) to advance its treatment performance and overcome the challenges of electron acceptors in CW [32, 33, 159]. However, the integration of CW-MFC has emerged as the promising technology for enhanced wastewater treatment with an added benefit of electricity generation and other resource recovery possibilities. Enhanced treatment efficiency in CW-MFC depends on the electron transfer rate from a less oxygenated to a more oxygenated region [160]. The electroactive microbes present in less oxygenated regions (anaerobic) oxidize the pollutants and employ the conductive materials/electrodes (anode) as an artificial electron acceptor [160-162]. The generated electron in anaerobic regions subsequently flows via an electric wire from anode to oxygenated regions (where the cathode is placed). The flow of electrons depends on the redox gradient of the anode, and the cathode, due to electron transfer, electricity generation occurs [80, 128, 163, 164]. Since the time CW-MFC was introduced (past 10 years) a lot of technological progress has been taken place. However, still the technology is in its infancy stage and several research areas such as electron recovery, treatment of different pollutants needs to be explored [165, 166]. González, et al. [167] has recently studied contaminant removal efficiency and to increase electrical efficiency in CW-MFC; the result indicated 18% higher organic removal in closed-circuit mode than the open-circuit mode, and the maximum power density achieved was 8.6 mW m^{-2}.

Several MFCs or bioelectrochemical systems have reported a direct or indirect reduction of inorganic electron acceptors such as SO_4^{2-} by the exo-electron transfer (EET) processes [168-170]. As mentioned before, microbes in bioelectrochemical systems generates electrons and protons. These electrons and protons move towards terminal electron acceptors through series of redox carriers/components and EET [168]. The oxidation and reduction of sulphur

compounds in bioelectrochemical systems act as intermediate electron acceptors and donors and finally pass the electrons to the electrode through several EET cascades [171]. In bioelectrochemical systems, SO_4^{2-} is reduced to elemental sulphur at the anode by sulphate reducing bacteria (SRB), which further oxidizes to sulphur oxides by the sulphate oxidizing bacteria (SOB) either bioelectrochemically or electrochemically. The oxidation/reduction processes of sulphur compounds can thus be interlinked with the other treatment processes such as nitrogen removal. Ge, et al. [172] has reported that pyrite based CW-MFC enhanced phosphorus and nitrogen removal with stable pH and low sulphate concentration in effluents.

In previous studies on CW-MFC, anaerobic organics and NH_4^+ oxidation has been reported where conductive material acts as an electron acceptor [65, 69, 131]. However, the presence of sulphur is very common in wastewater and its redox behaviour could influence organics and NH_4^+ oxidation in CW-MFC. Additionally, on the longer operation of CW-MFC, accumulated sulphur compounds can also influence treatment performance of organics and NH_4^+. Tinterrelation between sulphur with anaerobic ammonium and other organic pollutants removal in the presence of conductive material has not been reported in CW-MFC. The accumulation of sulphur compounds in CW can be minimized by redox coupling in the presence of conductive material, and the redox coupling of sulphur compounds can also play a significant role in treatment processes involved in the system. Therefore, the main objective of this study is to explore further the interrelation between sulphate and conductive materials for reducing precipitates build-up and its impact on the removal of ammonium and organic pollutants in CW-MFC and to compare this process with the normal CW.

4.2. Materials and method

4.2.1. Microcosm configurations

Three laboratory-scale CW microcosms were fabricated using a polyvinyl chloride (PVC) pipe of 320 mm x 85 mm (Length x Diameter) dimension. Two of the three CW microcosms were

integrated with an MFC. Both the MFC integrated CW microcosms were filled with granular graphite gravel (diameter 4-5 mm) to form the anode and cathode. The layer of graphite gravels from the bottom of the microcosm had a height of 105 mm to form the anode, which was overlayed by the normal gravels (garden pebbles) of height 150 mm graphite gravel of 60 mm to form the cathode. At the anode and cathode, carbon felt was used as a charge collector and charge dispenser, respectively. The dimension of the charge collector used at the anode was 102 x 73 mm (length x width), whereas at the cathode, the dimension was 100 x 55 mm (Length x Width). The smaller dimension of the cathode was due to the availability of terminal electron acceptors such as oxygen at the upper surface. The charge collector at the anode portion was placed at the height of 95 mm from the bottom, while at the cathode one-quarter of the collector was in the air to avail sufficient atmospheric oxygen as a terminal electron acceptor. The charge collector and dispenser were connected with a titanium wire of a diameter 1 mm. The size and configuration of the electrode remained the same in both MFC integrated CWs. The third microcosm was CW, which was fabricated with normal gravel (garden pebbles) of size 4-5 mm diameter without any compartmentation.

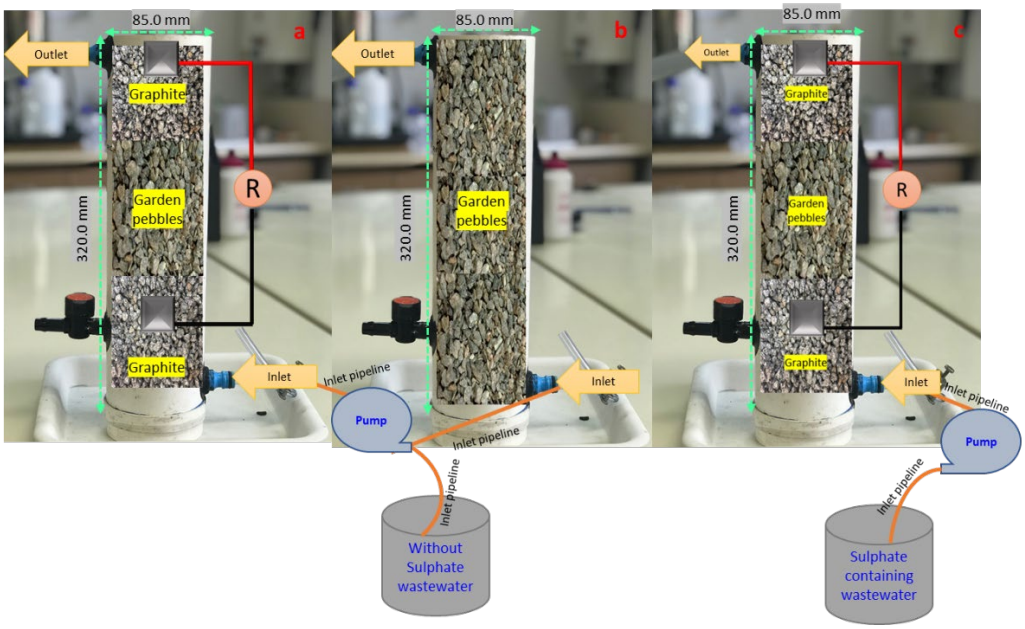

Figure 4-1. The schematic diagram of laboratory-scale microcosms: a. CW-MFC-deplete, b. CW, c. CW-MFC-replete.

4.2.2. Synthetic wastewater preparation

The wastewater used in this study was the synthetic wastewater having the composition: $C_6H_{12}O_6$ (0.80 g L^{-1}), NH_4Cl (0.15 g L^{-1}), KCl (0.13 g L^{-1}), $NaHCO_3$ (1.50 g L^{-1}) and $MgSO_4$ (0.12 g L^{-1}) or $MgCl_2$ (0.10 g L^{-1}) [173]. All the chemicals were purchased from Chemsupply, Australia. The wastewater compositions used in both CW-MFCs were the same except for sulphate presence (*S-replete*) or absence (*S-deplete*). One of the two MFC integrated CW microcosms was fed with sulphate containing wastewater (*CW-MFC-replete*), while the other was without sulphate containing wastewater (*CW-MFC-deplete*). The *CW-MFC-replete* feed contained 96 mg L^{-1} of SO_4^{2-}, and the concentration of $MgSO_4$ was adopted from the previous studies [174, 175]. The CW microcosm was initially operated with sulphate-free wastewater (*CW-deplete*) to observe the treatment performance. It was later operated on sulphate containing wastewater (*CW-replete*).

4.2.3. Inoculation and operation

The inoculum used in this study was taken from the local sewage wastewater treatment plant run by TasWater in Launceston, Tasmania, Australia. The 2% (v/v) sludge inoculum was mixed with synthetic wastewater and inoculated into all the microcosms. The microcosms were fed regularly in batch mode on a 1:1 ratio, one ratio of inoculum taken from the microcosm, mixed with freshly prepared wastewater. The experiment was then acclimatized for a further month with continuous feeding of the freshly prepared wastewater each day until steady state was achieved. All the experiments were run at room temperature (~23°C). All microcosms were run in a continuous mode using a peristaltic pump (Atalyst, Masterflex by Cole-Parmer) at a 12 h hydraulic retention time (HRT). The *CW-MFC-deplete* and *CW-MFC-replete* were continuously operated for six months. The performance of *CW-deplete* was observed for six months, and then it was switched to sulphate containing wastewater (*CW-replete*). After completion of the continuous mode operation, batch mode operation tests were conducted for

one month for *CW-MFC-deplete*, *CW-MFC-replete,* and *CW-replete* microcosms to evaluate the participation of SO_4^{2-} in the treatment performance and electricity generation. Contact time of the batch experiments was varied from 12 to 96 h. Samples from the anode of *CW-MFC-replete*, *CW-MFC-deplete,* and the bottom of the *CW-replete* were taken after 12 h, 24 h, 48 h, 72 h and 96 h, which were collected over a period of one month and analyzed for COD, NH_4^+, S^{2-} and SO_4^{2-}.

4.2.4. Chemical and electrochemical analysis

All the samples were filtered through a cellulose syringe filter (0.45 μm, diameter = 25 mm, MicroScience) before the analysis. Total organic carbon (TOC) and Total nitrogen (TN) were analysed using Shimadzu TOC-TN analyser (Model TNM-L ROHS). Ammonium (NH_4^+) and sulphate (SO_4^{2-}) were analyzed by ion chromatography (Eco IC, MEP instruments, Metrohm). The chemical oxygen demand (COD) was analyzed by APHA Standard Method 5220D [84]. Sulphite (SO_3^{2-}) and sulphide (S^{2-}) were analyzed using the Iodometric method described in APHA Standard Methods 4500B and 4500E, respectively [84]. The statistical calculation was performed with the Origin software 2019b.

The redox potentials of the anode and cathode of CW-MFC were measured against Ag/AgCl reference electrode, which was transposed to the standard hydrogen electrode (SHE) by calculation. Further, electromotive force from the measured anode and cathode potentials was calculated using Eq. 1:

$$E_{emf} = E_{cathode} - E_{anode} \qquad Eq.1$$

In continuous mode experiments, voltage (E_{cell}) was recorded every day using PC^{link} multimeter. In the batch mode experiment, E_{cell} was recorded using PC^{link} multimeter after feeding the microcosm until the sample was taken. The polarization study was carried out when *CW-MFC-deplete* and *CW-MFC-replete* microcosms achieved the steady-states. Based on higher E_{cell} potential, 2.2 KΩ of external resistance for the microcosm was selected. The

Coulombic efficiency (CE) for continuous mode operation of the *CW-MFC-deplete* and *CW-MFC-replete* were calculated using Eq. 2:

$$CE = \frac{MI}{Fbq\Delta COD} \qquad Eq.2$$

where M is the molecular weight of oxygen (g mol^{-1}), I is current density (A m^{-3}), F is Faraday's constant, b is charge transfer, q is flowrate of wastewater (Ls^{-1}), and ΔCOD (mgL^{-1}) is the difference between initial and final COD concentrations. In addition, the CE of batch mode operation was calculated using Eq. 3:

$$CE = \frac{MIt}{Fbv\Delta COD} \qquad Eq.3$$

Where t is the time (s), and v is the anodic volume (L) of the microcosms.

4.2.5. Characterizations of deposits

The chemical depositions at the anode of the *CW-MFC-deplete*, *CW-MFC-replete* and *CW-replete* were further analyzed with several characterization techniques after completion of the experiments. The gravels from the anode of all the microcosms were washed and dehydrated before the solid characterization by submerging in glutaraldehyde solution (2.5%) for 1 h, rinsed with phosphate buffer (pH = 7) three times and then submerged in ethanol (30%, 50%, 70%, then 90%) each for 10 min [176]. All the samples were freeze-dried (-18°C) and the samples were coated with platinum for surface morphology analysis using Scanning Electron Microscopy (SEM), (Hitachi SU-70 field emission SEM). The elemental composition of the samples was determined by the Energy Dispersive X-ray (EDX) spectrophotometer (Oxford AZtec XMax80 EDX system). Additionally, precipitates on the graphite and normal gravels were characterized with X-ray diffraction (XRD, D2 PHASER, Bruker) and later with X-ray photon spectroscopy (XPS, ESCALAB250Xi, Thermo Scientific, UK).

4.2.6. Microbiology

The microbiological samples were taken after the completion of all the experiments. The initial samples were taken from the fresh inoculum and from each microcosm after completion of the experiments. The samples were a mixture of gravels and wastewater from the anode (since anode had a main role in the microcosm) of the microcosms, which were sent to the Australian Genome Research Facility (AGRF) for DNA extraction and diversity profiling. The amplicon sequencing was performed with the target 27F, read length 300 bp, reverse primer (GWATTACCGCGGCKGCTG), and forward primer (AGAGTTTGATCMTGGCTCAG), similar to previous studies [131, 177].

4.3. Results and discussions

4.3.1. Simultaneous NH_4^+, COD, and SO_4^{2-} removal

The treatment performance of CW-MFC in comparison to CW in *S-deplete* and *S-replete* conditions was assessed based on organics and nitrogen removals in liaison with sulphate conversion or removal. The initial TOC and COD concentrations of *S-deplete* wastewater were 497±24 and 853±100 mgL^{-1}, respectively; from this 290±30 mgL^{-1} of TOC and 679±57 mgL^{-1} of COD were removed in *CW-MFC-deplete*, whereas 260±32 mgL^{-1} of TOC and 568±30 mgL^{-1} of COD were removed in *CW-deplete*. The initial TOC and COD concentrations of *S-replete* wastewater were 520±27 and 926±74 mgL^{-1}, respectively, from which 322±24 mgL^{-1} of TOC and 757±36 mgL^{-1} of COD were removed in *CW-MFC-replete*. In contrast, 283±41 mgL^{-1} of TOC and 600±52 mgL^{-1} of COD were removed in *CW-replete*. From the results summarized in *Table 4-1*, it can be observed that TOC and COD removal of CW-MFC were significantly higher than CW ($p< 0.05$). There was also a significant difference in the removal based on *S-replete* and *S-deplete* conditions of all the microcosms ($p< 0.05$). The mean COD removal followed the sequence: *CW-MFC-replete>CW-MFC-deplete>CW-replete>CW-deplete*.

The measured initial NH_4^+concentration was 60±7 mgL^{-1} in both S-replete and S-deplete wastewater, CW-MFC-replete and CW-MFC-deplete removed 40±8 and 35±4 mgL^{-1} of NH_4^+ respectively, whereas CW-replete and CW-deplete removed 28±5 and 22±7 mgL^{-1} of NH_4^+, respectively. The TN removal of CW-MFC-replete and CW-MFC-deplete was not significantly different at the beginning stage of the experiments, but after a few weeks, there was a significant difference in the removal pattern of both the microcosms. The TN removal in CW-MFC-replete was significantly higher than those of CW-MFC-deplete, CW-replete, and CW-deplete ($p< 0.05$). The statistical graph based on the data range of TN, NH_4^+, TOC, and COD removal represented in Figure 4-2 illustrates the performance of microcosm, which showed higher removal in CW-MFC-replete than the other microcosm.

Table 4-1. The mean TOC, COD, TN, and NH_4^+ removal concentration in continuous mode operation.

	Initial (*S-replete*)	*CW-MFC-replete*		*CW-replete*		Initial (*S-deplete*)	*CW-MFC-deplete*		*CW-deplete*	
	($mg\ L^{-1}$)	($mg\ L^{-1}$)	%	($mg\ L^{-1}$)	%	($mg\ L^{-1}$)	($mg\ L^{-1}$)	%	($mg\ L^{-1}$)	%
TOC	520±27	322±24	61±24	283±41	54±41	497±24	290±30	58±30	260±32	52±32
COD	926±74	757±36	82±36	600±52	66±52	853±100	679±57	79±57	568±30	64±30
TN	60±7	20±4	66±6	36±5	46±8	60±7	25±8	58±8	35±6	40±10
NH_4^+	60±7	40±8	65±8	28±5	46±5	60±7	35±4	58±4	22±7	36±7

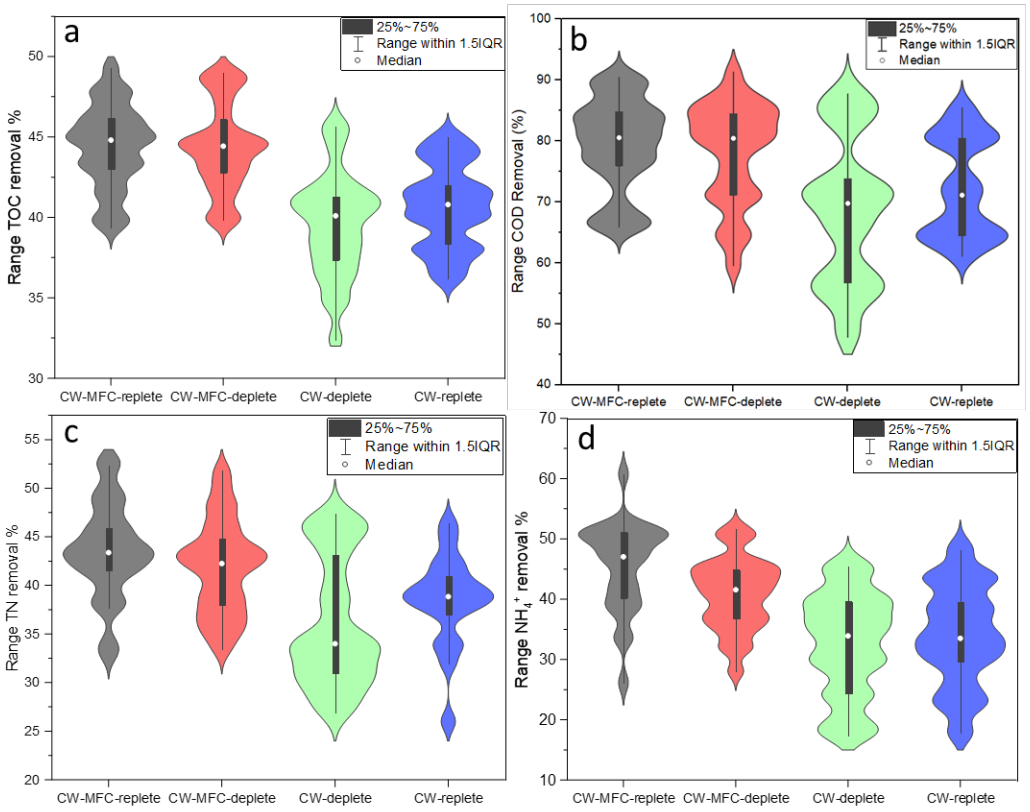

Figure 4-2. Statistical analysis of overall percentage removal in continuous mode operation: a. TOC; b. COD; c. TN; and d. NH_4^+. The wide range of data lies in the wider portion of the shape and the narrow portion indicates a small number of data points. Hence, CW-MFC-replete shows higher ranges of removal in comparison to the other systems.

The reduction of SO_4^{2-} was analysed in the form of sulphite (SO_3^{2-}) and sulphide (S^{2-}) from the effluent samples. The mean S^{2-} concentrations in effluent of *CW-MFC-replete* and *CW-replete* were 21±7 and 33±9 mg L^{-1}, respectively, but it was not detected in all the samples. In addition, no trace of SO_3^{2-} was detected in the effluent samples. The low determination of SO_3^{2-} and S^{2-} could be due to the detection limitation or contact of effluent with the atmospheric oxygen or stability of the ions [178, 179]. The high concentration of S^{2-} in *CW-replete* is evident from Figure 3, which shows dissolved concentration only; the precipitate characterization details in Section 3.4 also signify higher S^{2-} precipitation in *CW-replete*. It can be observed that in *CW-MFC-replete* SO_4^{2-} removal was up to 81±3% along with a low S^{2-} accumulation (*Figure 4-3*). In *CW-MFC-replete,* reduced sulphur products' reduction and probable re-oxidation could have contributed to lesser precipitate deposition even at higher SO_4^{2-} removal. However, SO_4^{2-} was

significantly consumed (since it is an electron acceptor) in *CW-replete* to remove the pollutants and its reduction can be attributed to high S^{2-} precipitation, which decreased the treatment performance of *CW-replete* at a later stage due to S^{2-} precipitate associated toxicity.

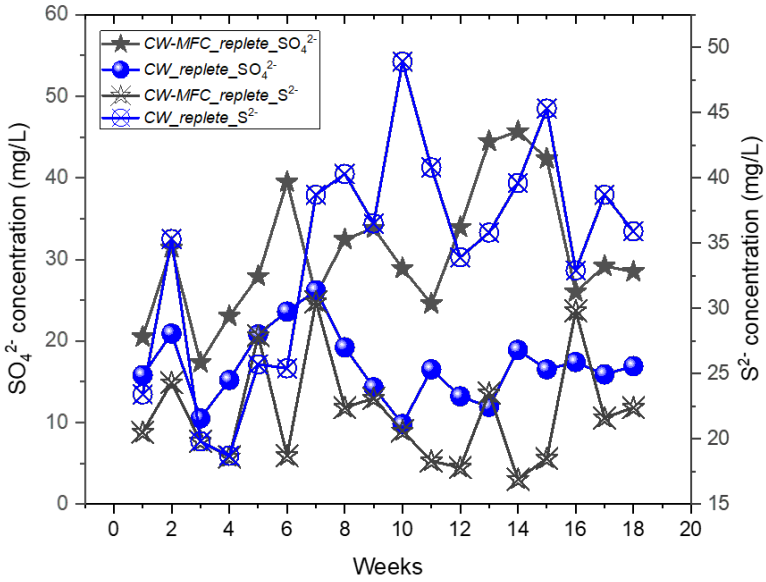

Figure 4-3. SO_4^{2-} and S^{2-} concentrations of CW-MFC-replete and CW-replete, excluding samples where S^{2-} was not detected.

The *CW-MFC-replete* and *CW-MFC-deplete* achieved higher treatment efficiency for NH_4^+ and COD compared to *CW-replete* and *CW-deplete.* However, NH_4^+ and COD removal efficiency was the highest in *CW-MFC-replete* than the other microcosms. The higher NH_4^+ removal in *CW-MFC-deplete* was due to the presence of conductive materials, which allowed higher oxidation of NH_4^+ and COD than *CW-replete* and *CW-deplete.* The conductive material in CW-MFC acts as an artificial electron acceptor in anaerobic conditions that allows higher oxidation of the pollutants [164, 166]. The high NH_4^+ removal efficiency in CW-MFC in comparison to CW has also been reported by Hartl, et al. [65], Xu, et al. [69], Srivastava, et al. [131], in which it is proven that the presence of conductive material at the anode enhances NH_4^+ removal efficiency. However, higher NH_4^+ removal in *CW-MFC-replete* among all the other microcosms was due to the abundance of SO_4^{2-} as an additional electron acceptor (other than conductive material) in *S-replete* conditions. The presence of electrode and SO_4^{2-} at the

anode of *CW-MFC-replete* allowed high oxidation of organic matter and NH_4^+ in anaerobic conditions. The presence of electrode in *CW-MFC-replete* was further responsible for the conversion of reduced SO_4^{2-} product (S^{2-}) back to its higher oxidation state, which decreased the S^{2-} and other sulphur bearing compounds build-up by reducing the amount of precipitate and enhanced treatment efficiency. In this study, the presence of SO_4^{2-} in *CW-MFC-replete* has an additional influence on the treatment efficiency, which signifies the synergetic correlation of sulphur and conductive material on the treatment efficiency of the pollutants.

The availability of electron acceptors in *CW-MFC-deplete* was limited due to the absence of SO_4^{2-}, where the treatment efficiency of NH_4^+ decreased compared to *CW-MFC-replete*. Additionally, in *CW-replete*, the presence of SO_4^{2-} provided an additional electron acceptor for removing COD and NH_4^+ compared to *CW-deplete* and the removal in *CW-replete* was higher for NH_4^+ than *CW-deplete*. However, in the absence of conductive material in *CW-replete*, S^{2-} conversion was lacking, which decreased the COD and NH_4^+ removal due to toxicity build-up. Hence, it can be concluded that SO_4^{2-} is positively intertwined with other elements present in wastewater, and it shows positive effect in the presence of conductive materials. Besides, the measured COD concentration from the effluent of *CW-MFC-deplete* was attributed to reduced chemical compound present in initial wastewater composition. On the contrary, in *CW-MFC-replete* the measured COD concentration was due to reduced sulphur metabolites and other chemical compositions present in effluent wastewater, such that on the same HRT *CW-MFC-replete* removed more COD than *CW-MFC-deplete*. Likewise, in *CW-deplete*, TOC and COD removal was higher compared to *CW-replete* at later stages, as a reduced product of SO_4^{2-} has increased the COD in *CW-replete*. Ter Heijne, et al. [179], Dai, et al. [180] have also stated that reduction of SO_4^{2-} into S^{2-} can increase COD since S^{2-} also acts as an electron donor. Jing, et al. [181] stated that the accumulation of S^{2-} inhibits the removal of organics and suppresses the microbial actions, whereas in *CW-MFC-replete* the presence of conductive material

decreased S^{2-} accumulation. The redox coupling of sulphur also influences the efficient electron transfer in the anaerobic region of *CW-MFC-replete*, minimizing the risk of toxicity build up in the system [182] in order to enhance the treatment efficiency. This suggests that the MFC component contributed to high treatment efficiency by assisting electron transfer through the conductive materials in anaerobic regions, and the presence of SO_4^{2-} positively influenced the performance of *CW-MFC-replete*.

The batch mode operation was also performed to study the detrimental effects of a toxic precipitate of reduced sulphur compounds without their washout. From the results of COD, NH_4^+, S^{2-} and SO_4^{2-} concentrations of batch mode operation presented in *Table 4-2*, it was observed that in the batch study, COD concentration at the anode of *CW-MFC-replete* was higher than *CW-MFC-deplete* due to the reduced product of SO_4^{2-}; however, the electrode assisted oxidation and reduction of sulphur compounds did not seem to impact the overall performance rather than the participates in enhanced treatment performance.

Table 4-2. The mean concentrations of COD, NH_4^+, S^{2-} and SO_4^{2-} batch mode operation.

(mg L^{-1})	*CW-MFC-replete* retention time (h)					*CW-MFC-deplete* retention time (h)					*CW-replete* retention time (h)				
	12	24	48	72	12	24	48	48	12	24	48	24	12	24	48
COD	500±12	456±8	386±7	COD	500±12	456±8	386±7	COD	500±12	456±8	386±7	COD	500±12	456±8	386±7
NH_4^+	39±5	28±4	2±3	NH_4^+	39±5	28±4	2±3	NH_4^+	39±5	28±4	2±3	NH_4^+	39±5	28±4	2±3
SO_4^{2-}	59±5	41±7	33±3	SO_4^{2-}	59±5	41±7	33±3	SO_4^{2-}	59±5	41±7	33±3	SO_4^{2-}	59±5	41±7	33±3
S^{2-}	12±3	18±6	26±2	S^{2-}	12±3	18±6	26±2	S^{2-}	12±3	18±6	26±2	S^{2-}	12±3	18±6	26±2

Furthermore, high NH_4^+ removal in *CW-MFC-replete* was due to the electrode acting as an electron acceptor, which was due to the presence of an additional electron acceptor in the form of SO_4^{2-} in wastewater. In case of *CW-MFC-deplete*, only the electrode acted as an artificial electron acceptor for NH_4^+ removal and thus, it was lower than *CW-MFC-replete.* In the case of *CW-replete,* removal was not high as CW-MFC microcosms due to the absence of electrodes

and also, low NH_4^+ removal with increased contact time in *CW-replete* was due to a decrease in electron acceptors with a reduction of SO_4^{2-} into S^{2-} over time. In the absence of an electron acceptor such as an electrode, the converted S^{2-} was unable to be re-oxidized in *CW-replete,* whereas the presence of an electrode in *CW-MFC-replete* converted S^{2-} by assisting the reoxidation that was responsible for the stable treatment performance even after 96 h of the retention time. In the batch mode operation, once wastewater was inoculated in the microcosm, it was retained in the microcosm for 96 h retention time and reduction, as well as oxidation of sulphur compounds, did not impact the treatment efficiency of *CW-MFC-replete* significantly. Rather the redox coupling enhanced COD and NH_4^+ removal.

Furthermore, in the batch mode operation, with an increase in the retention time, S^{2-} concentration also increased in both the *S-replete* microcosms and it was significantly higher in *CW-replete* than *CW-MFC-replete* (*Table 4-2*). The high accumulation of S^{2-} could increase the toxicity, which might negatively impact the treatment performance. Agostino and Rosenbaum [182] reported that high amount of S^{2-} precipitate can harm the living organisms present in the microcosms. However, in bioelectrochemical systems, the presence of conductive materials can again oxidize S^{2-} to SO_4^{2-} and reduce the toxicity level [182]. Thus, in *CW-MFC-replete,* reduction of sulphur compounds and oxidation has decreased the toxicity build-up of the reduced sulphur metabolites with the redox reactions. Thus, incorporation of MFC into CW can be an effective approach to treat the sulphate containing wastewater, and due to the presence of conductive materials, treatment performance can be improved.

4.3.2. Cell Voltage of CW-MFC-replete and CW-MFC-deplete

The polarization study of *CW-MFC-replete* and *CW-MFC-deplete* was performed after achieving steady-state conditions in the microcosms and polarization curves of both the microcosms are presented in *Figure 4-4*. From the polarization curves, the maximum current densities achieved in *CW-MFC-replete* and CW-*MFC-deplete* were 25.6 mAm^{-3} and 22.8

mAm^{-3}, respectively. Nevertheless, the maximum power densities achieved in *CW-MFC-replete* and CW-*MFC-deplete* were 1.1 mWm^{-3} and 0.48 mWm^{-3} at 1.2 KΩ, respectively. In the continuous mode experiment of *CW-MFC-replete* and *CW-MFC-deplete*, E_{cell} and current density throughout the operational period was always higher in *CW-MFC-replete*. *Figure 4-4 (b, c)* illustrate the correlation between the cell performance (E_{cell}) and the current density of *CW-MFC-replete* and *CW-MFC-deplete*. The E_{cell} of *CW-MFC-replete* varied between 50.0 and 60.0 mV, while in case of *CW-MFC-deplete,* it was 30.0 and 40.0 mV throughout the continuous mode operation. A similar pattern was also observed for current density, where the maximum current density was 15.4 mAm^{-3} in *CW-MFC-deplete* and 21.8 mAm^{-3} in *CW-MFC-replete* throughout the continuous mode operation. The maximum CE of *CW-MFC-replete* in a continuous mode operation was 0.78%, whereas in *CW-MFC-deplete,* CE was 0.76%. *Figure 4-4 (b)* illustrates the cumulative correlation of E_{cell} with COD concentration.

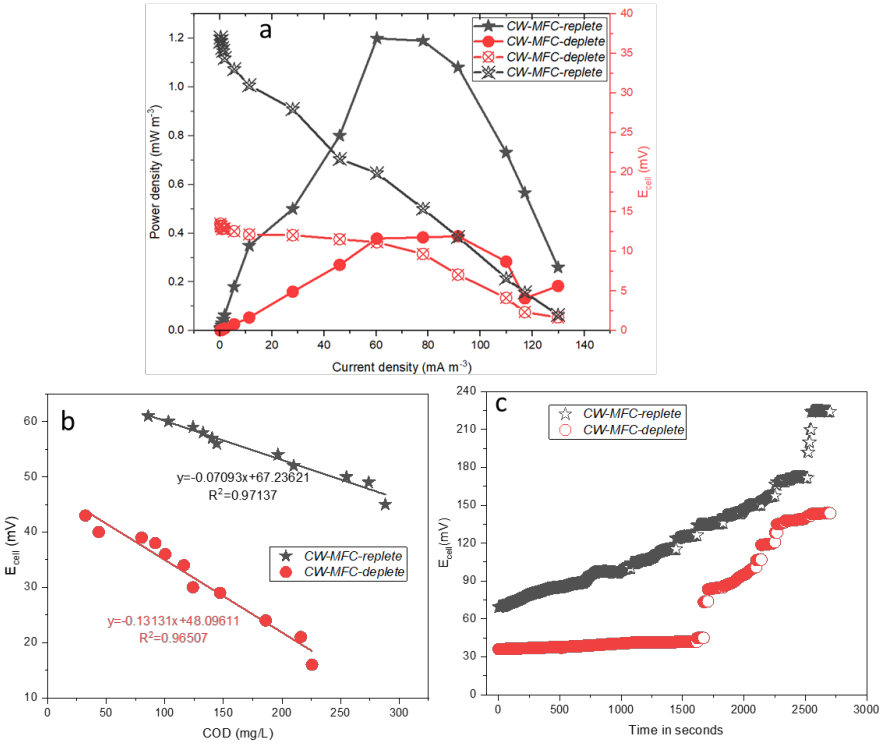

Figure 4-4. Performance in continuous mode operation, a. Polarization study of CW-MFC-replete and CW-MFC-deplete; b. correlation of COD and E_{cell}; and c. E_{cell} output of the CW-MFC-replete and CW-MFC-deplete in batch mode operation.

The redox potential of anode and cathode zones of *CW-MFC-deplete* and *CW-MFC-replete* were almost similar. *CW-MFC-replete*'s anodic potential was within -33.8 to -213.8 mV, while the cathodic potential was 177.2 to 285.2 mV. In *CW-MFC-deplete,* the anodic potential was within the range of -56.8 to -267.8mV, and for cathodic potential, it was 69.2 to 266.1 mV. The mean E_{emf} of *CW-MFC-replete* and *CW-MFC-deplete* was 296±200 mV and 260±155 mV. The detailed potential and E_{emf} values are provided in *Table A1 (Appendix 2)*. Both the microcosm's redox potentials were favourable for the electron transfer since anode potential was more negative than the cathode potential. Even with the favourable potential, the achieved current and power density were relatively lower than the other CW-MFC studies [164, 172, 174, 183]. The lower power and current density values in the present study could have resulted from the high external resistance and low retention time (12.0 h). González del Campo, et al. [184] reported that external resistance (based on polarization study) regulates the cell voltage, which is based on the difference between anodic and cathodic potential (redox). Additionally, electroactive bacteria (EAB) have their own doubling time [99]; due to a retention time of only 12.0 h, the growth of EAB would have slowed down, which influenced the electron transfer mechanism. Logan [99] discussed those microbes present in the nature usually have a doubling time of one day or longer; for instance, *G. sulfurreducens* co-cultured with *W. succinogens* take around 6-8 h doubling time, but for *Desulfovibriode sulfuricans* it takes 30 h.

In batch mode operation, the E_{cell} of *CW-MFC-replete* was 60.0 mV in 12.0 h, but it increased to 224.0 mV in 96.0 h of the retention time. Likewise, *CW-MFC-deplete* achieved 30.0 mV in 12.0 h and increased to 143.0 mV after 96.0 h of retention time. With the longer retention time of 96 h, the current density achieved in *CW-MFC-replete* was 51.5 mAm^{-3}, whereas, in case of *CW-MFC-deplete,* the achieved current density in 96 h retention time was 34.9 mAm^{-3}. By increasing the retention time, E_{cell} of both the microcosms increased, but the *CW-MFC-replete* again achieved high E_{cell} performance (*Figure 4-4 (c)*). Additionally, the CE of *CW-MFC-*

replete in 96 h retention time reached up to 12.2%, while in case of *CW-MFC-deplete*, it reached to 10.3%. The increase in retention time could provide appropriate doubling time to EAB and complete degradation of the pollutants at the anode. Additionally, in *CW-MFC-replete*, the presence of SO_4^{2-} assisted the redox reactions between microbial cells and the electrode, which favours higher E_{cell} output. Sun, et al. [185] suggested that in case of MFC, SO_4^{2-} first get reduced to S^{2-} and subsequent oxidation of S^{2-} results in electricity generation. In a continuous mode operation, due to the presence of SO_4^{2-} and its reduction to S^{2-}, followed by re-oxidation to SO_4^{2-} as a part of redox cycle would help in indirect extracellular electron transfer to the anode [176]. Additionally, it also acts as an electron shuttle for an adequate electron transfer to the electrode. The microbial and electrochemical electron release mechanism based on SO_4^{2-} reduction and S^{2-} oxidation in the presence of organic carbon (glucose and acetate) can be explained below using Eqs. 4 to 7 [186]:

$$C_6H_{12}O_6 + 2H_2O \xrightarrow{microbial} 4H_2 + 2CH_3COOH + CO_2 \qquad Eq.4$$

$$4H_2 \xrightarrow{electrochemical} 8H^+ + 8e^- \qquad Eq.5$$

$$CH_3COOH + SO_4^{2-} \xrightarrow{microbial} 2CO_2 + 2H_2O + S^{2-} \qquad Eq.6$$

$$4H_2O + S^{2-} \xrightarrow{electrochemical} 8H^+ + 8e^- + SO_4^{2-} \qquad Eq.7$$

The above equations show the influence of SO_4^{2-} on the release of electrons, which were responsible for the enhanced electricity generation in *CW-MFC-replete*. On the other hand, for *CW-MFC-deplete,* the absence of SO_4^{2-} would have enhanced the resistance for efficient electron transfer, resulting in a low E_{cell} output in *CW-MFC-deplete;* similar results were also reported by Srivastava, et al. [166]. It is also clear from the batch mode operation that when wastewater (media) within the microcosms becomes old, it gives higher E_{cell} than wastewater that change continuously. The high E_{cell} output was due to the redox-active metabolites in old

media, which had a strong oxidation capability than the media changing continually in a continuous operation mode [187]. Due to redox coupling with sulphur metabolites, *CW-MFC-replete* performed better than *CW-MFC-deplete* even after a longer contact time, and no toxicity effect was observed.

4.3.3. Characterisation of precipitates

In CW, the removal of SO_4^{2-} is mainly dominated by the adsorption onto organics or precipitation in the form of metal sulphides [114]. Therefore, after the completion of experiments, graphite and normal gravels from the anode of all the microcosms were analyzed using several characterization techniques. The SEM-EDX was used to characterize the morphology and structure of the biofilm as well as the precipitation that occurred at the anode. SEM imaging of the anodes of all the microcosms showed a thin visual biofilm onto the surface of gravels. The microbes were scattered and embedded in extracellular polymeric substances, with some linkages observed linking the biotic aggregates.

Nevertheless, the biofilm in *CW-MFC-replete and CW-MFC-deplete* showed different microbial structures than for *CW-replete* (*Figure 4-*5 (a, b, and c)). The *CW-replete* showed a chain like microbial structure (*Figure 4-5(c)*), whereas *CW-MFC-replete and CW-MFC-deplete* showed a tubular microbial structure (*Figure 4-5* (a, b)). The difference in microbial structure could be due to the presence of the conductive material, which may have influenced microbial adaptation. Furthermore, EDX imaging associated with SEM imaging in *Figure 4-5 (a, b, and c)* offers insights into the deposition of chemical constituents, indicating that *CW-MFC-replete* and *CW-replete* had sulphur precipitates along with other chemical constituents on the gravels. The total counts of sulphur deposited on the graphite gravels of *CW-MFC-replete* was 1.4%, whereas in *CW-replete,* it was 3.5%. The precipitation of sulphur was high in *CW-replete* than *CW-MFC-replete*, which agreed with the theory explained previously for the removal efficiency and electricity generation.

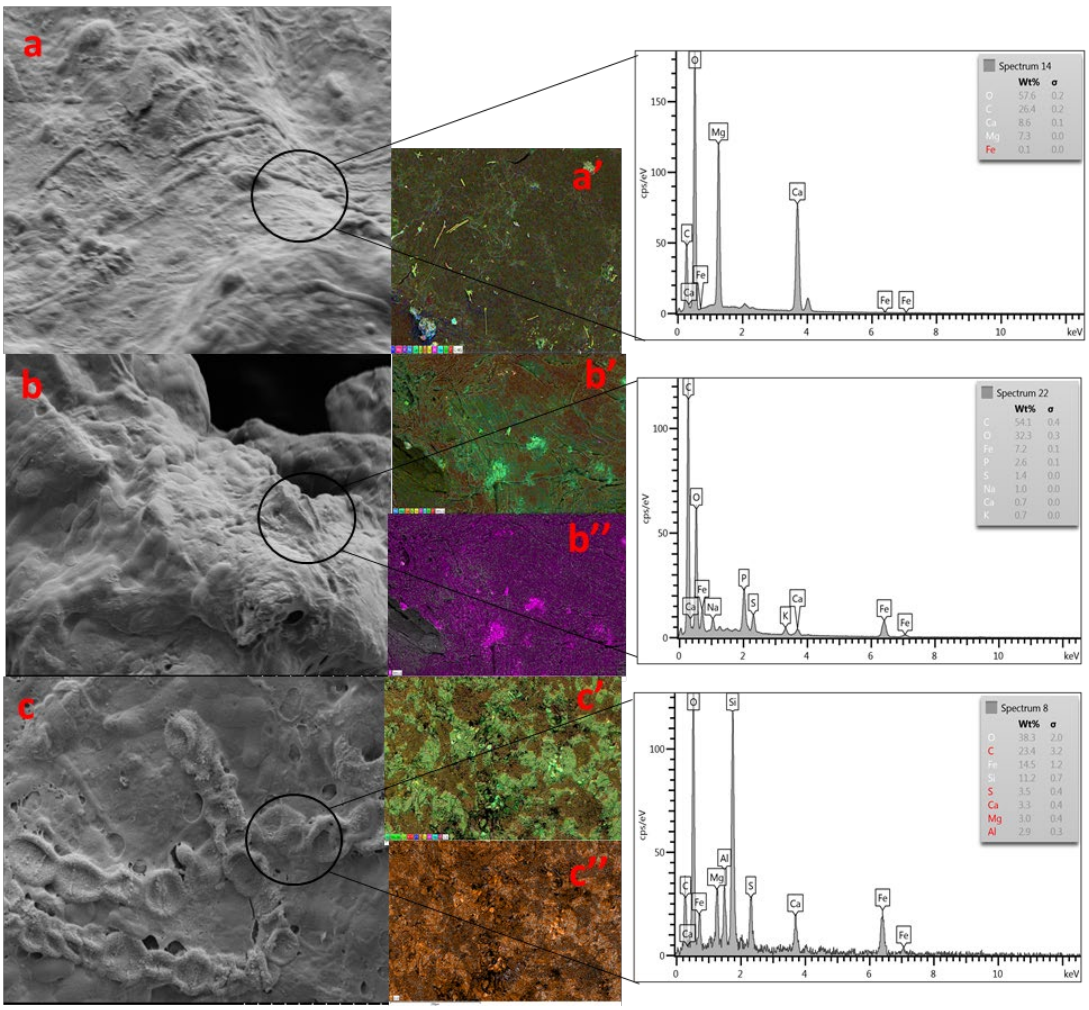

Figure 4-5. SEM imaging with associated EDX analysis of the anode of: a. CW-MFC-deplete; b. CW-MFC-replete; and c. CW-replete. Figure a' is a coloured image of precipitation of all chemical constituents, b' and b" are the precipitation of all chemical constituents and sulphur precipitation, respectively; c' and c" are the precipitation of all chemical constituents and sulphur precipitation, respectively.

Additionally, the XRD analysis was also performed on the precipitate samples; however, no apparent diffraction peaks were observed at 2θ from 10° to 90°, which indicates amorphous nature of the samples, as shown in *Figure A3 and Table A2 (Appendix 2)*. Therefore, XPS analysis was also performed to analyze the chemical components of the precipitate. *Figure 4-6* illustrate the survey of all the anode samples from each microcosm, which indicates a sulphur peak below 200 eV in *CW-MFC-replete* and *CW-replete* that is absent in *CW-MFC-deplete*. Additionally, Figure 6d and 6e demonstrate a broad S2p spectra for the anode of *CW-replete* and *CW-MFC-replete,* respectively. The broad peaks were determined between 161 and 168

eV binding energy (BE). The peak was further divided into one doublet and one singlet: S2p3/2 and S2p1/2 components, which were further assigned as S^{2-} and SO_4^{2-} [185]. In general, the lower energy peak signal is assumed to be the most reduced forms of sulphur such as sulphide, whereas higher energy peak signal denotes the most oxidized form of sulphur such as sulphate; the remaining peak can be assigned to sulphite and polysulphide [188]. The reduction of SO_4^{2-} into S^{2-} followed by oxidation to elemental sulphur has been studied by Ter Heijne, et al. [179]. The XPS peak of *CW-MFC-replete* and in *CW-replete* (Figure 6d and 6e) revealed that the highest binding energy (BE) peak is for SO_4^{2-} and then S^{2-}. The more intense peaks of S2p3/2 and S2p1/2 were observed, and based on BE, it can be concluded that the precipitate of SO_4^{2-} and S^{2-} was significantly higher in *CW-replete* than the *CW-MFC-replete*. The total atomic mass % of sulphur in *CW-MFC-replete* and in *CW-replete* were 0.84% and 2.49%, respectively, that also signifies higher sulphur precipitation in *CW-replete* than *CW-MFC-replete.* Further, low atomic % of sulphur content in *CW-MFC-replete* also signifies that S^{2-} was again converted into SO_4^{2-} or was being re-utilized either for electricity generation or reduction/oxidation of other chemical constituents.

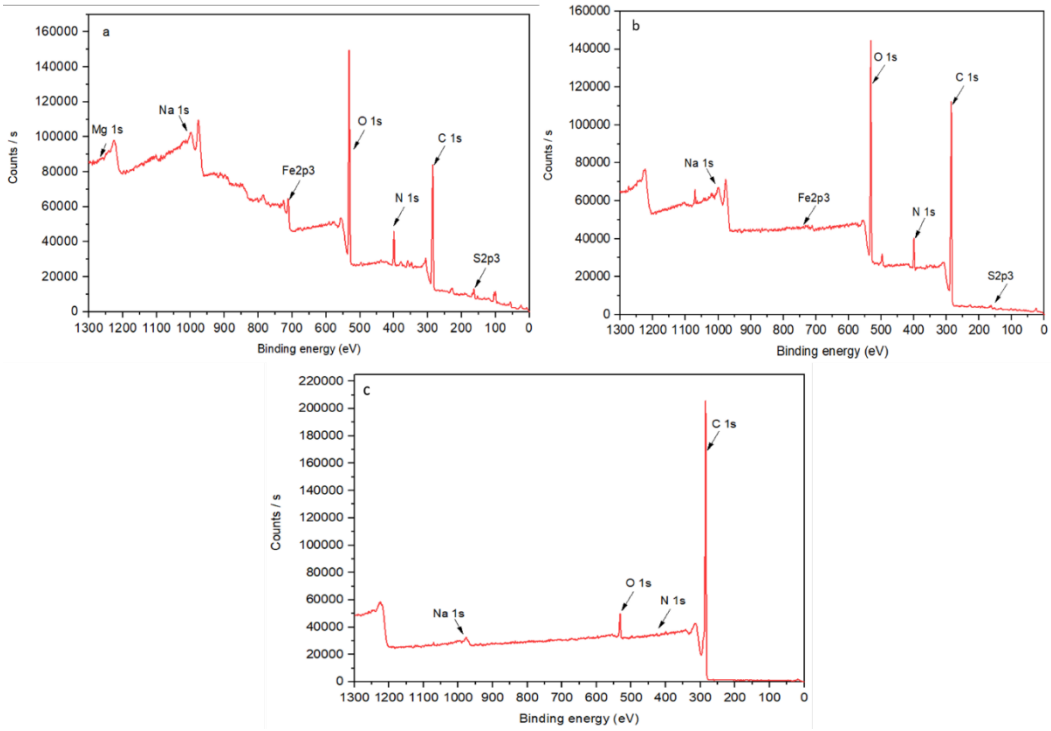

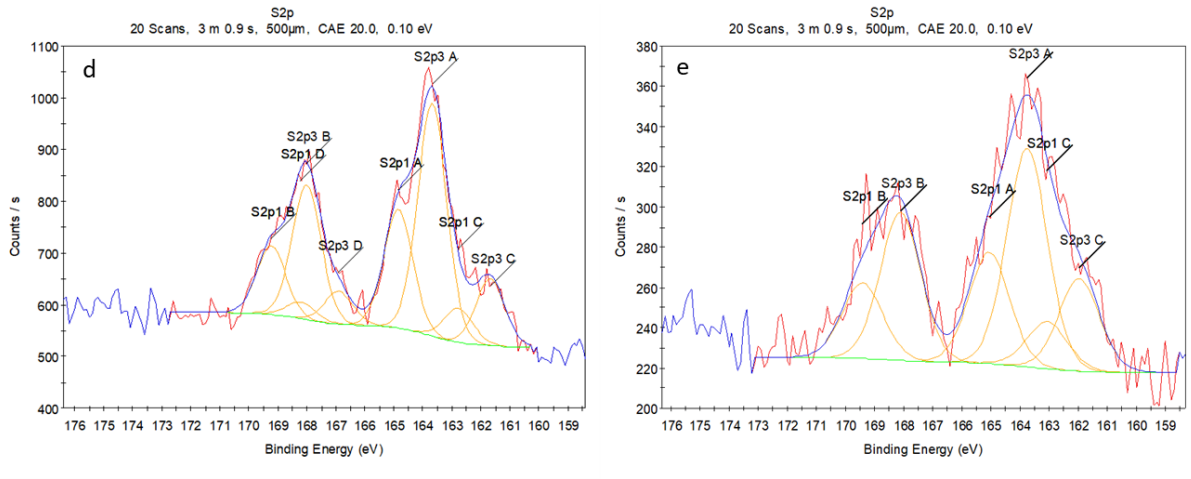

Figure 4-6. XPS survey of a. CW-MFC-replete; b. CW-replete; and c. CW-MFC-deplete; and high-resolution spectra of: d. CW-replete; and e. CW-MFC-replete. In Figure d and e fitting of the recorded spectrum detected several signals of sulphate (denoted in the figures).

4.3.4. Microbiology

Microbiological analysis of all the samples from the microcosms along with the inoculum sample was performed after the completion of the experiments. In the amplicon sequencing test, a total number of 169767, 291479, 283908, 325072 and 194077 effective reads were present after the quality control steps in *CW-MFC-replete, CW-MFC-deplete*, CW-*replete, CW-deplete* and inoculum, respectively. The Shannon index was used to find the species richness (diversity) and evenness of all the microcosms. The Shannon index of *CW-MFC-replete, CW-MFC-deplete*, CW-*replete, CW-deplete* and inoculum were 3.5,3.2, 2.9, 3.2, and 2.4, respectively. The maximum Shannon index was found in *CW-MFC-replete*, and the lowest was in the inoculum. The high Shannon index in *CW-MFC-replete* indicates high microbial richness followed by *CW-MFC-deplete*, *CW-deplete, CW-replete* and inoculum. The low Shannon index in samples indicates that it was mainly inhabited with a specific microbial community, whereas high Shannon index denotes higher diversity. With the low Shannon index, the inoculum was mainly inhabited with the microbes from the phylum *Firmicutes* (89.3%) followed by *Actinobacteria* (7.2%) and *Proteobacteria* (2.1%).

The microbial community changed significantly from inoculum after inoculation into the microcosms, particularly in *S-replete* and *S-deplete* conditions (*Figure 4-7*).

At the phylum level, *CW-MFC-replete* was densely populated with *Spirochaetes* (31.3%), followed by *Firmicutes* (29.7%), *Proteobacteria* (12.1%)*, Chloroflexi* (10.9%), *Actinobacteria* (6.9%), *Bacteroidetes* (4.3%) and *Synergistetes* (1.6%). Additionally, the *CW-MFC-deplete* was enriched at the phylum level with *Firmicutes* (54.6%) followed by *Actinobacteria* (18.8%), *Spirochaetes* (11.8%), *Bacteroidetes* (3.6%), *Proteobacteria* (2.8%) and *Synergistetes* (1.5%). The *CW-replete* was enriched with phylum *Firmicutes* (31.2%), followed by *Proteobacteria* (21.8%)*, Spirochaetes* (16.7%)*, Chloroflexi* (9.6%), *Actinobacteria* (9.2%) and *Bacteroidetes* (6.9%). On the other hand, *CW-deplete* microcosms were dominated by phylum *Firmicutes* (55.7%), followed by *Proteobacteria* (19.1%)*, Spirochaetes* (9.6%), *Actinobacteria* (6.1%), *Chloroflexi* (4.4%), and *Bacteroidetes* (2.2%). The high abundance of phylum *Firmicutes* in all the microcosms was due to its dominance in the inoculum; however, in *S-replete* conditions, the abundance was less than the *S-deplete* conditions. In CW-*replete* and *CW-deplete* *Firmicutes* was main enriched microbes, which are known as fermentative microbes and are mostly present in anaerobic conditions for organic degradation. However, in the presence of conductive material, these *Firmicutes* also participated in electricity production by the degradation of organics. Besides, *Firmicutes* were reported to be responsible for sulphate reduction in bioelectrochemical systems [182]. Thus, *Firmicutes* plays an important role in interlinking the sulphur cycle with other pollutants and influence the electron transfer in CW-MFC. The presence of *Actinobacteria,* and *Bacteroidetes* in CW-MFC are also recognized for organic degradation and electricity production in bioelectrochemical systems [172, 180, 189]. Furthermore, *Spirochaetes* was abundant in *CW-MFC-replete,* which are mainly anaerobic microbes and their enrichment participates in the glucose oxidation with acetate as an end

product [190]. Further, *Spirochaetes* are also known for enhancing electricity generation, and they adapt easily even in variable environmental conditions [191].

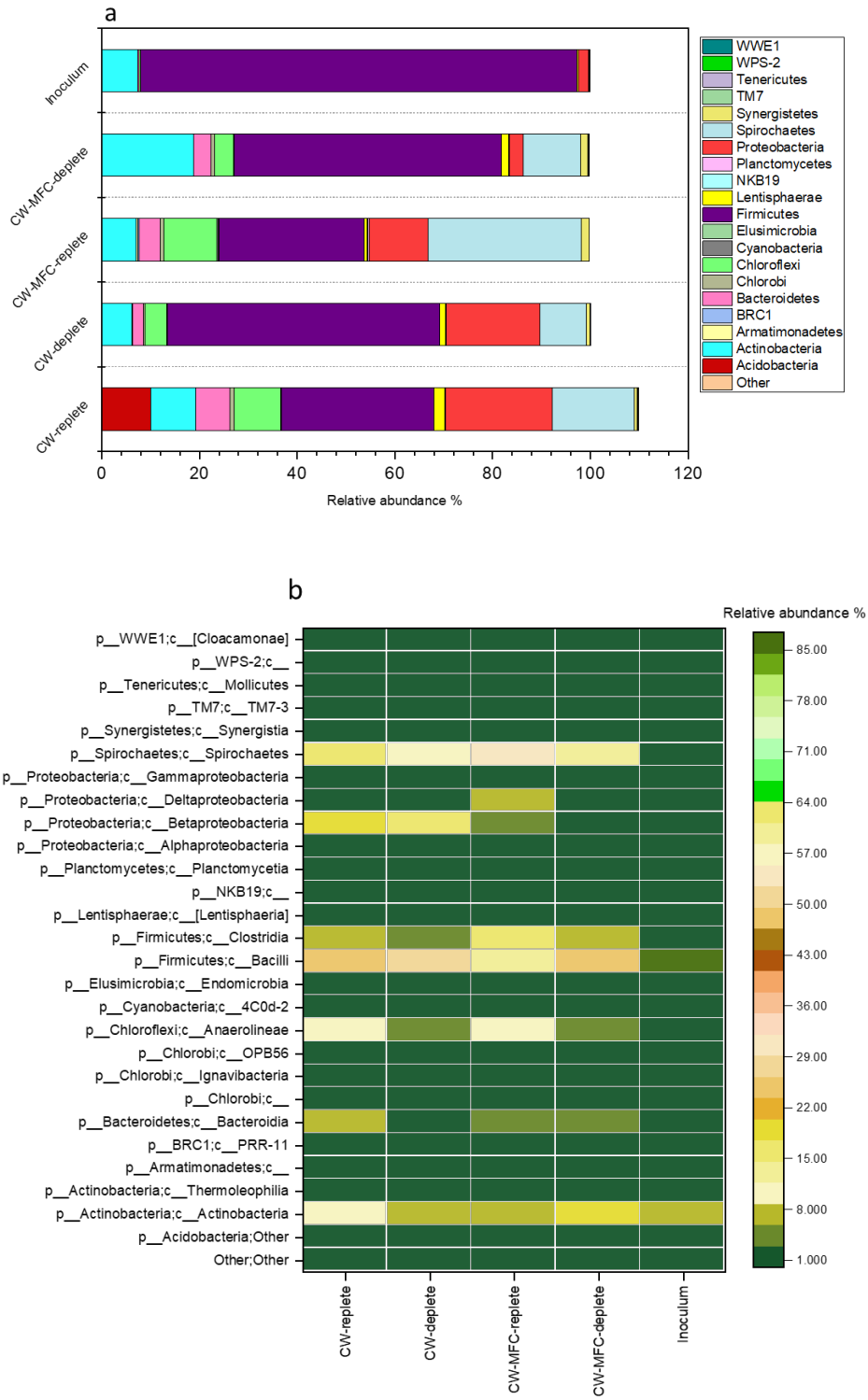

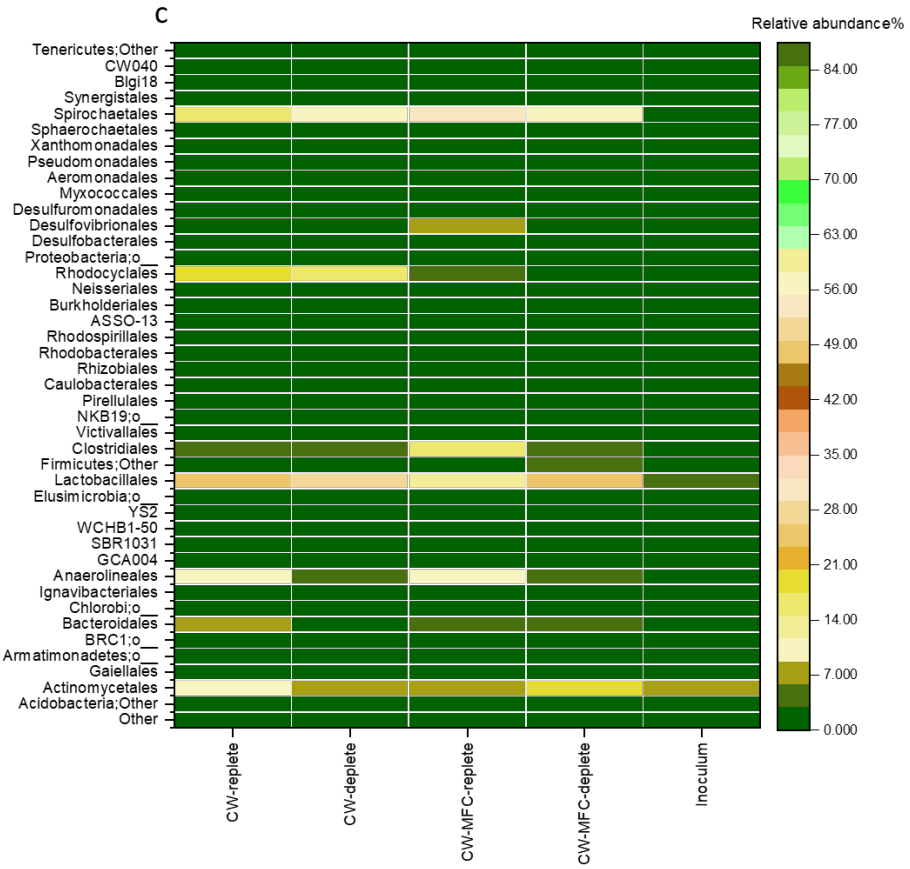

Figure 4-7. The microbiological analysis of CW-MFC-replete, CW-MFC-deplete, CW-replete, and CW-deplete, based on: a. Phylum, and heatmap based on b. Class, and c. Order.

The microbes from the phylum *Proteobacteria* have a crucial role in electrochemical activities. They include a wide range of microbes involved in sulphur metabolism [172, 192]. Most of the species from class *Deltapreoteobacteria* are recognized as sulphate reducing bacteria (SRB) and EAB. The abundance of *Deltapreoteobacteria* was higher in *CW-MFC-replete* (7.3%) in comparison to *CW-MFC-deplete* (1.2%), CW-*replete* (1.5%), and *CW-deplete* (1.0%). The presence of genus *Desulfovibrio* (6.2%), *and Desulfobulbus* (0.8%), SRB and SOB, respectively, from class *Deltapreoteobacteria*, and order *Desulfovibrionales* and *Desulfobacterales* in *CW-MFC-replete* implies the mechanism of sulphur reduction and oxidation in *CW-MFC-replete* [180, 185]. However, the presence of *Desulfovibrio*, an SRB in *CW-replete* was only 0.9%. The richness of order *Desulfovibrionales* and *Desulfobacterales* in *CW-MFC-replete* was higher than the other microcosm (*Figure 4-7 (c)*), which signifies the

efficient electron transfer in *CW-MFC-replete* since they are considered in a category of exoelectrogenic bacteria, which uses electrode as an electron acceptor in bioelectrochemical systems. Besides, they have a strong linkage between the sulphur and other pollutants. The low efficiency of *CW-MFC-deplete* for electricity generation could be due to less abundance of *Deltapreoteobacteria,* which is an important electrogenic microbes. In addition, SOB also belongs to *Gammaproteobacteria,* which was 0.5% in *CW-MFC-replete* and 0.1% in *CW-replete* [193]. The higher relative abundance of *Gammaproteobacteria* in *CW-MFC-replete* was due to the presence of electrodes, which acted as an electron acceptor and assisted oxidation of S^{2-} due to which reoxidation was high. The SRB also considered from genus *Clostridium* that was present in *CW-MFC-replete* (0.4%) and *CW-replete* (0.1%) [185]. The microbial community analysis demonstrates the presence of SRB and SOB in the *CW-MFC-replete* which was higher than *CW-replete,* responsible for reduction and oxidation of sulphur and high bioelectricity generation. The microbial community at phylum, class and order level is illustrated in (*Figures 4-7 (a*, *b, and c))* respectively. The high abundance of microbes and performance of *CW-MFC-replete* also shows that there was no influence of toxicity build up on the microbial performance even in the long-term operation of the experiment.

4.4. Conclusions

The present study establishes the positive association of SO_4^{2-} and conductive materials on ammonium and organic pollutants removal along with the electricity production in CW-MFC. Further, it signifies that conductive materials can help in reducing the adverse impact of reduced sulphur compounds on microbial diversity by re-oxidising them. The presence of SO_4^{2-} could play a significant role in CW-MFC, whereas in a traditional CW, it started impacting the treatment efficiency due to the precipitation of toxic S^{2-} and associated toxicity build-up. The presence of SO_4^{2-}containing wastewater in traditional CW starts impacting the treatment efficiency due to the precipitation of toxic S^{2-} and associated toxicity build-up. Further, a

comparison of treatment efficiency between *CW-MFC-replete* and *CW-MFC-deplete* shows that the presence of SO_4^{2-} in wastewater has a substantial influence on the treatment efficiency and electricity generation. This study also concludes that the redox coupling of SO_4^{2-} and its reduced product in the presence of electrodes have positive impact in CW-MFC, and no toxicity buildup was observed in the substrate; rather, it increased its treatment and electricity performances. The microbiological study also proved that *CW-MFC-replete* had higher microbial diversity (high Shannon index) with the abundance of SRB and SOB for reduction and oxidation of sulphur compounds. Thus, CW-MFC has proven as a promising alternative technology for treating SO_4^{2-}containing industrial or mine wastewaters without obstructing the treatment performance even with the long-term operation. However, still a clearly proven pathway for nitrogen removal in association with sulphur should be explored in pilot level planted CW-MFC. In prospective with the economic value of CW-MFC it is suggested to use reusable low-cost conductive material of natural origin such as natural coal. In this study the conductive material was mainly carbon-based natural material and was cost-effective. Thus, the studied process is economical and sustainable.

Acknowledgments

The authors would like to acknowledge the facilities provided by the Central Science Laboratory (CSL), the University of Tasmania for SEM-EDX analysis. The authors would also like to acknowledge the XPS facility provided by Mark Wainwright Analytical Centre, The University of New South Wales. Further, the authors would like to extend the acknowledge for the financial support received from the University of Tasmania and the Grant received from the Tasmanian Community Fund (31Medium00171).

Chapter 5: Influence of applied potential on treatment performance and clogging behaviour of hybrid constructed wetland-microbial electrochemical technologies

Graphical Abstract

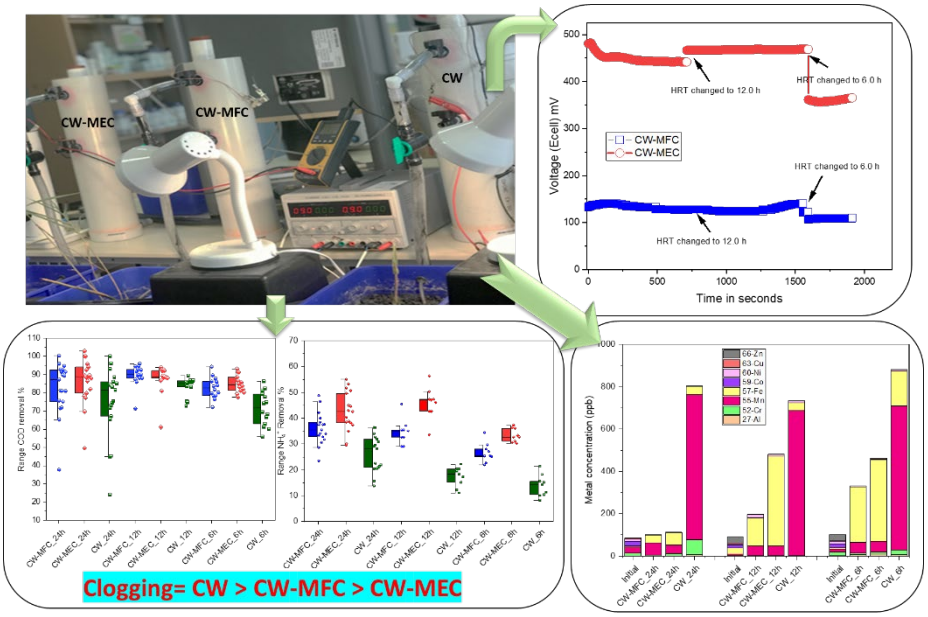

Abstract

A two-stage hybrid Constructed Wetland (CW) integrated with a microbial fuel cell (MFC), and microbial electrolysis cell (MEC) has been assessed for treatment performance and clogging assessment and further compared with CW. The CW-MEC was operated with applied potential to the working electrode and compared with the performance of naturally adapted redox potential of the CW-MFC system. A complex synthetic municipal wastewater was used during the study, which was composed of trace metals, organics, inorganics, and dye. The study demonstrated that providing a constant potential to the working electrode in CW-MEC has resulted in high treatment performance and reduced sludge generation. The maximum chemical oxygen demand (COD), ammonium (NH_4^+), and phosphate (PO_4^{3-}) removal achieved during

treatment by CW-MEC at 24h hydraulic retention time was 89±6%, 72±6% and 93±2%, respectively. ICP-MS results indicated that trace metal removals were also higher in CW-MEC than in CW alone ($p < 0.05$). At the end of the experiment, a significant volumetric change (total volume of the microcosm) occurred in CW (1.3L), indicating high sludge generation. In contrast, it was lesser in CW-MEC (0.3 L) and in CW-MFC (0.5 L). Further, Energy Dispersive X-ray (EDX) spectroscopy results indicated low levels of metal precipitation in the CW-MEC system. Based on the Shannon diversity index, the CW-MEC was assessed to be characterised by high species richness and diversity. The observations from this study indicate that the applied potential at the working electrode has a significant impact on the system's treatment performance and clogging behaviour.

5.1. Introduction

Biological treatment processes are eco-friendly and cost-effective techniques for wastewater treatment. They are widely used to treat various pollutants such as nutrients, organic matter, heavy metals, and dyes [194, 195]. One class of biological wastewater treatment systems, constructed wetlands (CWs), have been used for the treatment of a variety of wastewaters, including municipal [196], domestic [197], industrial [198] and mining [199] effluents. The CWs are considered sustainable technology based on their main features, including low maintenance, operation, and construction cost [19, 183]. As it is a biological process, the treatment performance of CWs is impacted by the operating conditions and composition of the wastewater [200, 201]. One primary concern for biological processes is excessive sludge formation, which requires further disposal or management that alone can account for 25-50% of total operating cost for the treatment processes [202].

Furthermore, clogging associated with sludge formation is common, and the accumulation of organic/inorganic constituents can lead to a decrease in a system’s lifespan [162]. Due to clogging, effective treatment of various pollutants such as nutrients, organic matter, dyes and

metals in the same system is complicated [203], and hinders treatment performance. Based on previous studies, uncoupled microbial metabolism plays a crucial role in the generation of excess sludge [202, 204]. Excess sludge production in biological treatment processes has always been linked to the microbial community's composition, thus change or transformation in the microbial community might reduce the sludge formation and enhance treatment performance [202, 205]. It has also been reported that the generation of excess sludge can be reduced by applied potential [202].

In recent decades, microbial electrochemical technologies (MET) have been widely used for improving wastewater treatment with electrogenic microbial activity [99, 176]. Recent MET-based CWs have proven to be an efficient biological method for improved wastewater treatment while simultaneously producing electricity [33, 159]. The integration of MET in CWs, either in the form of CW-Microbial Fuel Cell (CW-MFC), CW-Microbial Electrolysis Cell (CW-MEC), or electroactive wetlands, enhances the reaction rate by assisting the normal microbial community and promoting electroactive microbes sometimes referred to as 'electrogens' [131]. These electroactive microbes use conductive materials as electron donors and acceptors, based on reactor configurations, to transfer an electron from anaerobic oxidative (anode) to aerobic reductive (cathode) regions [160, 164]. The recovery of electrons from the microbial cell is mainly based on the redox potential between the anode and the cathode [99]. To date, the high internal resistance of CW-MET is the major cause of low voltage output or electron recovery, even with high treatment performance [206, 207]. Several studies have attempted to obtain high electron recovery and higher electrical performance in CW-MFC [207, 208].

On the other hand, a few studies analysed CW-MET performance by applied potential targeting specific pollutants such as nitrate removal [71]. Similarly, Xiao, et al. [206] have applied voltage to the anode of CW-MFC to study nitrogen removal performance and its effect on reed

planted in CW-MFC. The study observed that at an applied potential of 3V, the 'giant reed' species *Arundo donax* was able to adapt, and growth was unaffected; however, at 5V, *A. donax* showed voltage stress. The study concludes that the level of applied potential used to recover maximum current should also be based on the sustainability of plants at that applied voltage. The applied voltage to the MET systems regulates the redox potential and impacts the system's overall environment. To date, the impact of redox potential on treatment performance, electron recovery, and clogging assessment has not been reported in CW-MET studies. In the present study, a constant potential has been applied to the working electrode (anode) to determine the impact on treatment efficiency and clogging. A complex synthetic municipal wastewater was chosen for the study since it contains a wide range of pollutants, including recalcitrant pollutants (such as trace metals and dyes) similar to real municipal wastewater. The study's main objective was to reduce sludge formation/clogging while achieving high treatment efficiency with maximum electron recovery.

5.2. Materials and methods

5.2.1. Reactor fabrication and start-up

To achieve higher treatment efficiency and reduced sludge generation, three sets of hybrid CW were set up in two stages where vertical up-flow CWs (VUF-CW) were followed by horizontal flow CWs (HF-CW). The laboratory-scale hybrid CW microcosms, VUF followed by HF, were set up using PVC pipes and plastic containers, respectively. The dimensions of the VUFs were 520 mm X 104 mm (length X diameter), and the HF was 259 mm X 181 mm X 140 mm (length X width X height) for all three sets of microcosms. The substrate used in two sets of hybrid CW microcosms was graphite gravel, whereas the third set of hybrid CW was filled with normal gravel (garden pebbles). The average substrate size used in all three sets of the hybrid CW was diameter (Ø) = 5-8 mm. The net volume (void volume) of each VUF-CW was 1.5 L, and HF-CW was 1.8 L. At the inlet and outlet of each microcosm, large-size gravel of Ø = 10-

12 mm was used to support equal distribution of wastewater and to avoid clogging at the inlet and outlet zones. One of the two sets of hybrid VUF-CW microcosms filled with graphite was integrated with MFC (CW-MFC). The other graphite-filled VUF-CW was integrated with a continuous voltage supply at the working electrode (CW-MEC).

The HF-CW of CW-MFC and CW-MEC were filled with graphite gravel without any compartmentation or electrical circuitry (electroactive wetlands). The third set of hybrid CWs was filled with regular gravel (garden pebbles) without any compartmentation in VUF-CW, followed by HF-CW. The HF-CW substrate configuration of CW-MFC and CW-MEC was as follows: at the bottom, 40 mm layer of large-sized normal gravel (Ø = 10-12 mm), overlaid by graphite gravel (Ø = 5-8 mm) up to the height of the microcosm. The VUF-CW of CW-MFC and CW-MEC filling was as follows: large size normal gravel to 40 mm from the bottom, overlaid by graphite gravel of thickness 170 mm (anode), followed by a normal gravel layer of 210 mm thickness as a separator, again overlaid by graphite gravel of thickness 80 mm (cathode). The anode and cathode of VUF were equipped with a charge collector of graphite plates (length x width = 100 x 100 mm) buried in graphite gravel. Graphite plates of the same dimension were used as the cathode with ¼ of the area in contact with the air. One end of each of the graphite plates was connected to a stainless-steel wire (0.1 mm). The VUF-CW of all three sets of microcosms were equipped with perforated PVC pipes to monitor the redox potential at the anode and regulate the mixing of wastewater in the microcosm. The pipes were 400 mm x 50 mm (length x diameter) with 2 mm holes along their lengths. These were buried in the layers to about 140 mm above the bottom of the microcosm. In CW-MFC, a reference electrode Ag/AgCl (Sigma Aldrich, Australia) was used to monitor redox potential through the perforated PVC pipe, whereas, in CW-MEC, the perforated PVC pipe was to provide a constant potential through a reference electrode to the working electrode (anode). The HF-CW of three sets of microcosms were planted with common reed (*Phragmites australis).*

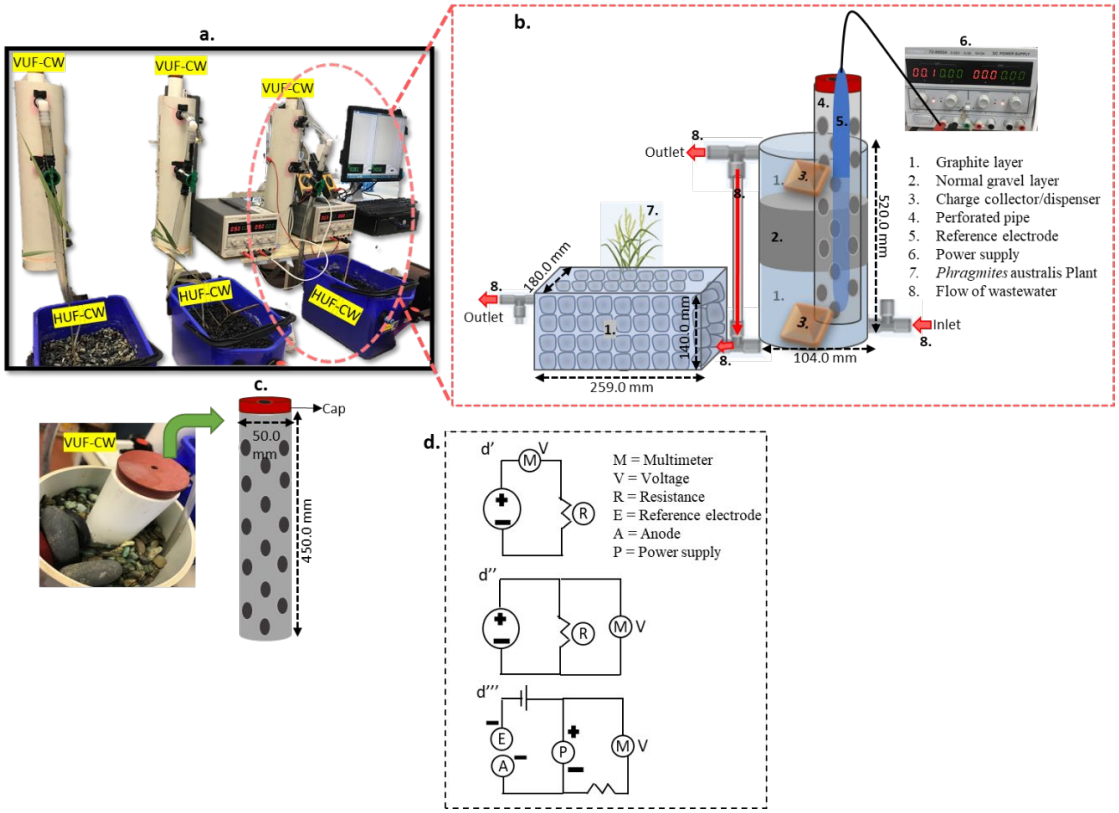

Figure 5-1. The laboratory setup of hybrid CW reactors: ***a.*** *laboratory photos of the three hybrid-CW setups,* ***b.*** *schematic diagram of one of the hybrids CW (CW-MEC),* ***c.*** *measurement of perforated pipe used in VUF-CW of all the microcosms,* ***d.*** *the electrical circuit used in CW-MET for the measurement of current (d'), voltage (d''), and applied potential through reference electrode (d''').*

5.2.2. Synthetic wastewater composition and inoculum

The reactors were fed with synthetic complex wastewater in a continuous mode. The composition of wastewater was adopted from Wang, et al. [202] with little modification except the addition of chromium and methylene blue dye as additional pollutants. The composition of wastewater was as follows: 118.0 mg/L $C_6H_{12}O_6$, 216.0 mg/L, $C_2H_3NaO_2$, 59.0 mg/L KH_2PO_4, 153.0 mg/L NH_4Cl, 28.0 mg/L, $CaCl_2$, 51.0 mg/L, $MgSO_4 \cdot 7H_2O$, 9.0 mg/L $FeSO_4 \cdot 7H_2O$, 0.005 mg/L H_3BO_3,0.005 mg/L $ZnCl_2$, 0.003 mg/L, $CuCl_2$, 0.005 mg/L $MnSO_4 \cdot H_2O$, 0.005 mg/L $(NH_4)_6Mo_7O_{24} \cdot 4H_2O$, 0.005 mg/L $AlCl_3$, 0.005 mg/L, $CoCl_2 \cdot 6H_2O$, 0.005 mg/L $NiCl_2$, 0.005 mg/L $K_2Cr_2O_7$ and 0.5 mg/L, $C_{16}H_{18}ClN_3S$ (methylene blue).

All the microcosms were inoculated with sludge inoculum (2.0% v/v) collected from a local wastewater treatment plant operated by TasWater in Launceston, Tasmania, Australia. At the beginning of the experiments, all three reactors were inoculated with 500 ml sludge inoculum mixed with 9.4 L of synthetic wastewater. The inoculum and synthetic wastewater were mixed and kept in the refrigerator overnight before using it in the microcosms. The media inside the microcosm was changed regularly using a 1:1 ratio, where 1 part of old media from the microcosm was mixed with 1 part of freshly prepared media, and microcosms were kept in batch mode of operation for two months. Afterwards, the microcosms were operated in continuous mode for another month. Once the microcosms reached a steady state, all the analysis was commenced.

5.2.3. Operation strategy and redox potential measurement

The microcosms were operated on over 420 days in a continuous mode with a constant chemical oxygen demand (COD) of 275 mg/L. The organic loading rate (OLR) was varied with decreasing HRT. At HRT of 24 h, the OLR was 11 mg/L-d, with decreased HRT of 12 h and 6 h; the corresponding OLR was 23 mg/L-d and 45 mg/L-d, respectively. The pollutant removal efficiency and clogging assessment was monitored on all three HRTs. In the first week of the experiment, the polarization of the cathode and anode of CW-MFC and CW-MEC was performed by applying potential through a power supply. The anode polarization of CW-MFC and CW-MEC was performed at an applied potential of -100 to -400 mV against an Ag/AgCl reference, and the cathode polarization at an applied potential from 100 to 400 mV. Based on the measured current, CW-MEC was configured to provide -400 mV at the anode continuously. The CW-MEC was continuously run at a fixed potential at the anode with the help of a DC power supply (TENMA, DC POWER SUPPLY).

5.2.4. Analysis and Calculations

The microcosms were monitored daily for pH, temperature and redox potential. The average room temperature was ~23°C. The wastewater treatment parameters, total organic carbon (TOC), chemical oxygen demand (COD), total nitrogen (TN), ammonium (NH_4^+), phosphate (PO_4^{3-}), dye and metals were analysed every week. All the samples were filtered through a syringe filter (0.45µm, MicroScience) before analysis. The TOC and TN analysis was performed with Shimadzu TOC-TN analyser (Model TNM-L ROHS), COD was analysed according to the APHA standard methods 5220D [84]. The NH_4^+, NO_3^-, NO_2^- and PO_4^{3-} was analysed with ion chromatography (Eco IC, MEP Instruments, Metrohm). Dye removal was analysed through UV-Vis Spectrophotometer (Agilent technologies) by comparing with the standard curve. The metal concentration was measured through Inductively coupled plasma mass spectrometry (ICP-MS). Furthermore, the voltage (E_{cell}) was recorded every 12 seconds using a PC_{LINK} multimeter connected to the computer. The internal resistance of CW-MFCs is a measure of the voltage against current. In the present study, the internal resistance was determined as the ratio of measured current and the voltage reduction from open-circuit voltage (OCV) to current at a particular operating point.

The gravels from each microcosm's anode were characterised by scanning electron microscopy (SEM, Hitachi SU-70 field emission SEM) to observe the precipitate on the gravels. The dehydration of gravels was performed by submerging in glutaraldehyde solution (2.5%) for 1 hour, then rinsing with phosphate buffer (pH = 7) three times and then submersion in ethanol (30%, 50%, 70% then 90%) each for 10 minutes [176]. All samples were freeze-dried (-18°C). Further, the samples were coated with platinum for surface morphology analysis by SEM. The samples' elemental composition was determined by the attached Energy Dispersive X-ray (EDX) spectroscopy (Oxford AZtec XMax80 EDX system).

5.2.5. Volatile suspended solids (VSS), Volumetric change, and Tracer test

Sludge generation and clogging were analysed by VSS analysis, volumetric change, and tracer test. These were compared with the conditions at the beginning and the end of the experiment. The VSS of all three sets of the hybrid CW was analysed at the beginning of the experiment and then after each HRT. Samples of 200 mL were taken from both HF-CW and VUF-CW of each set of microcosms. Samples were filtered through a Whatman glass microfibre filter paper of 0.7 μm pore size and dried at 500°C in a furnace (Labec, manufactured in Australia) for one hour. The VSS was calculated based on Equation (Eq.) 1,

$$VSS\ \left(\frac{mg}{L}\right) = I_W - F_W \qquad Eq.1$$

Where I_w is the initial weight of the samples, and F_w is the final weight of the samples after drying.

The volumetric change (net volume) was estimated by discharging the whole volume from the microcosms at the start of the experiment and after completion of the 24 h, 12 h and 6 h HRT experiments. The volume difference was calculated by subtracting the final volume from the initial volume each time, Eq. 2. The net volume was the volumetric change of each microcosm.

$$Net\ volume\ (L) = Initial\ Volume - Final\ Volume \qquad Eq.2$$

At the end of the experiment, a dye tracer test was performed where 2 g of methylene blue dye was dissolved in 1 L of tap water and injected in the inlet pipeline of each microcosm. The HRT was determined from the time taken for the dye to travel from injection to its appearance at the outlet. Clogging was analysed based on the differences between initial HRT and the HRT of dye within the system at the end of the experiment. The retention time of dye within each setup was calculated by Eq.3,

$$Hydraulic\ time\ (h) = Retention\ time\ -\ Injection\ time \qquad Eq.3$$

5.2.6. 16s RNA sequencing

Microbiological samples were taken from each component (VUF and HF) of the hybrid-CWs after completion of the experiments to monitor the change in microbial diversity of each microcosm. The gravels and 50 mL of wastewater were taken from each microcosm's anode (VUF and HF of all three sets of microcosms). DNA extraction and diversity profiling were performed by AGRF, Australia. The Amplicon sequencing was performed to analyse the data with target 27F with reverse and forward primer of AGAGTTTGATCMTGGCTCAG and GWATTACCGCGGCKGCTG, respectively. The total read length was 300 bp. Diversity profiling analyses were performed with QIIME 2 2019.7 [209]. The demultiplexed raw reads were primer trimmed and quality filtered using the cutadapt plugin followed by denoising with DADA2 (via q2‑dada2) [210]. Taxonomy was assigned to ASVs using the q2‑feature classifier [211] classify‑sklearn naïve Bayes taxonomy classifier.

5.3. Results and discussion

5.3.1. Electric potential measurements

Figure 5-2 demonstrates the current generation of CW-MFC and CW-MEC with the varied anodic and cathodic potential; the maximum measured current in both microcosms was at an applied potential of -400 mV. As shown in *Figure 5-2*, with more negative applied potential (-400 mV) at the anode and more positive applied potential (400mV) at the cathode, the current generation was higher in CW-MFC than in CW-MEC. Based on this, the working electrode (anode) of CW-MEC was held at a constant voltage of -400 mV throughout the experiment. On the other hand, to verify the role of redox potential gradient for the recovery of electrons in terms of E_{cell} (cell potential) in CW-MFC, cell potential was monitored and compared with CW-MEC. Since the anode of CW-MEC was held at a negative potential due to the favourable redox gradient, the maximum E_{cell} measured was 480 mV at 24 h HRT, which decreased to 466 mV and 359 mV at 12 and 6 h HRTs, respectively. On the other hand, the mean value of natural

anode potential in the CW-MFC was -237 mV, lower than the desired potential to generate maximum voltage as obtained from *Figure 5-2*, i.e., the measured E_{cell} in the CW-MFC was lower than the CW-MEC at all HRTs. The maximum measured E_{cell} in the CW-MFC was 141, 130 and 109 mV at HRTs of 24 h, 12 h and 6 h, respectively (*Figure 5-3*). Subsequently, the power density of CW-MFC with the decrease in HRTs was 22.1 mWm^{-2} at 24 h, 18.8 mWm^{-2} at 12 h, and 13.2 mWm^{-2} at 6 h. The E_{cell} in the CW-MEC did not significantly vary even with higher OLR, whereas the CW-MFC had lower E_{cell} at all OLRs. The mean cathode potential of CW-MFC and CW-MEC was 238 and 273 mV, respectively, which was similar for both microcosms.

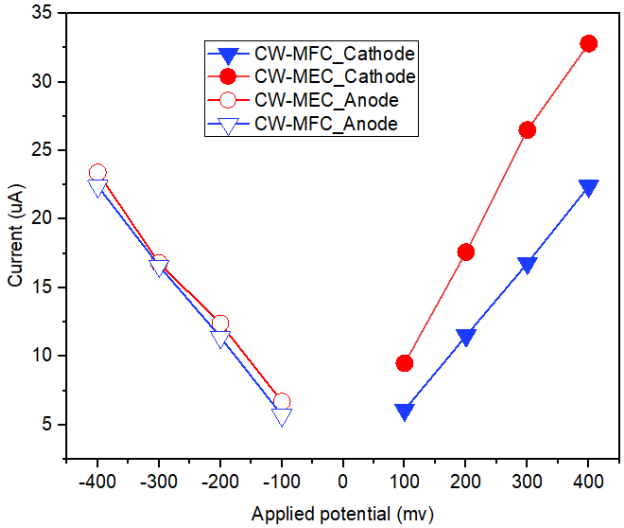

Figure 5-2. The polarization of CW-MFC and CW-MEC: cathodic and anodic polarization on the applied potential of 100 to 400 mV and -100 to -400 mV, respectively.

Additionally, monitoring the redox potential of CW indicated no variation throughout the vertical upflow microcosm bed. Typically, due to the lack of an electron acceptor in traditional CW, microbial metabolism and flow of electrons do not occur through nonconductive gravels; thus, no variation can be observed throughout the gravel bed [212]. Due to enhanced microbial metabolism in the presence of an artificial electron acceptor in the CW-MFC, a sharp redox variation can be observed spatially and temporally. On the other hand, the redox gradient in

CW-MEC further enhances the flux of ions in wastewater, allowing the current flow in the circuit, hence improving the electron recovery [212]. With the applied potential at the anode of CW-MEC, the redox gradient created in the system was favourable for the microbes, decreasing the resistance and enhancing the electron transfer between microbes and electrodes [65, 166].

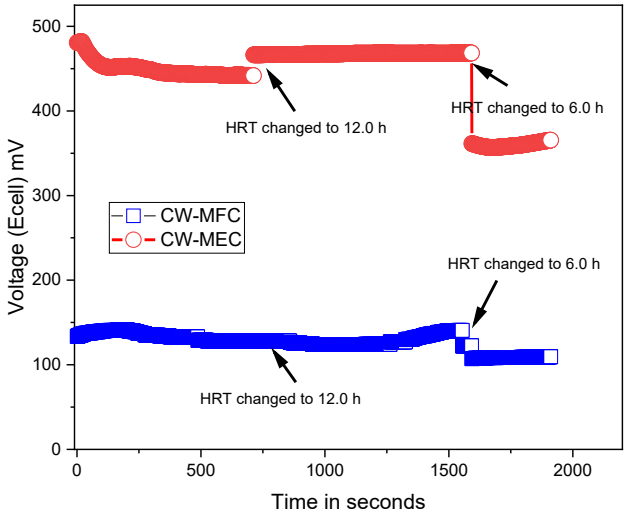

Figure 5-3. Cumulative E_{cell} of CW-MFC and CW-MEC at different HRTs; the time in seconds is the average time that data was collected for different HRTs.

When the anode potential was more negative, it was also closely related to a higher electron flux and higher reduction at electrodes in the microcosms. Mixed microbial communities mainly dominated the CW-MFC and CW-MEC microcosms, and each microbial community has its own optimal potential [99, 166]; in the CW-MFC, the anode potential was allowed to float to a relatively constant potential in comparison to the CW-MEC, where applied potential was constant. Thus, the variation in anodic potential can create losses in electron flow and subsequently decrease electricity generation [207]. Thus, applied potential in the CW-MEC can significantly impact electron flux generated in the microcosm. The low E_{cell} performance of the CW-MFC was due to the high internal resistance of the microcosm. In general, CW-MFCs have high internal resistance due to their large dimension and high surface area. The

internal resistance of CW-MFCs was 1200 Ω at 24 h, which changed to 1450 Ω at 12 h, and 1380 Ω at 12 h. The change in internal resistance was because the internal behaviour of CW-MFC can change with the condition of the cell, with changes of chemistry and physical conditions at the anode and cathode individually. Maintaining constant potential at the working electrode using external power sources might decrease internal resistance resulting in higher E_{cell} performance.

5.3.2. Treatment performance

5.3.2.1. Based on redox potential and different HRT

In previous reported CW-MFC studies, integration of the MFC has always improved the treatment performance of a CW due to the inclusion of an electrode for pollutant removal in the absence of other electron acceptors [128, 131, 207, 213]. The enhancement in treatment performance mainly comes from the pollutant oxidation by electroactive bacteria (EAB) at the CW-MFC's anode. However, due to unfavourable redox potential between EAB and the electrode and further between anode and cathode, electron recovery from microbial cells is usually challenging. Therefore, to understand the influence of redox potential on electron flow, the CW-MFC and CW-MEC treatment performance compared to a CW was evaluated at different HRT. The treatment efficiency was evaluated based on the final effluent flowing through VUF-CW to HF-CW.

Figure 5-4 shows the removal efficiency for several pollutants in a CW-MEC, a CW-MFC and a CW. At 24h HRT, the order of pollutant removal efficiency was: CW-MEC > CW-MFC > CW. The removal efficiency decreased when decreasing HRT (increased OLR) from 24 to 6 h; still, there was a significant difference in the removal performance of CW-MEC in comparison to CW-MFC and CW ($p < 0.05$). The mean COD removal in CW-MEC was 89±6% at 24 h HRT, further decreasing to 84±6% at 6 h HRT. On the other hand, in CW-MFC, the mean COD removal was 85±5% at 24 h HRT, which decreased to 79±9% at 6 h HRT. Likewise,

in CW, the mean COD removal was 76±9% at 24 h HRT, which decreased to 69±6% at 6 h HRT. *Figure 5-4* shows that the treatment efficiency of CW-MEC was better than other microcosms at all the HRTs. Furthermore, the same pattern was observed for other pollutants such as TN, NH_4^+, and PO_4^{3-} shown in *Table 5-1*, where maximum removal was achieved in the CW-MEC which had a significant treatment performance difference compared to CW at 6 h HRT ($p < 0.05$). A significant difference in treatment performance was also observed between CW-MFC and CW-MEC ($p < 0.05$) at HRT of 6 h. Doherty, et al. [143] reported removal of 64-81% COD, 48-52% TN, 55-59% NH_4^+-N for treating swine wastewater in a vertical graphite based CW-MFC. The methylene blue dye was also used as a model pollutant, which was 100% removed in all the reactors at 24 and 12 h HRTs, whereas this dropped to 65±10 % removal in CW at 6 h HRT. Yadav, et al. [33] has also reported 80% of methylene blue removal from the initial concentration of 2000 mgL^{-1} in HRT of 4 days in vertical graphite-based CW-MFC.

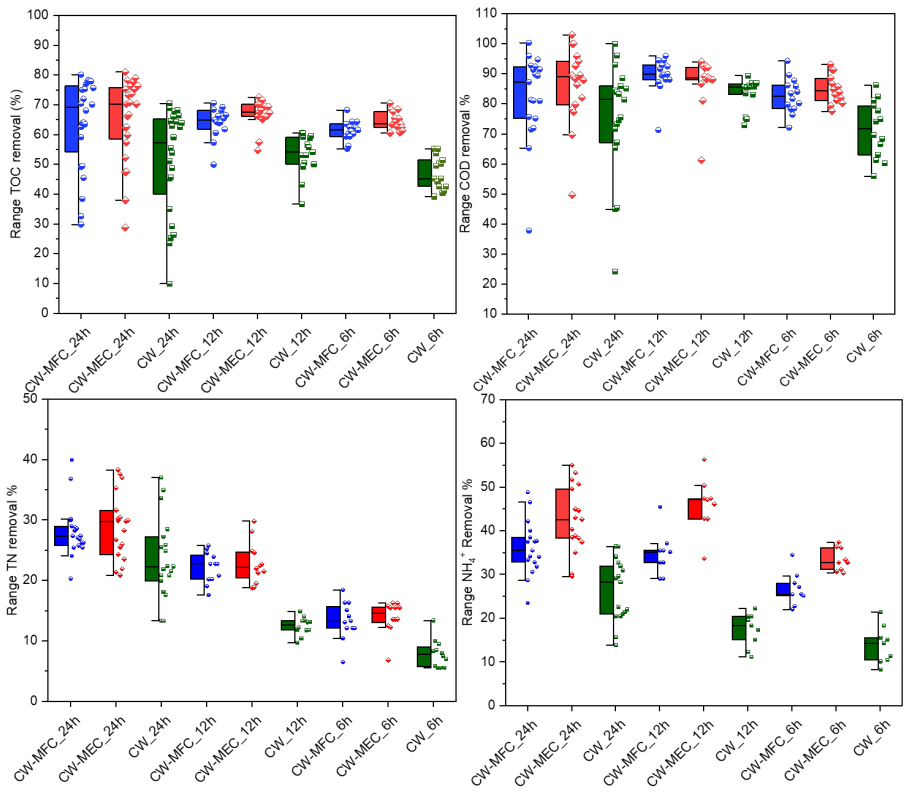

Figure 5-4. The range of TOC, COD, TN, and NH_4^+, removal in all reactors at different HRTs.

Table 5-1. The mean influent concentrations and removal efficiencies of pollutants at different HRTs in CW-MFC, CW-MEC and CW.

		CW-MEC (%)			CW-MFC (%)			CW (%)		
		HRT (h)								
	Initial (mg/L)	24	12	6	24	12	6	24	12	6
TOC	108±12	65±7	66±5	64±8	63±9	64±12	61±6	53±6	53±10	47±9
COD	267±8	89±6	87±4	84±5	85±5	86±8	80±9	76±9	74±4	69±6
TN	67±4	59±5	33±9	24±5	48±9	22±6	13±3	35±6	12±4	8±5
NH_4^+	66±7	72±6	55±5	38±7	66±5	42±4	26±8	48±7	17±4	13±5
PO_4^{3-}	210±4	93±2	89±5	74±6	92±6	86±4	71±3	79±6	65±9	50±7

The low treatment performance of CW was due to limited organics oxidation in the absence of an electron acceptor since normal gravels cannot participate in charge transfer, and the electron acceptor (oxygen) was mainly present at the surface (most of the portion was anaerobic) [172, 197]. On the other hand, the CW-MFC had better performance than the CW due to the electrodes' availability, enhancing pollutant oxidation at the anode and reduction at the cathode. However, the treatment performance of CW-MEC was higher since the redox potential of the system played a significant role in electron recovery and subsequently in the treatment performance. The CW-MEC was supplied with a constant anode potential that maintained positive redox potential between anode and cathode, along with microbes and electrodes that favoured efficient electron recovery from the microbial cells. The CW-MFC treatment performance and the CW-MEC indicate that the redox gradient substantially influenced treatment performance. The results imply that with applied potential in CW-MEC, the redox potential was consistent and microbial metabolism was satisfactory; hence the electron recovery and pollutant removal were high. Nevertheless, with the natural potential differences in CW-MFC, the microbial metabolism was interrupted at a higher loading rate since microbes had to maintain the potential naturally, which causes low treatment efficiency in CW-MFC at higher OLR.

5.3.2.2. Based on different metals

Metals are often present in wastewater in variable concentrations; however, in municipal wastewater, metals are expected to be relatively low. In the previous studies of electroactive wetlands, chromium removal was reported to be 99.9%, even at a high loading rate [177]. In the present study, trace levels of Al, Zn, Cr, Mn, Ni, Cu, Fe and Co, each with an initial concentration of 5µg/L, were studied. All the metals were quite low in the effluent of all the microcosms except Fe and in some cases Mn. The Mn concentration was high in the CW effluent at all three HRTs compared to the CW-MFC and CW-MEC (*Figure 5-5*). However, the composition of normal gravels used in CW revealed a high level of Mn (confirmed from SEM analysis), the likely source of high Mn in the effluent. Since microcosms were operated for a quite long time (>12 months) the gravels could have released Mn in the system. The other reasons for high Mn in the effluent of the CW, CW-MEC and CW-MFC other than the influent concentration could be due to oxidation and reduction state of Mn in the microcosms. The Mn would have first oxidized from Mn^{2+} to $Mn^{4+,}$ which is highly insoluble, and its accumulation and later oxidation to MnO_2 (soluble form) would have accounted for the increase in concentration. Moreover, the Mn concentration was not very high in the CW-MEC and CW-MFC. On the other hand, most metals such as Al, Zn and Co in the effluent were below the detection limit range in CW-MFC and CW-MEC. The Al range in the CW was 5.6 to 8ppb, while Zn and Co were below the detection limit. The observed Fe concentration in CW-MFC at 24 h HRT was 36.3 ppb, which increased to 130ppb at 12 h HRT and 262.5 ppb at 6 h HRT. In the CW-MEC, the observed Fe concentration at 24 h HRT was 58.5 ppb, which increased to 425.0 ppb at 12 h HRT and 386.8 ppb at 6 h HRT.

On the other hand, the maximum observed Fe concentration at 6 h HRT in CW was 166.0 ppb. The Fe concentration was high in the CW-MFC effluent and the CW-MEC with decreased HRT (at a high loading rate). Under oxidising conditions, Fe is readily oxidised from Fe^{2+} to

$Fe^{3+,}$ which readily forms insoluble oxyhydroxides. Under reducing conditions, this is readily converted back to the highly soluble Fe^{2+}. Alternately, the high flowrate required to produce a 6 h HRT, could force precipitates of Fe compounds through the system. The other reason for higher Fe concentration in CW-MET than the CW could be due to participation of Fe in pollutant removal in CW, which consumed Fe, whereas in CW-MET the role of Fe was limited. Other metals were not significantly high in the effluent of CW-MFC and CW-MEC even at 6 h HRT. However, at decreased HRT in the CW the concentration of Cr in the effluent reached 21.7 ppb. The dominating reaction mechanisms involved in the removal of metals in a CW are adsorption to organic complexes and precipitation on the substrate [214]. Like Fe oxyhydroxides, Mn oxides can also undergo reductive dissolution under anoxic conditions, where Mn^{4+} is reduced to Mn^{2+} [215, 216]. The accumulation of Fe is usually high in the CW substrate due to its less reductive nature and low redox potential. Zn has a lower adsorption affinity typically to the substrate than Cu and Pb; however, complexes of Zn with Mn and Fe are the major mechanism for removal in CW [216]. Additionally, the high removal of metals in MET integrated CWs could be due to mainly electroactive microbial mediated reaction mechanisms [177]. Several other studies have reported biological activity for removing metals from wastewater [150, 217]. Electroactive bacteria have also been shown to efficiently remove metals from the wastewater in MET [177, 217].

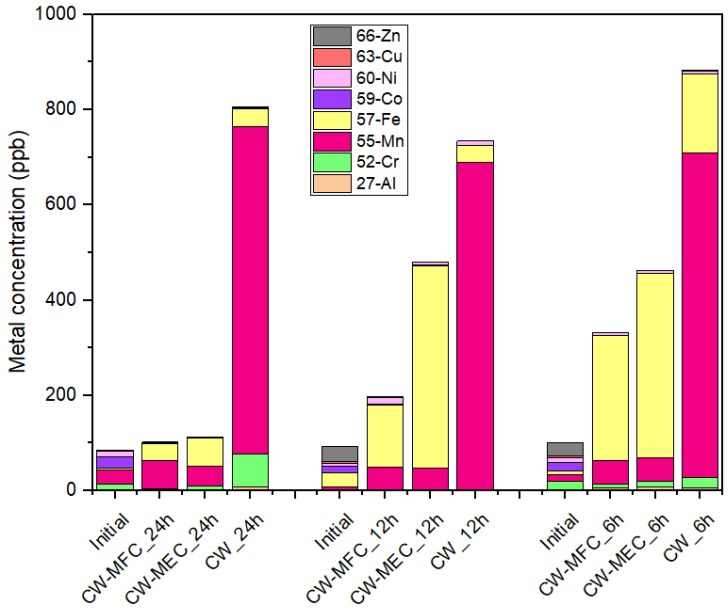

Figure 5-5. The mean value of different trace metals in CW-MEC, CW-MFC, and CW at different HRTs.

5.3.3. Clogging tendency assessment

Due to inefficient pollutant removal, sludge generation and solids accumulation typically occur in a traditional CW. This, in turn, results in clogging and hinders the operation and retention time of the pollutants. Thus, the impact of electron flow on clogging was evaluated in CW-MFC, CW-MEC and CW systems. Clogging at high OLR was assessed based on net volume, VSS, and HRT of each microcosm at the beginning and end of each HRT experiment. *Table 5-2* gives details of the volumetric change, VSS and tracer tests.

Based on *Table 5-2*, the change in net volume (void volume of the microcosm) from the beginning of the experiment to the end of an experiment was not substantial in the CW-MEC and CW-MFC; however, it was substantially different in the CW. At the end of the experiment, the net volume change was 0.3 L in the CW-MEC_VUF and 0.5 L in the CW-MFC_VUF; this was 0.6 L in the CW_VUF. While there was no change in the net volume in the CW-MEC_HF, it decreased to 0.2 L in the CW-MFC_HF and 0.7 L in the CW_HF from the initial volume.

Table 5-2. The difference in net volume and VSS, and tracer test for all microcosms at the beginning and at the end of the experiments.

	Net volume (L)				VSS (mg/mL)				Tracer test	
	Initial	HRT (h)			Initial	HRT (h)			Before HRT (h)	After HRT (h)
		24	12	6		24	12	6		
CW-MEC									24	26
VUF	1.5	1.4	1.2	1.2	332	777±123	1277±117	1655±78		
HF	1.8	1.8	1.8	1.8	208	1155±94	2029±107	2233±96		
CW-MFC									24	27
VUF	1.5	1.4	1.0	1.0	145	923±86	2423±123	3083±111		
HF	1.8	1.8	1.7	1.6	131	2247±135	2099±115	3389±87		
CW									24	30
VUF	1.5	1.3	1.0	0.9	103	998±120	2148±110	3516±122		
HF	1.8	1.5	1.3	1.1	396	2297±112	2328±134	3587±99		

Additionally, the accumulation of sludge/biomass was considered by determining the VSS of each microcosm at the start of the experiment and comparing it to the VSS at the end of each HRT experiment. A considerable change in VSS was observed for all the microcosms, among which CW_VUF and CW_HF had higher VSS than the other microcosms. In contrast, the lowest VSS at the end of the experiment was observed in CW-MEC_VUF and CW_MEC_HF. The high sludge formation in the CW was mainly due to two reasons. Firstly, the lower removal of organics accumulated on the substrate in the microcosm, and secondly, the formation of dense biofilm of the substrate (confirmed from SEM). However, due to high treatment efficiency, the CW-MFC_VUF and CW-MEC_VUF only had low organics accumulation, leading to a volumetric change of 0.3 L in CW-MEC_VUF and 0.5 L in CW-MFC_VUF at the end of the experiment. As most of the pollutants were removed in the VUF, due to a faster reaction rate, there was no substantial volumetric change nor major sludge generation observed in CW-MEC_HF and CW-MFC_HF. The high treatment efficiency in CW-MET decreased the system's organic and biomass accumulation, which decreased the high sludge generation.

Tracer tests using methylene blue dye were also performed at the end of the experiment to observe any differences in HRT. The change in HRT was not large in either the CW-MFC or the CW-MEC and the HRT of 24 h at the start of the experiment increased only to 25 h at the end of the experiment. On the other hand, it increased to 30 h in the CW due to sludge formation in both the CW_VUF and CW_HF. Due to the decreased flow rate in the CW, it was only able to treat a lower volume of wastewater in a given time compared to the CW-MEC and the CW-MFC. Since in a given time, a low amount of wastewater was passing through the system in comparison to the other microcosms.

The CW-MFC and CW-MEC results show that the systems were quite adaptable even at high OLRs. As mentioned earlier, most of the pollutants were removed in the first stage of hybrid systems leading to less sludge generation and high performance. The other indicator for less sludge generation in the system is electron recovery. Corbella, et al. [162] has mentioned that sludge generation is negatively correlated to electron recovery, and high sludge generation restricts electron recovery. In the present study, the high electron recovery in CW-MEC through to the end of the experiment indicates sludge generation should be low, and electron flow remained unrestricted.

Furthermore, with a maintained redox potential of CW-MEC the reaction mechanism of CW-MEC enhanced resulted in high treatment efficiency with reduced sludge generation. Overall, due to the high treatment performance of CW-MEC and CW-MFC in comparison to CW, the system had low solid accumulation thus low sludge generation. Whereas low performing CW had higher solid accumulation with high sludge generation. Thus, conductive material-based CWs have proven an efficient way to avoid clogging/sludge formation even at high OLR and over a longer period (greater than 12 months) of operation.

5.3.4. Microbiology

The microbial diversity and richness in all VUF and HF components of the CW-MEC, CW-MFC and CW microcosms were analysed. The CW_HF, CW_VUF, CW-MEC_HF, CW-MEC_VUF, CW-MFC_HF and CW-MFC_VUF exhibited 39212, 32925, 40700, 45355, 43890 and 22615 non-chimeric sequences, respectively, with an average read of 300 bp.

The Shannon diversity index was used to characterize calculated species richness and diversity. The Shannon indices of the various microcosms were CW_HF 4.3; CW_VUF 5.1; CW-MEC_HF 0.88; CW-MEC_VUF 5.3; CW-MFC_HF 2.9; and CW-MFC_VUF 4.4. The maximum Shannon index was observed in the VUF of all three sets of microcosms, while the HF had a low index. The CW_HF had the highest Shannon index (4.3) among the HF regions, while the CW-MEC_VUF (5.3) highest index overall. This shows that the CW-MEC_VUF had higher microbial diversity and richness than any other region examined.

The lowest Shannon index was determined for the CW-MEC_HF (0.88). This is not unexpected as the hybrid CW-MEC was an integrated system with the VUF component preceding the HF component. It would be expected that in such a system, a significant fraction of pollutants were removed in VUF, leaving only low carbon levels and hence microbial growth in the HF. The higher Shannon index in CW-MEC_VUF indicates increased diversity and richness of a limited number of specific microbes, which contributed to high treatment efficiency with low sludge generation [202, 218]. The CW, CW-MFC and CW-MEC's microbial community identification indicates microbes from 44 different phylum (*Figure 5-6*). The dominant microbes present in all the microcosms were from the phylum *Firmicutes, Actinobacteria, Chloroflexi, Proteobacteria* and *Bacteriodetes.* The dominant phyla were consistent with our previous CW-MFC and electroactive wetlands, both of which used the same source inoculum as the current study [131, 177].

At the Class level, 106 classes were identified (*Figure 5-6*), of which class *Gammaproteobacteria* (17.3%) was the most dominant microbes in CW-MEC_HF from phylum *Proteobacteria* followed by class *Bacilli* (14.0%) from phylum *Firmicutes*. In contrast, in another microcosms class, *Bacilli* from phylum *Firmicutes* was the dominating microbes. These microbes' abundance shows higher performance in electrode-assisted microcosms for improved treatment and reduction in sludge generation. The microbes from phylum *Firmicutes, Actinobacteria*, *Bacteroidetes,* and *Proteobacteria*, are known to be responsible for organic degradation and electron transfer in the anaerobic region [172, 189]. In addition, *Proteobacteria* play an important role in bioelectrochemical activities and are responsible for the degradation of recalcitrant pollutants such as metals [172]. The phylum *Bacteriodetes* are well recognized as capable of degradation of proteins and polysaccharides, which may be correlated with settleability and reduction of sludge in CW-MFC and CW-MEC [202, 219]. The other non-electrogenic bacteria, such as heterotrophic anaerobes, also participate in organic degradation at an enhanced rate and assist electron shuttling in electroactive wetlands [220, 221]. The observed microbial diversity indicates their role in treatment efficiency and the reduction of sludge generation. The applied potential allows the growth of diverse microbes with a higher metabolic reaction rate, which enhances higher treatment efficiency to reduce sludge generation.

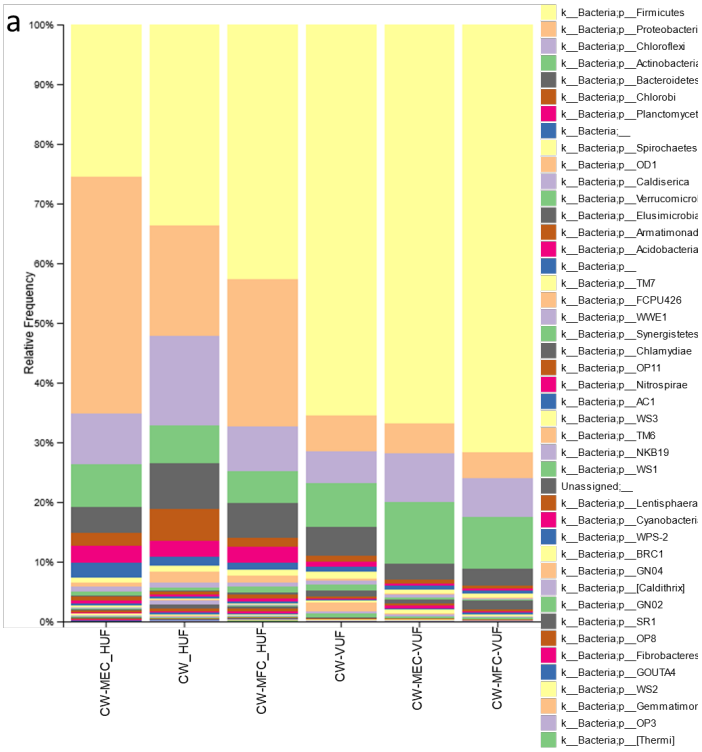
a
Relative Frequency
100%
90%
80%
70%
60%
50%
40%
30%
20%
10%
0%
CW-MEC_HUF
CW_HUF
CW-MFC_HUF
CW-VUF
CW-MEC-VUF
CW-MFC-VUF
k__Bacteria;p__Firmicutes
k__Bacteria;p__Proteobacteri
k__Bacteria;p__Chloroflexi
k__Bacteria;p__Actinobacteria
k__Bacteria;p__Bacteroidetes
k__Bacteria;p__Chlorobi
k__Bacteria;p__Planctomycet
k__Bacteria;__
k__Bacteria;p__Spirochaetes
k__Bacteria;p__OD1
k__Bacteria;p__Caldiserica
k__Bacteria;p__Verrucomicro
k__Bacteria;p__Elusimicrobia
k__Bacteria;p__Armatimonad
k__Bacteria;p__Acidobacteria
k__Bacteria;p__
k__Bacteria;p__TM7
k__Bacteria;p__FCPU426
k__Bacteria;p__WWE1
k__Bacteria;p__Synergistetes
k__Bacteria;p__Chlamydiae
k__Bacteria;p__OP11
k__Bacteria;p__Nitrospirae
k__Bacteria;p__AC1
k__Bacteria;p__WS3
k__Bacteria;p__TM6
k__Bacteria;p__NKB19
k__Bacteria;p__WS1
Unassigned;__
k__Bacteria;p__Lentisphaera
k__Bacteria;p__Cyanobacteri
k__Bacteria;p__WPS-2
k__Bacteria;p__BRC1
k__Bacteria;p__GN04
k__Bacteria;p__[Caldithrix]
k__Bacteria;p__GN02
k__Bacteria;p__SR1
k__Bacteria;p__OP8
k__Bacteria;p__Fibrobacteres
k__Bacteria;p__GOUTA4
k__Bacteria;p__WS2
k__Bacteria;p__Gemmatimor
k__Bacteria;p__OP3
k__Bacteria;p__[Thermi]

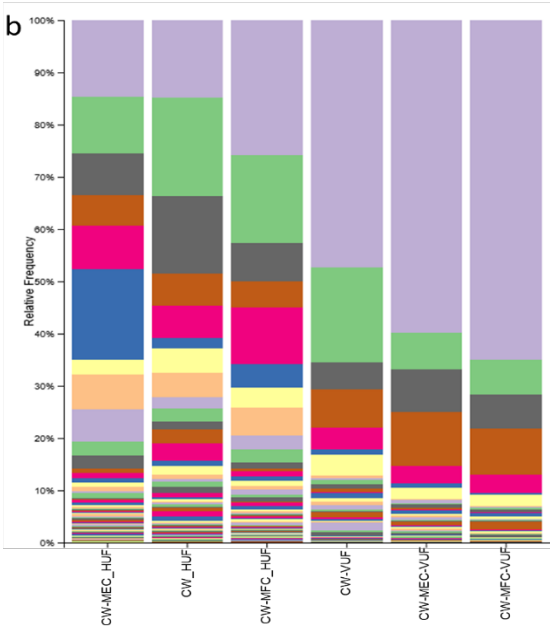
b
Relative Frequency
100%
90%
80%
70%
60%
50%
40%
30%
20%
10%
0%
CW-MEC_HUF
CW_HUF
CW-MFC_HUF
CW-VUF
CW-MEC-VUF
CW-MFC-VUF

Figure 5-6. Microbial communities in the CW-MFC_VUF, CW-MFC_HF, CW-MEC_VUF, CW-MEC_HF, CW_VUF and CW-HF, based on a. Phylum, and b. Class.

5.3.5. Characterisations of precipitates

Scanning electron microscopy was used to characterise the precipitates on the anode gravels of the VUF and HF of the CW-MEC, CW-MFC and CW. The SEM analysis revealed rod-shaped biofilm formation and organic aggregates on the gravel of the CW-MFC_HF and CW-MFC_VUF (*Figure 5-7*). Similar biofilm and aggregates were observed on the gravel of the CW-MEC_VUF, though with some linkages to form bio-aggregates.

Less bio-aggregation and less biofilm were observed on the CW-MEC_HF anode gravels (*Figure 5-7*). This is in good agreement with the Shannon index that indicates low microbial diversity and richness on these gravels. Again, this is not unexpected as the higher treatment efficiency in CW-MEC_VUF led to lower levels of organic pollutants flowing to the CW-MEC_HF, limiting microbial growth in this region. On the other hand, CW_VUF and CW_HF were observed to be covered with a dense biofilm of organic aggregates (*Figure 5-7*).

The EDX analysis provides insights into the chemical constituents precipitated on the gravels of each microcosm (*Figure 5-7*). The majority of the surface of the gravels were covered with organic aggregates and inorganic elements. The results reveal that only low metal levels were precipitated on the gravels in the CW-MFC and CW-MEC. However, in CW_VUF and CW_HF, considerable levels of a small number of metals were observed. In the CW_VUF, the relative abundance (based on total counts) of Al was 8.5%, followed by Cr (3.7%), Ni (0.5%), Fe (3.1%), along with minor amounts of other metals. Similarly, in CW_HF, the relative abundance of Fe was 22.2%, followed by Al (3.4%), Zn (2.3%), Mn (0.6%) and again minor amounts of other metals. In contrast, Fe was the major metal species precipitated in the CW-MFC and CW-MEC.

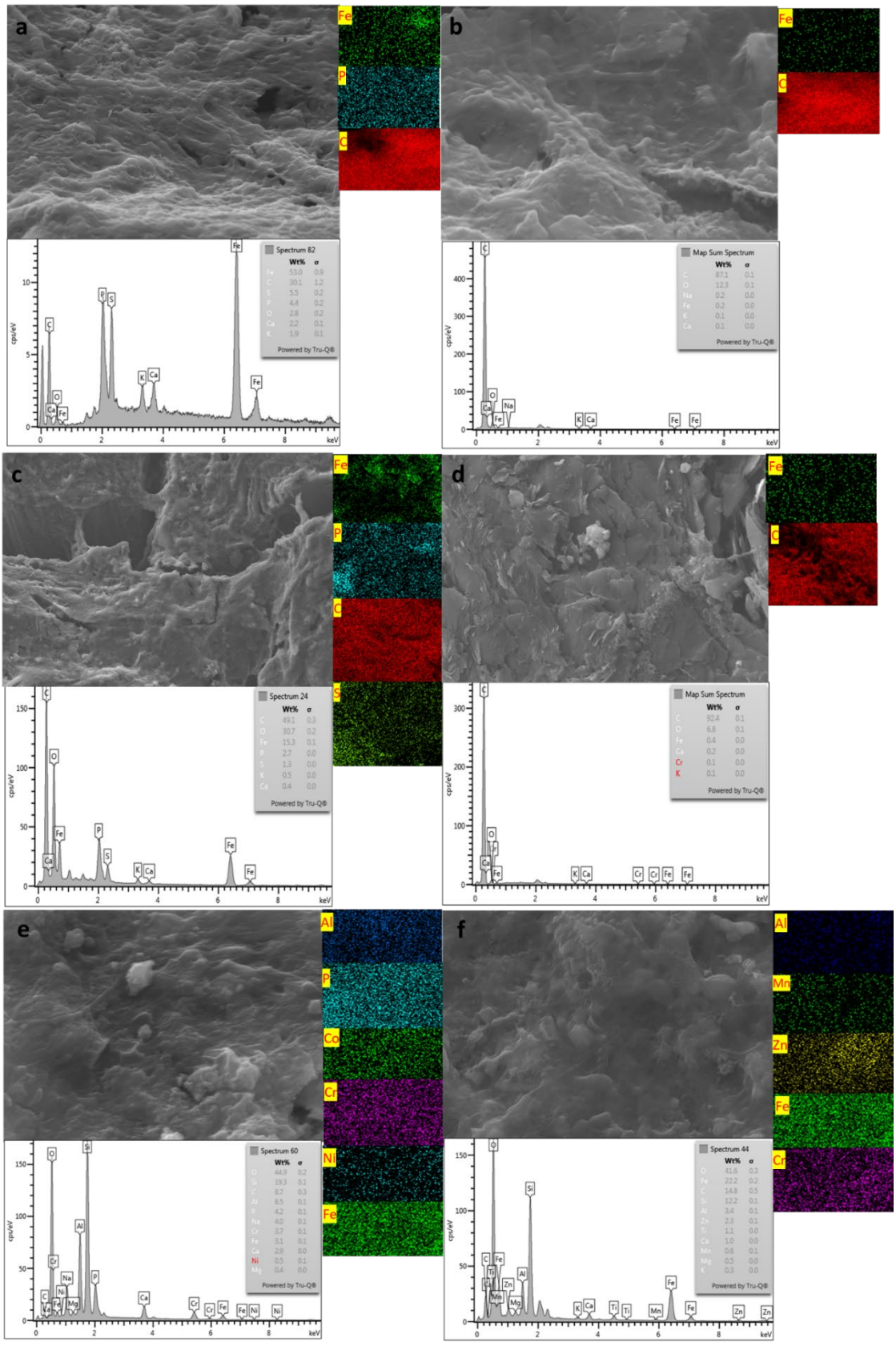

Figure 5-7. SEM-EDX image along with elemental mapping image of a. CW-MFC_VUF, b. CW-MFC-HF, c. CW-MEC_VUF, d. CW-MEC-HF, e. CW_VUF, and f. CW_HF. The abundance of elements is highlighted with different elemental colour mapping.

The coloured mapping associated with SEM imaging in *Figure 5-7* indicates the abundance of elements. The coloured mapping associated with *Figure 5-7 (a, b, c, d)* indicates the lower abundance of metals, while the coloured mapping associated with *Figure 5-7 (e, f)* indicates high abundance of metal in the precipitates. The results indicate that CW-MFC and CW-MEC do not have significant levels of metal precipitates but rather, it might be consumed or mobilised on the microbial surfaces. Moreover, in CW_HF and CW_VUF, high levels of metals were clearly seen in the precipitate. Thus, it is evident that, due to bioelectrochemical reactions in CW-MFC and CW-MEC, metal precipitation was very low in these systems, while in CW, without MET components, metal precipitation was significantly higher.

5.4. Conclusions

The applied potential in CW-MEC had a significant contribution to maintaining redox potential, resulting in higher electron recovery and treatment performance. The treatment performance of CW-MEC was higher than CW-MFC and CW at all HRTs. Even at decreased HRTs (higher OLR), the CW-MEC adapted quickly and performed greater removal of all pollutants included in the feedstock. However, in CW-MFC, the microbes could not adapt easily as the redox potential changed with changing OLR. This resulted in a decrease in treatment performance at an HRT of 6h. Even though the treatment performance decreased in the CW-MFC at decreased HRT, it was still significantly higher than in the CW ($P < 0.05$).

The microbial community exhibited high diversity and richness of a few specific microbes, contributing to high treatment efficiency with low sludge generation in CW-MEC. The VSS, tracer test and volumetric change in net volume also revealed that sludge generation was lower in a CW-MEC and CW-MFC than in the CW. CW's net volume decreased from an initial net volume of 3.3 L to 2.0 L at the end of the experiment. Trace metal precipitation was also higher in CW than in the CW-MEC and CW-MFC. In summary, providing an adequate, stable potential to a conducting substrate working electrode in a CW-MET improves the recovery of

electrons. It allows the development of a more favourable microbial community to improve treatment efficiency.

Acknowledgments

The authors would like to acknowledge facilities provided by the Central Science Laboratory (CSL), the University of Tasmania, for SEM-EDX analysis. The authors would also like to acknowledge the ICP-MS facility provided by The University of New South Wales. Additionally, the authors would like to extend their acknowledgement to the University of Tasmania for the financial support and grant from the Tasmanian Community Fund (31Medium00171).

Chapter 6: Low-power energy harvester from constructed wetland-microbial fuel cells for initiating a self-sustainable treatment process

Graphical Abstract

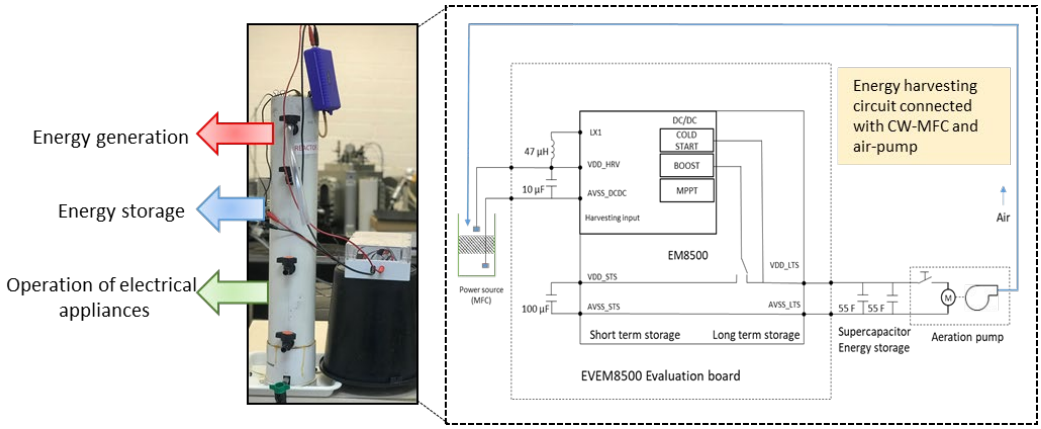

Abstract

This is the first study that demonstrates developing a Power Management System (PMS) for initiating a self-automated Constructed wetlands (CW)-microbial fuel cell (MFC). The developed PMS helps by harvesting and storing low power generated from CW-MFC and using it to operate an air-pump used as a part of treatment processes. The great potential for self-generating energy harvester to power electrical instruments makes the CW-MFC technology a sustainable candidate for many applications. In this paper, two laboratory-scale CW-MFC were used for this purpose, the cathode of one CW-MFC (R1) intermittently aerated (IA) with the self-automated air-pump, and the performance compared with the second CW-MFC (R2). An energy harvesting system was configured specifically optimised to suit the low energy output from the CW-MFC. The maximum power generated by R1 and R2 CW-MFC was 54.6 µW and 41.2 µW, respectively, which increased up to 90 µW after IA. The pollutant treatment performance of R1 with IA increased significantly from R1 without aeration and R2 microcosms. The ammonium (NH_4^+) removal in R1_IA was 10% higher than R1 without

aeration and 12% higher than in R2. With the IA, dissolved oxygen at the cathode of R1 increased, which influenced redox potential for better electron recovery and reduced the internal resistance. The use of generated energy from the system makes the technology self-sustainable and high performing.

6.1. Introduction

The emerging water and energy "water-energy-nexus" related environmental challenges requires upgrading various technologies towards sustainability. The strategic use of natural energy such as wind, solar, and tidal is necessary to achieve a sustainable society [222]. Based on the impact of fossil-fuels on socio-economic and environmental perspectives, the search for alternative renewable energy sources is increasing rapidly [223, 224]. Microbial fuel cells (MFC) have been studied as a promising technology for generating renewable energy while concurrently treating wastewater [225, 226]. The main principle behind producing energy from MFC technology is converting chemical energy stored in organic matter into electrical energy by bacterial metabolism [227-229]. That feature of MFC makes it a platform for several other integrated wastewater treatment processes, such as sediment-MFC, benthic-MFC, Photo-MFC, Plant-MFC, Plug flow-MFC, Baffled air-cathode-MFC [207, 230-232]. Among other MFC integrated platforms, the most practical innovation to intensify wastewater treatment while generating electricity is the integration of MFC with CW [32, 33].

In the past ten years, CW-MFC technology has gained considerable attention for intensive wastewater treatment and electricity generation [61, 76, 91, 100, 128, 160, 166, 233, 234]. The CW-MFC works on the MFC principle where organics at the anode are oxidised by electroactive bacteria (EAB), and generated electrons flow through the electric wire to the cathode, which results in electricity generation [75, 80, 235]. The CW-MFC has often been considered a low voltage generating device due to several challenges such as low oxygen availability at the cathode [69, 100] and high internal resistance [207, 236]. The internal

resistance is a measure of the voltage vs current characteristic of a non-ideal power source. The internal resistance can be determined as the ratio of the voltage reduction from OCV to current at a particular operating point. For an MFC, the internal resistance of the cell can change with the condition of the cell, with changes of chemical and physical conditions at the anode and cathode individually, and with significant changes in the current drawn from the cell. Due to the cell's (CW-MFC) low output voltage, it has not been explored much for electrical applications; however, several studies have attempted modification in design, material, and electrode configurations to increase the voltage output [69, 100, 233, 234, 237].

Despite recent advancements to enhance the power output of CW-MFC, the power output has not increased substantially. Thus, CW-MFC major research's areas are focused on treatment performance enhancement to achieve an improved efficiency [65, 69, 208, 238]. Several studies have reported that the generated electricity from CW-MFC can have biosensor applications in order to monitor environmental parameters within the systems [80, 160]. Xu, et al. [207] attempted the first study to increase maximum energy harvest from an open-air bio-cathode CW-MFC. This study adopted the capacitor engaged duty cycling (CDC) strategy to minimise the energy losses from CW-MFC and proven it as a worthwhile strategy to maximize the energy harvested.

On the other hand, despite low power generation, single MFCs have been used for energy harvesting. Yamashita, et al. [222] developed an ultra-low-power energy harvester that requires only 2.09 μW power from the MFC to charge a supercapacitor to 3.3V. The study further utilised the produced stored energy for environmental sensing. Furthermore, Nguyen, et al. [239] used three MFCs with a net volume of 100mL and connected them to an upconverter, which boosted the output voltage to a sufficient level for operation. They also used this setup to develop a high conversion power management system. Several other studies have reported energy harvesting from MFCs treating wastewater, and its use for different applications

including environmental sensing, operation of small electronic devices, and wastewater treatment [223, 227, 240]. However, due to low power output, the use of energy production from CW-MFC has not been reported so far, except a few studies as a biosensor [241, 242]. In low power generating MFCs, boosting of power has been attempted by recent studies by connecting several MFCs into series without voltage reversal [243]. Kim, et al. [243] attempted to boost power output by avoiding degradation in electrical performance using electrical harvesting circuits and by connecting power management system (PMS) to several MFCs. The voltage performance of single PMS connected in parallel achieved maximum of 3.3V. However, PMS connected several MFCs boosted voltage performance up to 6.6 V [243]. Similarly, a sediment microbial fuel cell (SMFC) improved its performance by modifying its design configuration and by connecting it to PMS. The study concluded that increasing cathode electrode surface (27 cm^3) had better electrical performance 800 mW/cm^2, than using multiple cathodes (three electrodes, and each 27 cm^3) that achieved 526 mW/cm^2. Further at last stage the SMFC was connected to a PMS to utilize the output voltage, which enhanced the electricity performance of SMFC upto 3.3 V. The generated energy from the CW-MFC can have several other applications to make the technology more sustainable and high performing. The present study is the first that demonstrates the use of generated energy from CW-MFC for operating an air-pump at the cathode. In several CW-MFC studies, it has been reported that cathode is a major challenge which restricts the flow of electrons due to low availability of oxygen [69, 166, 208, 244]. Oon, et al. [244] stated that 600 mL/min aeration of aeration at the cathode was optimum for highest energy recovery since the terminal electron acceptor in the form of oxygen at the cathode was sufficient for the electron flow. Srivastava, et al. [127] used radial oxygen loss (ROL) from plants as a low-cost aeration system to aerate the cathode of CW-MFC and supplementary aeration to overcome the cathodic challenges. The ROL based CW-MFC performed almost equal to supplementary aeration based CW-MFC; however, supplementary

aeration had better performance. Teoh, et al. [245] stated that supplementary aeration enhanced dissolved oxygen concentration at the cathode, which enhanced NH_4^+ removal by 67% compared to planted and non-planted CW-MFCs. In most of CW-MFCs, aeration was provided by an air-pump by an external electrical supply, which increases the operational cost.

The operation of an air-pump with the self-generated energy can overcome the cathode challenges of CW-MFC while providing aeration to maximise electron recovery from the anode. Aeration is also required for degrading complex pollutants in wastewater, and in CW-MFC aeration has usually been provided by external electrical supply for efficient treatment performance, requiring additional cost [127, 159, 244-246]. The use of self-generated energy should be able to make the technology self-sustainable by reducing external energy demand and operational costs. In the present study, a harvester was designed to harvest low energy generated by CW-MFC and further use it for powering an air-pump to intermittently aerated the cathode of CW-MFC. This was in order to enhance the voltage output by minimizing the cathode challenges and enhancing the pollutant removal rate. It was a self-sustainable CW-MFC system where the generated energy was used for real electrical applications.

6.2. Materials and methods

6.2.1. Power harvester design

The energy harvesting equipment used in this study consisted of a harvester and energy storage by means of supercapacitors. The harvester used was an EMEVB8500 (EMEVB8500 Evaluation Board, in, 2020, [247]) evaluation board from EM Microelectronic SA (Marin, Switzerland). The board is based on the EM8500 device, which is a high-performance energy collection device capable of operation from sources with very low power output. The EM8500 contains a boost converter and low voltage start-up circuits, enabling a system to start up from very low voltage and high impedance sources, such as a CW-MFC. We had previously tested different harvester models, including systems based on the LTC3108 highly-integrated DC/DC

converter from Analog Devices Inc. (Massachusetts, US) [248]. Our initial tests showed that this device, when in a completely de-energised state was not able to start operation with the amount of power available from CW-MFC cells. Hence, the EM Microelectronic device was used, as the specifications suggested that it would be able to start at a lower power input. This is consistent with reports from Vondrak, et al. [249]. We configured our evaluation board for a low threshold of power and high impedance source, which allowed a cold start of the system, but with a trade-off of limiting the maximum output voltage available.

In order to maximise power collection, the effective impedance on the input of the harvester needs to be matched to the impedance of the cell. As the cell's impedance will vary with the condition of the cell, ideally, the harvesting equipment should vary its operating point to maximise power collection. The EMEVB8500 uses Maximum power point tracking (MPPT) to adjust the effective input impedance of the harvesting system to the present condition of the cell. The harvester measures the open-circuit voltage (OCV) of the fuel cell to estimate the cell's condition. The maximum operating power point calculation can be adjusted from 50 % OCV to 88 % OCV. The polarisation tests showed the peak power output of the CW-MFC occurred at around 50 % OCV. The harvester repeatedly measures the open-circuit voltage of the CW-MFC and controls the current drawn to maintain the input voltage at the specified proportion of it. As the main goal was to maximise the power output of the CW-MFC, it was set to configured harvester to track and operate at the 50 % OCV point.

The collected power was stored in two 55 Farad (F) super-capacitors in parallel, being 110 F in total. The power was switched to an aquarium pump by the connected timer. The pump was a commercial aquarium aeration pump, an Aqua One Battery Air 250, (Aquarium Spare Parts, Edwardstown, South Australia), modified to allow for the use of external 1.5 V power. The pump was evaluated at 1.5 V (nominal), but was tested to run effectively at voltages of 1.5 to 1.7 V. The pump operated for 30 s at a time at 8-hour intervals until the capacitor voltage

dropped to the minimum pump operating voltage of 1.5 V. After this, pump operation was inhibited until the storage voltage returned to 1.7 V. So, the available power (E) to use can be calculated using Equation 1.

$$E = C(Vmax^2 - Vmin^2) \qquad Eq.1$$

Where *C* is 110 F, *Vmax* is 1.7 V, and *Vmin* is 1.5 V.

The harvester's output current was also limited, so two 55 F supercapacitors were used and connected in parallel to store the energy generated. This was to provide sufficient current capacity to run the commercial aquarium pump used for aeration. The pump was measured under maximum current draw to require 410 mA. The circuit used for the tests is illustrated in *Figure 6-1*.

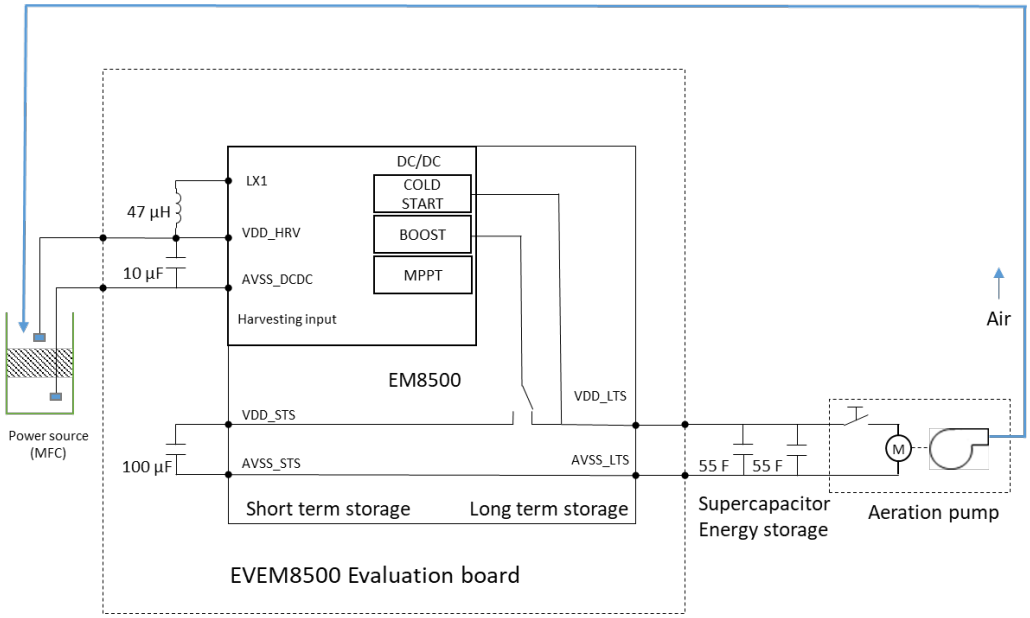

Figure 6-1. Electrical schematic of the power harvester and a capacitor connected to the air pump.

6.2.2. Reactor fabrication and start-up

Two laboratory-scale CW-MFC microcosms (R1 and R2) were constructed from polyvinyl chloride (PVC) pipes (height 600 mm x diameter 104 mm). Both the microcosms were constructed with the same filling configuration - the bottom filled with large bolder (gravel)

(diameter 12-15 mm) of 10 mm height to avoid clogging, overlined with graphite gravel (conductive materials) of 220 mm (anode), that was overlined with normal gravel (garden pebbles) of 200 mm, and the top layer was again overlined with graphite gravels of 150 mm (cathode). The anode and cathode were equipped with a charge collector of graphite felt and graphite plate, respectively. The graphite felt dimension was diameter 830 mm x width 90 mm, and it was placed 170 mm from the bottom of the cell. The graphite plate was of dimension length 100 mm x width 55 mm and placed at the cathode's air-water interface. The net volume of R1 and R2 were 1.5 L each. Four ports were provided to collect the samples, the first port (P1) at a distance of 100 mm from the top of the microcosm, port 2 (P2) at 120 mm below P1, port 3 (P3) 200 mm below P2, port 4 (P4) 120 mm from P3, and port 5 (P5) was connected at the bottom of the microcosm, with the distance between P4 and P5 60 mm. The considerable distance between P2 and P3 was to separate the anode and cathode chambers. The R1 microcosm was connected to the harvester to collect its output voltage, and it was further equipped with an air-pump at the cathode at 130 mm from the top of the microcosm. *Figure 6-2* illustrates the schematic of the laboratory scale R1 and R2 CW-MFC microcosms.

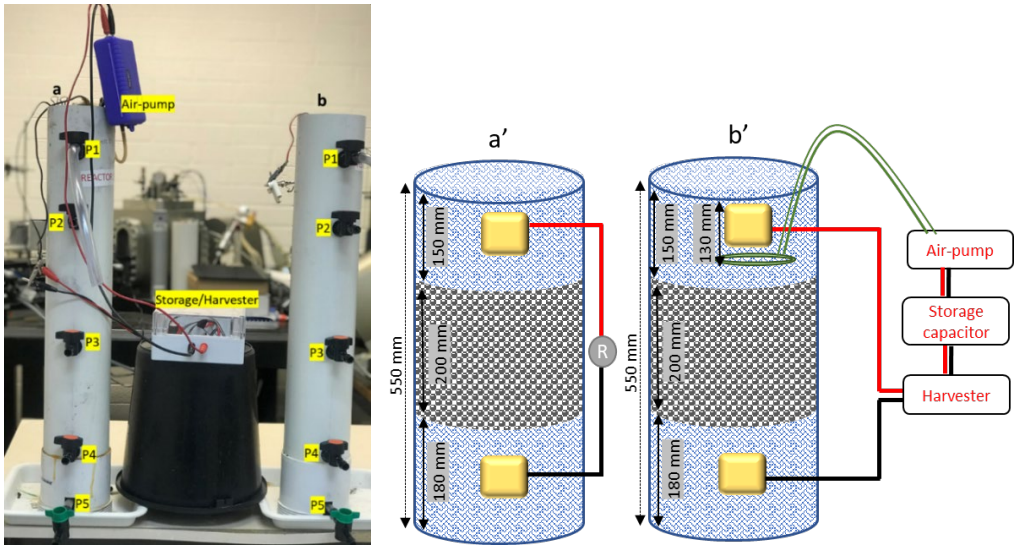

Figure 6-2. Laboratory scale and schematic of microcosms: 2a and 2b is laboratory picture of R1 and R2 microcosms respectively; 2a' and 2b' is schematic of R1 and R2 microcosms respectively, and 2c is a picture of harvester/storage capacitor used for the microcosm.

6.2.3. Inoculation and Operation

The R1 and R2 were inoculated with inoculum from an old running laboratory, CW-MFC microcosm. Both reactors were operated on the synthetic municipal wastewater adapted from Wang, et al. [202]. The composition of wastewater was as follows: 118.0 mg/L $C_6H_{12}O_6$, 216.0 mg/L, $C_2H_3NaO_2$, 59.0 mg/L KH_2PO_4, 153.0 mg/L NH_4Cl, 28.0 mg/L, $CaCl_2$, 51.0 mg/L, $MgSO_4 \cdot 7H2O$, 9.0 mg/L $FeSO_4 \cdot 7H_2O$, and trace metal solution. The inoculum of 100 mL was taken from an old microcosm and mixed with 3 L synthetic wastewater and kept in the refrigerator overnight for microbial enrichment. Afterwards, it was inoculated in the microcosm and kept for acclimatization in a batch mode operation until steady-state conditions were achieved. The synthetic wastewater (1.5 L) during the acclimatization period was changed every day, and voltage output was recorded to decide the microcosms' steady-state conditions. The total period of acclimatization was 90 days (d). Once the steady state was achieved, polarization was performed, and the microcosm was connected to the harvester. The microcosm was operated in a batch mode operation, and the contact time was 24 h.

The influent wastewater was poured simultaneously in the R1 and R2 microcosm, and the samples were collected from both the microcosms without IA. The samples from cathode, anode, and overall sample were taken from P1, P4, and P5, respectively, from both

microcosms. The samples from the R1 microcosm were named R1_anode, R1_cathode, and R1_overall. Similarly, the samples from the R2 microcosm were named R2_anode, R2_cathode, and R2_overall. Afterwards, the cathode of R1 microcosm was provided with IA (R1_IA) and again samples from the cathode (R1_cathode_IA), the anode (R1_anode_IA), and overall sample (R1_anode_IA), were taken from P1, P4, and P5, respectively. The treatment efficiency was then compared between R1, R2, and R1_IA.

6.2.4. Chemical and Electrochemical analysis

The dissolved oxygen (DO) of R1, R2, and R1_IA was assessed regularly from the anode and the cathode. The DO of R1_IA was also evaluated for continuous 8 h after IA in order to observe the changes in DO conditions concerning time. The DO meter (Hanna Instruments) was used to analyse DO. The cathode and anode potential were analysed by Ag/AgCl (Sigma Aldrich) reference electrode. The other chemical parameters, such as total organic carbon (TOC), chemical oxygen demand (COD), total nitrogen (TN), ammonium (NH_4^+), were analysed twice a week. The TOC and TN were analysed with Shimadzu TOC-TN analyser (Model TNM-L ROHS), COD was analysed by APHA standard method 5220D. The NH_4^+ was analysed with Ion chromatography (Eco IC, MEP Instruments, Metrohm).

The voltage of R1 and R2 microcosms were recorded regularly with PC_{LINK} multimeter, except during the period when the harvester was collecting the energy from R1. The polarization of both the microcosms was performed every 15 days during the experimental period by varying the external resistance. At the beginning, the external resistance was used within a range of 1000 KΩ to 150 Ω. The obtained results were subsequently changed to a range of 20 KΩ to 26 Ω. The external resistance determined the power output and current, and calculations were performed based on Equations 2 and 3.

$$I = \frac{V}{R} \qquad Eq.2$$

$$P = VI \qquad Eq.3$$

Where I is current (A), V is voltage (V), R is external resistance (Ω), and P is power (W).

6.3. Results and discussions

6.3.1. Electrical performance of CW-MFCs

The two identical CW-MFCs, R1 and R2 have almost similar voltage performance with a small variation in the performance of R1. The mean voltage performance of R1 and R2 microcosm was 394±53 mV and 307±34 mV, respectively (*Figure 6-3*). The polarization test was performed every 15 d during the experimental period (*Figure 6-4*). The polarization test was used to identify the maximum withdrawing power capacity of the microcosm with time. The polarization test indicated that the microcosms' voltage and power output changed with time on varying resistance. The maximum power achieved in R1 and R2 microcosm was 54.6 µW and 41.2 µW, respectively; however, it increased in R1 after IA up to 90.0 µW. The internal resistance decreased with time as the condition of the microbial cells changed in the microcosm. The harvesting system operates at 50% OCV. The CW-MFC's internal resistance at that operating point from the measured current and the drop in cell voltage as compared to the OCV in R1 had an effective internal resistance of 1360 Ω at 150 d, 870 Ω (165 d), and 800 Ω (180 d), and R2 had internal resistance of 920 Ω (150 d), 1180 Ω (165 d), and 870 Ω (180 d). These values vary depending on the condition of the respective cells and agree with the trends in performance shown in the polarisation curves in *Figure 6-4*. At low load resistance, there was a reduction in current and hence power output, likely due to the extended test compromising systems to maintain relatively high current output. When the voltage dropped below approximately 0.2V, the harvester was disconnected from the cell. It maintained monitoring of the output voltage of the cell but not recommenced collecting energy until the cell voltage rises above this minimum level. This prevents further significant current flow from the cell until its output was restored to a satisfactory operating state. It also means that the

storage capacitors are disconnected from the CW-MFC and maintained their stored charge. In some cases, the voltage performance in R1 was higher than the R2 microcosm. The electrical output of the two identical microcosms may differ due to microbial composition. Even with the same inoculum and operational conditions, the microbiological growth may differ [250]. The difference in voltage and power output could also be different due to several other factors, such as ohmic losses, activation losses, and mass transfer losses [250, 251]. The internal resistance and overpotential of electrodes can drive ohmic and mass transfer losses in the systems, whereas substrate unavailability can be a reason for activation losses. Kim, et al. [250] also mentioned that despite using the same designs and operational conditions, the electrochemical performances of four identical MFCs were different. Moreover, in the present study, the electrical output of R1 microcosm was higher than R2 microcosm, and due to this, the harvester was connected to the R1 microcosm for voltage storage and operation of the air-pump.

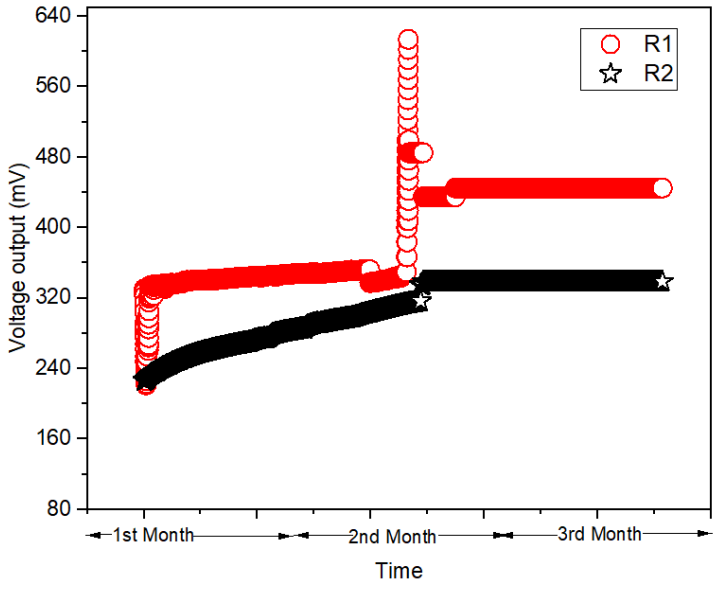

Figure 6-3. The voltage represented in the graph is a cumulative voltage over three months except for the period when harvested was connected to R1. An average of 3000 readings each month is presented in the graph. The rise in the second month was the period where aeration was provided to the R1 microcosm.

The performance of the system was strongly dependant on the output of the CW-MFC. The initial tests with a harvester based on the LTC3108 could not start collecting energy due to the low power available from the cell, which was lower than that required for the device to start. The EM8500 based system was more sensitive and could bootstrap itself from the low voltage output and commence collecting energy. As configured, the system could cold-start from an input voltage of 0.28 V. The polarizations tests had suggested that the cell's output impedance was around 800-1200 Ω. Due to the high output impedance of the cell, the harvester could not effectively boost the voltage to the high voltages. In this configuration, the voltage output will be less than 2 V, so it was necessary to use a power storage circuit configuration suitable for operation under this level. Use of two 55 F capacitors in parallel and operation between 1.7 and 1.5 V from Eq.1 had 70.4 J (equivalent to Ws) available for each cycle, which allowed operation of the aeration pump for 60 s before the voltage dropped to the 1.5 V minimum operating voltage. However, another consequence of the large capacitance configuration was that it takes 318 Ws to charge the storage capacitors to 1.7 V from 0 V, so with the circa 54 µW available from the cell, it required around 70 days for the initial charge.

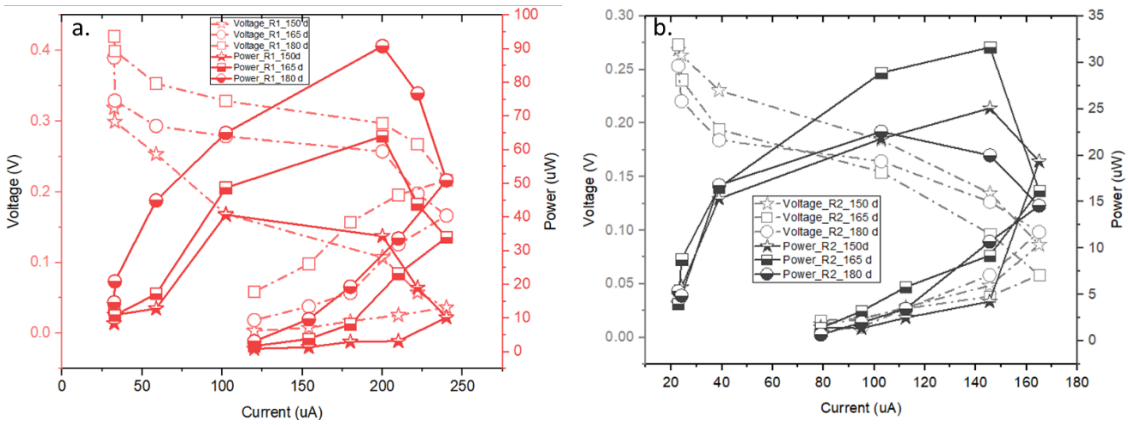

Figure 6-4. Polarization curve of R1 and R2 microcosm after 150th day of operation.

6.3.2. Energy harvesting and operation of an air-pump

Initially, due to the low power output of the CW-MFCs, the energy harvester was first connected to both R1 and R2 microcosms in parallel to withdraw maximum power from the microcosms to store the start-up voltage. The parallel connection in the MFCs has been reported to increase the voltage output [250]. In the initial phase, the harvester took a long time to withdraw power from the microcosms; moreover, once it achieved the OCV, the storage capacity increased. However, the harvester took a longer time to reach the required voltage of 1.5 V for the start-up. To achieve 1.5 V, it required 86,400 minutes for the storage from R1 and R2 microcosms in parallel connections. Thus, practically, a single microcosm's power output was not enough to store that much energy. Once the harvester achieved its start-up voltage, the harvester was connected only with the R1 microcosm during the rest of the experiment. The maximum power output of the R1 microcosm increased from 1.6 µW to 54.6 µW from day 30 to day 90. However, power output changed with the variation in operational conditions, which is normal in any BES. Once 1.5 V was reached in the harvester, it was kept constant throughout the experimental period, and the operating voltage of 0.2 V was stored from R1 and used for the air-pump to provide IA. For the operational voltage of 0.2 V, R1 microcosm charges the harvester for 8,640 minutes. Once the harvester achieved 1.7 V, a connected timer starts IA in R1 for 30 seconds (s) each time after ~8 h and ~16 h since the wastewater as poured in the microcosms. The air-pump used 0.1V from the harvester for the 30s of aeration at the cathode each time. After two operations of IA, the harvester's voltage decreased to 1.5 V again, and then it resumed recharging the 0.2 V. Hence, the aeration provided at the cathode of R1 microcosm was two times in 24 h duration and it was self-regulated through the harvester storage voltage.

6.3.3. Dissolved oxygen (DO) and redox potential of CW-MFC

DO has been considered a key factor in the effective treatment of pollutants in CW [244, 252]. The DO acts as an electron acceptor for organics' oxidation, which is typically lacking in CW and CW-MFC systems due to design configurations. In the CW-MFC study, the electrode acts as an artificial electron acceptor at the anode. It allows the flow of electrons from the anode to the cathode, where the electron goes to the terminal electron acceptor, i.e., oxygen. Due to the low oxygen concentration at the cathode, electron losses occur, and electrical output decreases [69]. The decrement in electrical output is also a result of the system's redox potential, and DO plays an important role in creating a potential difference between the anode and the cathode [244, 253]. However, it is reported that oxygen diffusion from the atmosphere [254] and wetland plants [255] in most cases is not sufficient [246] as an electron acceptor, particularly in anaerobic regions. Moreover, IA in CW-MFC is well justified for an increase in electrical output and treatment performance in literature [127, 159, 238, 246] though it is provided by the external electrical supply, which requires additional cost. A self-regulated air-pump was provided for IA in the present study, which uses electricity generated from the CW-MFC itself.

The DO graph illustrated in *Figure 6-5(a)* indicates the microcosms' DO concentration before and after aeration. The mean DO concentration at the cathode of R1 and R2 microcosm was 0.99±0.30 mg L^{-1} and 0.95±0.20 mg L^{-1}. However, after providing IA at the cathode of R1, the DO concentration increased from 0.99±0.30 mg L^{-1} to 5.1±2.5 mg L^{-1}. The increased DO at the cathode of R1_IA also influenced the redox potential. The R1_IA cathode potential increased from 90±85 mV to 250±47 mV, and the anode potential was -250±120 mV throughout. The cathode potential of R2 was 95±70 mV, similar to R1 before IA, and the anode potential was -260±90 mV. Though, there was not any significant change in the DO concentration at the anode of R1_IA. Due to an increase in the DO concentration at the cathode and influence in the redox

potential of R1_IA, the electron transfer rate increased from anode to the cathode, which resulted in high electrical output [93, 127, 159, 245, 253].

Further, to determine the stability of DO at the cathode of R1_IA, it was measured hourly up to 8h after IA (*Figure 6-5(b)*). The DO concentration considerably decreased after 8h of IA; at 2nd h, the decrement was not significant with the DO value of 5.1±3.5 mg L^{-1}; however, it gradually decreased with time until the second IA was provided (8h) (*Figure 6-5(b)*). The DO concentration at the anode did not change and was stable throughout; however, redox potential slightly changed with the change in DO concentration after 8h. The decrement in the DO condition from the cathode could be due to releasing oxygen from the surface since the aeration was provided only to the microcosm's upper portion. The other reason for the decrement in DO concentration was the use of oxygen for pollutant treatment (detailed discussion in *Section 6.3.4*) and involved in the half-cell reaction of MFC [245]. In the half-cell reaction, DO acts as a terminal electron acceptor at the cathode, which enhanced the electron transfer rate from the anode to the cathode.

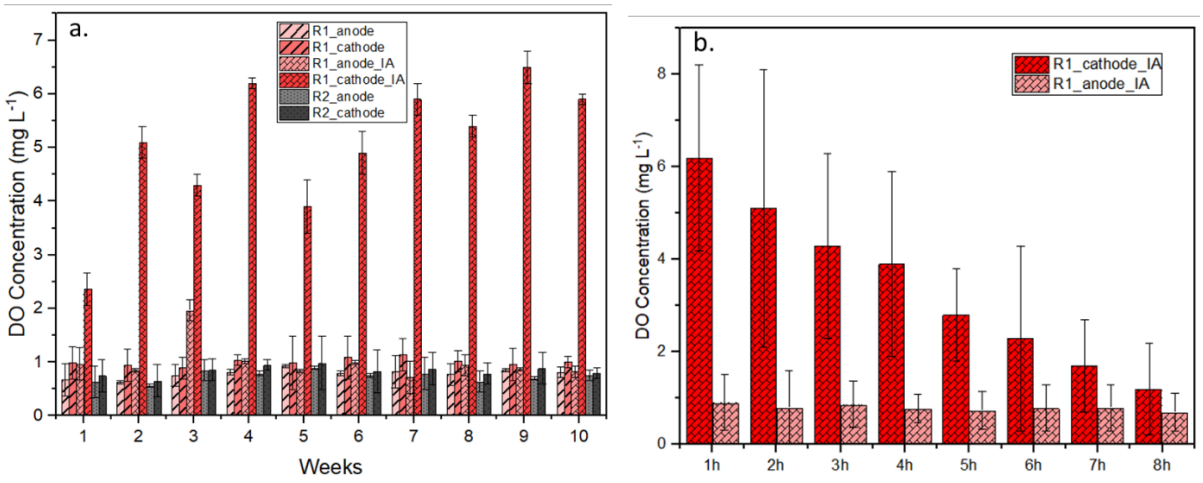

Figure 6-5. a) DO conditions of R1, R2, and R1_IA, at the cathode and anode; b) monitoring of DO conditions with time after IA.

6.3.4. Pollutant Treatment and Electrical performance after IA

The treatment performance of R1 and R2 microcosm was evaluated based on TOC, COD, TN, and NH_4^+ removal, represented in *Figure 6-6*. The treatment performance of R1 and R2 was evaluated and then compared with R1_IA. The treatment performance was based on the removal efficiency at the cathode, anode, and overall removal. The mean COD removal in R1_anode, R1_cathode, R2_anode, and R2_cathode was 79±4%, 84±2%, 78±6%, and 80±4%, respectively. The mean overall COD removal efficiency of R1 and R2 microcosm was 82±4% and 80±6%. However, after providing IA at the cathode of R1, the mean COD removal in R1_cathode_IA, R1_anode_IA, and R1_overall_IA was 90±4%, 86±5%, 91±4%. The COD removal of R1_IA increased significantly after providing two aerations for the 30s each during 24 h of contact time. The overall COD removal efficiency of R1_IA increased by 9% from R1 and 11% from R2. Likewise, the TOC, TN, and NH_4^+ removal also increased (*Figure 6-6*). The mean overall TOC removal in R1, R2, and R1_IA was 52±7%, 48±5%, and 63±9%, respectively. The mean overall TN removal in R1, R2, and R1_IA was 70±2%, 69±2%, and 78±3%, respectively, and the overall NH_4^+ removal was 70±2%, 80±3%, and 67±2%, respectively. The overall removal efficiency for all the parameters significantly increased in R1_IA. The increment in removal was due to providing IA at the cathode, which influenced the system's DO concentration and redox potential. The COD and NH_4^+ removal efficiency was higher than the other CW-MFC studies [256-258]. Xu, et al. [256] attempted pretreatment of wastewater with Fe_3C and further pass it to CW-MFC, the ammonium-nitrogen removal achieved was 96.38 ± 1.87%, total phosphorus (96.52 ± 1.25%) and chemical oxygen demand 74.70 ± 1.67%. Wang, et al. [257] used air-cathode CW-MFC using four different electrode materials. The COD removal of the system 1, 2, 3, and 4 were 42.30%, 37.42%,48.78%, and 35.73%, respectively. The study concluded that carbon fibre felt (CFF) and foamed nickel (FN) was more efficient for treatment and electricity generation.

The low TOC removal compared with the COD removal is also reported in the previous study and stated that low TOC removal could result from high dominance of autotrophic bacteria that were more dependent on inorganic pollutants removal such as NH_4^+ than the organics [259-261]. It is also clear from the substantial enhancement in NH_4^+ removal of R1_IA, which was due to higher oxygen availability since NH_4^+ requires oxygen for the conversion into other oxidation states. Also, in CW-MFC, the electrode act as an electron acceptor at the anode for NH_4^+ oxidation even in anaerobic conditions [131], which is why the overall NH_4^+ removal was 70±2%, and 67±2% in R1 and R2, respectively. This significantly increased after IA at the cathode due to the higher availability of DO and adequate electron transfer mechanism. The higher availability of oxygen at the cathode allowed efficient electron flow from the anode to the cathode, enhancing the removal rate at the anode, hence the overall removal efficiency [127, 244]. Guo, et al. [262] also reports the increment in ammonium removal efficiency up to 90% with IA. TN removal in R1_IA states that the IA provided was enough to support nitrification and denitrification processes. Since the IA aeration only aerated the cathode for a few seconds, the DO concentration first increases, supporting the nitrification process, and with time DO decrease, which allowed the denitrification process [69, 245, 246]. The mineralisation of pollutants with enhanced DO at the cathode can also be observed with high COD removal at R1_cathode_IA [238].

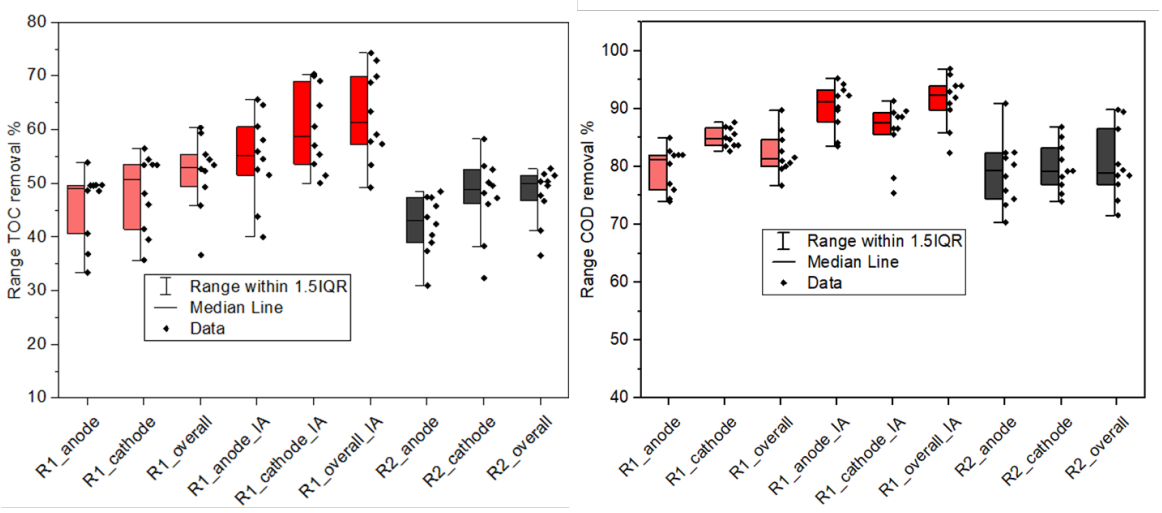

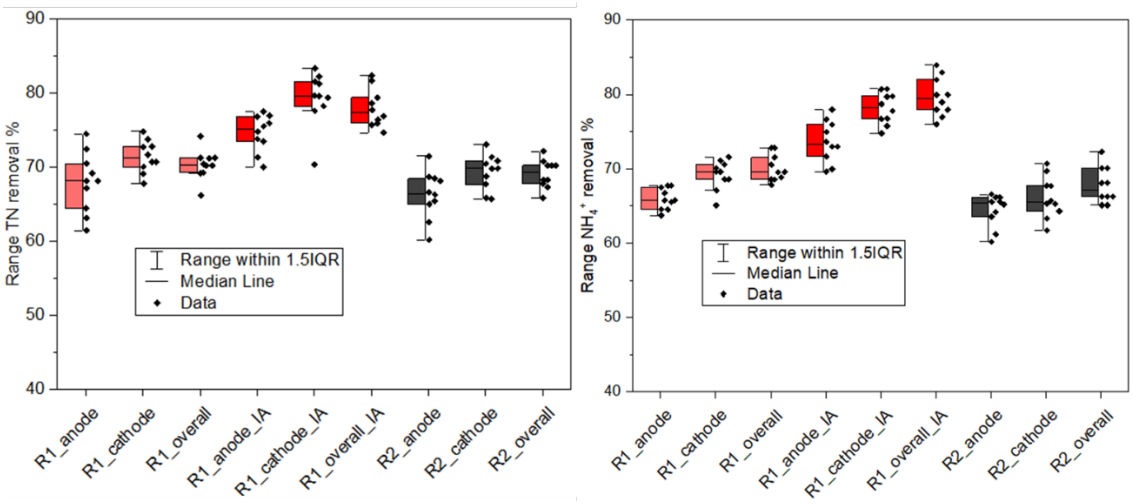

Figure 6-6. Range removal of TOC, COD, TN, and NH_4^+, in R1, R2, and R1_IA.

Furthermore, with the IA in R1 microcosms, the voltage performances increase, with the voltage output of R1_IA significantly increasing from that of R1 and R2 microcosm. The mean voltage performance of R1 microcosm before aeration was 394±53 mV, but with IA, it increases to 435±25 mV. The IA also decreased the internal resistance of the R1 microcosm, which was noticed with the help of the polarization curve drawn after every 15 days. The flow of electrons from the anode is mainly regulated with a terminal electron acceptor present at the cathode; with increased DO conditions, electron flow was not restricted, which decreases the internal resistance. The polarization graph of R1 and R2 is represented in *Figure 6-4*. With the aeration in the R1 microcosm, the maximum power output increased to 90.0 µW, whereas in R2, it was quite similar throughout. Moreover, IA impacted the R1 microcosm's performance significantly.

Table 6-1. Comparison of DO concentration with anode and cathode potential of R1, R2, and R1_IA and its voltage performance.

	DO Concentration (Cathode, mg/L)	Voltage performance (mV)	Anode potential (mV)	Cathode potential (mV)
R1	0.99±0.30	394±53	-250±120	90±85
R1_IA	5.1±2.5	435±25	-250±120	250±47
R2	0.95±0.20	307±34	-260±90	95±70

For the effective degradation of specific pollutants such as organics and NH_4^+ in CW, artificial aeration has generally been provided [244-246], which requires energy input and increases the overall cost of wastewater treatment systems. In CW-MFC studies, it is widely reported that less oxygen availability at the cathode inhibits the electron transfer rate, limiting the cathodic reduction [69, 183, 208]. However, the results of this study clearly illustrate that providing a self-automated aeration system without any extra cost would provide high impact treatment performance in CW-MFC.

6.4. Conclusions and recommendations

The low energy generated from CW-MFC can be used for activating the low-power electrical devices by amplifying the power generated by the device. The present study demonstrates the use of generated energy for operating a low power air-pump, which was successfully utilized for providing intermittent aeration at the cathode of R1 microcosm. The aeration at the cathode enhances the DO concentration, enhancing the removal efficiency of different pollutants and the electron flow. Due to IA, the system's internal resistance also decreased with a change in environmental conditions, which increased the microcosm's power generating capacity. However, initially, the harvester required a longer time to store the start-up voltage due to low power generation. Even during the experiment for storing 0.2 V, it required 8,640 minutes each time to store the voltage. Thus, it is recommended for future studies to use highly conductive electrode materials in CW-MFC systems to decrease internal resistance and enhance power generation. The high conducive or hydrophilic electrode material would be able to generate enough power to minimize the required period for storage. The parallel connection of more than one CW-MFC would also decrease the storage time and produce a higher electrical output. It is also advisable to use an efficient power management system that can amplify the low power generation. Overall, this study demonstrates a self-automated practical application of

electricity generated by CW-MFC for operating an electronic device, enhancing the system's performance.

Acknowledgments

The authors would like to extend their acknowledgment to the University of Tasmania and Macquarie Universities for the financial support and also the grant received from the Tasmanian Community Fund (31Medium00171).

Chapter 7: Summary & Conclusion

7.1. Summary

The integration of a constructed wetland and a bioelectrochemical system improved the rate and efficiency of treating wastewater from various sources. The integration of a microbial fuel cell enhanced the anaerobic microbial metabolism resulting in a high reaction rate and efficiency. Similarly, the integration of a microbial electrolysis cell provided energy for catalysing the reaction rate and efficiency in a constructed wetland. The incorporation of conductive materials/electrodes into the constructed wetland system (electroactive wetland) also allowed an efficient electron flow due to a better redox gradient resulting in efficient removal of pollutants via higher oxidation and higher reduction. Furthermore, the generated electricity from the system is an essential factor as it a means of resource recovery. The recovered energy can be used for operating electrical appliances to further improve the efficiency of the process. Thus, the integration of bioelectrochemical systems overcomes several problems associated with the traditional constructed wetlands as well as providing additional benefits such as recovering energy.

7.2. Conclusions

The foremost conclusions of this research are listed below according to the organisation of the thesis chapters:

- A new process was developed for the anaerobic ammonium oxidation along with organics removal. The process was named an Electroannamox process since the anode electrode acted as an artificial electron acceptor to efficiently remove ammonium-nitrogen. The MFC integrated CW also produces low biomass quantity while achieving high treatment efficiencies. Further, the study conclusively demonstrates that anaerobic

ammonium oxidation can occur using a solid electron acceptor. This information might give the possibility of other new pathways for anaerobic ammonium oxidation and could change the existing understanding of nitrogen cycle.

- The role of conductive material in an anaerobic environment was investigated to treat Cr(VI) contaminated wastewater. The redox susceptible nature of conductive material was investigated. The study indicated that even without any external electrical circuit, the electron transfer could occur in a conductive material packed column. Due to such electron transfer, microbes are able to tolerate higher loading of pollutants and efficiently treat them even under what would normally be toxic conditions (high metal concentration). The presence of conductive material also influences the microbial diversity and biomass in electroactive CW.
- A positive synergetic relation of sulphate and conductive material was identified and further optimised to improve nitrogen and organics removal. The sulphate-based CW-MFC exhibited improved performance for ammonium and organics removal compared to a traditional CW. Additionally, toxicity build-up due to the reduction of sulphate to toxic sulphide does not occur in CW-MFC; thus, treatment performance was stable. Furthermore, redox coupling of sulphate in the presence of conductive material enhanced electron transfer hence the electricity generation and treatment performance improved.
- A method was developed to efficiently recover more electrons by maintaining a stable redox potential of the CW-BES. The CW-BES was designed to treat complex wastewaters, including the presence of multiple pollutants, while efficiently recovering electricity. By maintaining stable redox potential in CW-BES, high treatment performance and low sludge generation were achieved. The low sludge generation in

CW-BES keeps the system operational for a longer period without the problem of clogging, enhancing the lifespan of technology.

- A power management system was developed to store generated electricity from CW-MFC and use the stored energy for the aeration process. Work has demonstrated a prototype unit where a power management system stored electricity generated in CW-MFC to run an air-pump to aerate the cathode of CW-MFC. This resulted in higher treatment efficiency and overcame cathodic challenges such as low dissolved oxygen levels. Due to aeration, the resistance of the system was also decreased, thus increasing electricity generation.

7.3. Future work

This research was conducted to improve CW-BES technology and bring it to the advanced level; however, several research areas still need attention in future research:

- Though laboratory-scale CW-BES showed promising results for the treatment of various wastewaters and electricity generation, field testing of the technology is essential to prove that it is competitive with conventional wastewater treatment technologies.
- The enhancement of electricity generation needs to be explored further, as the current electricity generation is not sufficient to run real-world appliances. The main reason for low electricity generation is the system's high resistance that needs to be overcome in further research.
- The real-world application of generated electricity is also important; even though the generated voltage is low, it can be stored through a power booster and can solve several problems which require low power appliances. Thus, real applications of the generated electricity should be explored further, as should possible low power applications.

References

[1] J. Garcia, D.P. Rousseau, J. Morato, E. Lesage, V. Matamoros, J.M. Bayona, Contaminant removal processes in subsurface-flow constructed wetlands: a review, Critical Reviews in Environmental Science and Technology, 40 (2010) 561-661.

[2] S.D. Wallace, R.L. Knight, Small-scale constructed wetland treatment systems: feasibility, design criteria and O & M requirements, IWA Publishing, 2006.

[3] K. Seidel, Zur Problematik der Keim-und Pflanzgewässer: Mit 4 Abbildungen, 4 Tabellen und 4 Skizzen im Text, Internationale Vereinigung für theoretische und angewandte Limnologie: Verhandlungen, 14 (1961) 1035-1043.

[4] R. Kickuth, Elimination gelöster Laststoffe durch Röhrichtbestände, Arbeiten des Deutsches Fischereiverbandes, 25 (1978) 57-70.

[5] H. Brix, Treatment of wastewater in the rhizosphere of wetland plants–the root-zone method, Water Sci. Technol., 19 (1987) 107-118.

[6] A.K. Kivaisi, The potential for constructed wetlands for wastewater treatment and reuse in developing countries: a review, Ecol. Eng., 16 (2001) 545-560.

[7] H. Brix, Use of constructed wetlands in water pollution control: historical development, present status, and future perspectives, Water Sci. Technol., 30 (1994) 209-223.

[8] J. Vymazal, Constructed wetlands for wastewater treatment: five decades of experience, Environmental science & technology, 45 (2011) 61-69.

[9] Y. Zhao, G. Sun, S. Allen, Purification capacity of a highly loaded laboratory scale tidal flow reed bed system with effluent recirculation, Sci. Total Environ., 330 (2004) 1-8.

[10] J. Wood, G. Fernandez, A. Barker, J. Gregory, T. Cumby, Efficiency of reed beds in treating dairy wastewater, Biosystems engineering, 98 (2007) 455-469.

[11] S.E. Mbuligwe, Comparative treatment of dye-rich wastewater in engineered wetland systems (EWSs) vegetated with different plants, Water Res., 39 (2005) 271-280.

[12] C.S. Calheiros, P.V. Quitério, G. Silva, L.F. Crispim, H. Brix, S.C. Moura, P.M. Castro, Use of constructed wetland systems with Arundo and Sarcocornia for polishing high salinity tannery wastewater, Journal of environmental management, 95 (2012) 66-71.

[13] M.Z. Justin, M. Zupančič, Combined purification and reuse of landfill leachate by constructed wetland and irrigation of grass and willows, Desalination, 246 (2009) 157-168.

[14] M. Borin, D. Tocchetto, Five year water and nitrogen balance for a constructed surface flow wetland treating agricultural drainage waters, Sci. Total Environ., 380 (2007) 38-47.

[15] R.K. Wieder, A survey of constructed wetlands for acid coal mine drainage treatment in the eastern United States, Wetlands, 9 (1989) 299-315.
[16] N.T.D. Trang, H. Brix, Use of planted biofilters in integrated recirculating aquaculture-hydroponics systems in the Mekong Delta, Vietnam, Aquaculture research, 45 (2014) 460-469.
[17] L. Scholes, R. Shutes, D. Revitt, D. Purchase, M. Forshaw, The removal of urban pollutants by constructed wetlands during wet weather, Water Sci. Technol., 40 (1999) 333-340.
[18] D. Istenič, C.A. Arias, J. Vollertsen, A.H. Nielsen, T. Wium-Andersen, T. Hvitved-Jacobsen, H. Brix, Improved urban stormwater treatment and pollutant removal pathways in amended wet detention ponds, Journal of Environmental Science and Health, Part A, 47 (2012) 1466-1477.
[19] J. Vymazal, Removal of nutrients in various types of constructed wetlands, Sci. Total Environ., 380 (2007) 48-65.
[20] R.H. Kadlec, S. Wallace, Treatment wetlands, CRC press, 2008.
[21] D.S. Brown*, J F. Kreissl*, R. A. Gearhart, and et al., MANUAL - CONSTRUCTED WETLANDS TREATMENT OF MUNICIPAL WASTEWATERS, in, EPA/625/R-99/010 (NTIS PB2001-101833), 2000.
[22] W.C. Allen, P.B. Hook, J.A. Biederman, O.R. Stein, Temperature and wetland plant species effects on wastewater treatment and root zone oxidation, Journal of Environmental Quality, 31 (2002) 1010-1016.
[23] O. Stein, P. Hook, J. Biederman, W. Allen, D. Borden, Does batch operation enhance oxidation in subsurface constructed wetlands?, Water Sci. Technol., 48 (2003) 149-156.
[24] O.R. Stein, P.B. Hook, Temperature, plants, and oxygen: how does season affect constructed wetland performance?, Journal of Environmental Science and Health, 40 (2005) 1331-1342.
[25] Y. Yang, Y. Zhao, S. Wang, X. Guo, Y. Ren, L. Wang, X. Wang, A promising approach of reject water treatment using a tidal flow constructed wetland system employing alum sludge as main substrate, Water Sci. Technol., 63 (2011) 2367-2373.
[26] J. Baptista, T. Donnelly, D. Rayne, R. Davenport, Microbial mechanisms of carbon removal in subsurface flow wetlands, Water Sci. Technol., 48 (2003) 127-134.
[27] J. García, E. Ojeda, E. Sales, F. Chico, T. Píriz, P. Aguirre, R. Mujeriego, Spatial variations of temperature, redox potential, and contaminants in horizontal flow reed beds, Ecol. Eng., 21 (2003) 129-142.

[28] J. Dušek, T. Picek, H. Čížková, Redox potential dynamics in a horizontal subsurface flow constructed wetland for wastewater treatment: Diel, seasonal and spatial fluctuations, Ecol. Eng., 34 (2008) 223-232.
[29] A. Pedescoll, R. Sidrach-Cardona, J. Sánchez, E. Bécares, Evapotranspiration affecting redox conditions in horizontal constructed wetlands under Mediterranean climate: influence of plant species, Ecol. Eng., 58 (2013) 335-343.
[30] A.N. Bezbaruah, T.C. Zhang, pH, redox, and oxygen microprofiles in rhizosphere of bulrush (Scirpus validus) in a constructed wetland treating municipal wastewater, Biotechnol. Bioeng., 88 (2004) 60-70.
[31] S. Wu, P. Kuschk, H. Brix, J. Vymazal, R. Dong, Development of constructed wetlands in performance intensifications for wastewater treatment: a nitrogen and organic matter targeted review, Water Res., 57 (2014) 40-55.
[32] A. Yadav, Design and development of novel constructed wetland cum microbial fuel cell for electricity production and wastewater treatment, in: Proceedings of 12th International Conference on Wetland Systems for Water Pollution Control (IWA), 2010, pp. 4-10.
[33] A.K. Yadav, P. Dash, A. Mohanty, R. Abbassi, B.K. Mishra, Performance assessment of innovative constructed wetland-microbial fuel cell for electricity production and dye removal, Ecol. Eng., 47 (2012) 126-131.
[34] M.C. Potter, Electrical effects accompanying the decomposition of organic compounds, Proceedings of the royal society of London. Series b, containing papers of a biological character, 84 (1911) 260-276.
[35] B. Cohen, The bacterial culture as an electrical half-cell, J. Bacteriol, 21 (1931) 18-19.
[36] D. Pant, G. Van Bogaert, L. Diels, K. Vanbroekhoven, A review of the substrates used in microbial fuel cells (MFCs) for sustainable energy production, Bioresour. Technol., 101 (2010) 1533-1543.
[37] P. Pandey, V.N. Shinde, R.L. Deopurkar, S.P. Kale, S.A. Patil, D. Pant, Recent advances in the use of different substrates in microbial fuel cells toward wastewater treatment and simultaneous energy recovery, Applied Energy, 168 (2016) 706-723.
[38] J.R. Trapero, L. Horcajada, J.J. Linares, J. Lobato, Is microbial fuel cell technology ready? An economic answer towards industrial commercialization, Applied energy, 185 (2017) 698-707.
[39] M. Rahimnejad, A. Adhami, S. Darvari, A. Zirepour, S.-E. Oh, Microbial fuel cell as new technology for bioelectricity generation: a review, Alexandria Engineering Journal, 54 (2015) 745-756.

[40] B.E. Logan, Scaling up microbial fuel cells and other bioelectrochemical systems, Appl. Microbiol. Biotechnol., 85 (2010) 1665-1671.
[41] H. Rismani-Yazdi, S.M. Carver, A.D. Christy, O.H. Tuovinen, Cathodic limitations in microbial fuel cells: an overview, J. Power Sources, 180 (2008) 683-694.
[42] A.P. Borole, G. Reguera, B. Ringeisen, Z.-W. Wang, Y. Feng, B.H. Kim, Electroactive biofilms: current status and future research needs, Energy & Environmental Science, 4 (2011) 4813-4834.
[43] U. Schröder, F. Harnisch, L.T. Angenent, Microbial electrochemistry and technology: terminology and classification, Energy & Environmental Science, 8 (2015) 513-519.
[44] D.R. Lovley, Extracellular electron transfer: wires, capacitors, iron lungs, and more, Geobiology, 6 (2008) 225-231.
[45] N. Risgaard-Petersen, L.R. Damgaard, A. Revil, L.P. Nielsen, Mapping electron sources and sinks in a marine biogeobattery, Journal of Geophysical Research: Biogeosciences, 119 (2014) 1475-1486.
[46] M. Villano, F. Aulenta, M. Beccari, M. Majone, Start-up and performance of an activated sludge bioanode in microbial electrolysis cells, CHEMICAL ENGINEERING, 27 (2012).
[47] C. Gao, A. Wang, W.-M. Wu, Y. Yin, Y.-G. Zhao, Enrichment of anodic biofilm inoculated with anaerobic or aerobic sludge in single chambered air-cathode microbial fuel cells, Bioresour. Technol., 167 (2014) 124-132.
[48] A. Escapa, M.I. San-Martín, A. Morán, Potential use of microbial electrolysis cells in domestic wastewater treatment plants for energy recovery, Frontiers in Energy Research, 2 (2014) 19.
[49] B. Min, J. Kim, S. Oh, J.M. Regan, B.E. Logan, Electricity generation from swine wastewater using microbial fuel cells, Water Res., 39 (2005) 4961-4968.
[50] B. Erable, N.M. Duţeanu, M.M. Ghangrekar, C. Dumas, K. Scott, Application of electro-active biofilms, Biofouling, 26 (2010) 57-71.
[51] P.S. Bonanni, G.D. Schrott, L. Robuschi, J.P. Busalmen, Charge accumulation and electron transfer kinetics in Geobacter sulfurreducens biofilms, Energy & Environmental Science, 5 (2012) 6188-6195.
[52] J.B. Arends, W. Verstraete, 100 years of microbial electricity production: three concepts for the future, Microbial Biotechnology, 5 (2012) 333-346.
[53] L. Mao, W.S. Verwoerd, Selection of organisms for systems biology study of microbial electricity generation: a review, International Journal of Energy and Environmental Engineering, 4 (2013) 1-18.

[54] B.R. Ringeisen, E. Henderson, P.K. Wu, J. Pietron, R. Ray, B. Little, J.C. Biffinger, J.M. Jones-Meehan, High power density from a miniature microbial fuel cell using Shewanella oneidensis DSP10, Environmental science & technology, 40 (2006) 2629-2634.
[55] P.D. Kiely, J.M. Regan, B.E. Logan, The electric picnic: synergistic requirements for exoelectrogenic microbial communities, Curr. Opin. Biotechnol., 22 (2011) 378-385.
[56] G. Reguera, K.P. Nevin, J.S. Nicoll, S.F. Covalla, T.L. Woodard, D.R. Lovley, Biofilm and nanowire production leads to increased current in Geobacter sulfurreducens fuel cells, Applied and environmental microbiology, 72 (2006) 7345-7348.
[57] Z. Du, H. Li, T. Gu, A state of the art review on microbial fuel cells: a promising technology for wastewater treatment and bioenergy, Biotechnol. Adv., 25 (2007) 464-482.
[58] C.E. Reimers, L.M. Tender, S. Fertig, W. Wang, Harvesting energy from the marine sediment− water interface, Environmental science & technology, 35 (2001) 192-195.
[59] L.M. Tender, C.E. Reimers, H.A. Stecher, D.E. Holmes, D.R. Bond, D.A. Lowy, K. Pilobello, S.J. Fertig, D.R. Lovley, Harnessing microbially generated power on the seafloor, Nat. Biotechnol., 20 (2002) 821-825.
[60] D.-Y. Huang, S.-G. Zhou, Q. Chen, B. Zhao, Y. Yuan, L. Zhuang, Enhanced anaerobic degradation of organic pollutants in a soil microbial fuel cell, Chem. Eng. J., 172 (2011) 647-653.
[61] C. Corbella, M. Garfi, J. Puigagut, Vertical redox profiles in treatment wetlands as function of hydraulic regime and macrophytes presence: surveying the optimal scenario for microbial fuel cell implementation, Sci. Total Environ., 470-471 (2014) 754-758.
[62] Y. Zhao, S. Collum, M. Phelan, T. Goodbody, L. Doherty, Y. Hu, Preliminary investigation of constructed wetland incorporating microbial fuel cell: batch and continuous flow trials, Chem. Eng. J., 229 (2013) 364-370.
[63] L. Doherty, Y. Zhao, X. Zhao, Y. Hu, X. Hao, L. Xu, R. Liu, A review of a recently emerged technology: constructed wetland–microbial fuel cells, Water Res., 85 (2015) 38-45.
[64] M.A. Aguirre Sierra, Integrating microbial electrochemical systems in constructed wetlands: a new paradigm for treating wastewater in small communities, (2017).
[65] M. Hartl, D.F. Bedoya-Rios, M. Fernandez-Gatell, D.P.L. Rousseau, G. Du Laing, M. Garfi, J. Puigagut, Contaminants removal and bacterial activity enhancement along the flow path of constructed wetland microbial fuel cells, Sci. Total Environ., 652 (2019) 1195-1208.
[66] A. Vilajeliu-Pons, C. Koch, M.D. Balaguer, J. Colprim, F. Harnisch, S. Puig, Microbial electricity driven anoxic ammonium removal, Water Res., 130 (2018) 168-175.

[67] M. Sgroi, C. Pelissari, P. Roccaro, P.H. Sezerino, J. García, F.G.A. Vagliasindi, C. Ávila, Removal of organic carbon, nitrogen, emerging contaminants and fluorescing organic matter in different constructed wetland configurations, Chem. Eng. J., 332 (2018) 619-627.
[68] J. Vymazal, The use of hybrid constructed wetlands for wastewater treatment with special attention to nitrogen removal: a review of a recent development, Water Res., 47 (2013) 4795-4811.
[69] L. Xu, Y. Zhao, X. Wang, W. Yu, Applying multiple bio-cathodes in constructed wetland-microbial fuel cell for promoting energy production and bioelectrical derived nitrification-denitrification process, Chem. Eng., 344 (2018) 105-113.
[70] J. Vymazal, The use of hybrid constructed wetlands for wastewater treatment with special attention to nitrogen removal: a review of a recent development, Water research, 47 (2013) 4795-4811.
[71] P. Srivastava, A.K. Yadav, R. Abbassi, V. Garaniya, T. Lewis, Denitrification in a low carbon environment of a constructed wetland incorporating a microbial electrolysis cell, J. Environ. Chem. Eng., 6 (2018) 5602-5607.
[72] D. Wu, X. Yi, R. Tang, C. Feng, C. Wei, Single microbial fuel cell reactor for coking wastewater treatment: Simultaneous carbon and nitrogen removal with zero alkaline consumption, Sci. Total Environ., 621 (2018) 497-506.
[73] N. Lu, S.-g. Zhou, L. Zhuang, J.-t. Zhang, J.-r. Ni, Electricity generation from starch processing wastewater using microbial fuel cell technology, Biochem. Eng. J., 43 (2009) 246-251.
[74] C. Santoro, C. Arbizzani, B. Erable, I. Ieropoulos, Microbial fuel cells: From fundamentals to applications. A review, J. Power Sources, 356 (2017) 225-244.
[75] C. Corbella, J. Puigagut, Microbial fuel cells implemented in constructed wetlands: Fundamentals, current research and future perspectives, Contribution to Science, 11 (2015) 113-120.
[76] Z. Fang, H.-L. Song, N. Cang, X.-N. Li, Performance of microbial fuel cell coupled constructed wetland system for decolorization of azo dye and bioelectricity generation, Bioresour. Technol., 144 (2013) 165-171.
[77] P. Srivastava, A.K. Yadav, B.K. Mishra, The effects of microbial fuel cell integration into constructed wetland on the performance of constructed wetland, Bioresour Technol, 195 (2015) 223-230.

[78] C. Corbella, J. Puigagut, Improving domestic wastewater treatment efficiency with constructed wetland microbial fuel cells: Influence of anode material and external resistance, Sci. Total Environ., 631-632 (2018) 1406-1414.
[79] P. Srivastava, A.K. Yadav, V. Garaniya, R. Abbassi, Constructed Wetland Coupled Microbial Fuel Cell Technology: Development and Potential Applications, in: Microbial Electrochemical Technology, Elsevier, 2018, pp. 1021-1036.
[80] A.K. Yadav, P. Srivastava, N. Kumar, R. Abbassi, B.K. Mishra, Constructed Wetland-Microbial Fuel Cell: An Emerging Integrated Technology for Potential Industrial Wastewater Treatment and Bio-Electricity Generation, in: Constructed Wetlands for Industrial Wastewater Treatment, Wiley, 2018, pp. 493-510.
[81] S. Puig, M. Serra, A. Vilar-Sanz, M. Cabré, L. Bañeras, J. Colprim, M.D. Balaguer, Autotrophic nitrite removal in the cathode of microbial fuel cells, Bioresour. Technol., 102 (2011) 4462-4467.
[82] N. Pous, S. Puig, M.D. Balaguer, J. Colprim, Cathode potential and anode electron donor evaluation for a suitable treatment of nitrate-contaminated groundwater in bioelectrochemical systems, Chem. Eng. J., 263 (2015) 151-159.
[83] Y. Yang, L. Xie, X. Tao, K. Hu, S. Huang, Municipal wastewater treatment by the bioaugmentation of Bacillus sp. K5 within a sequencing batch reactor, PLoS One, 12 (2017) e0178837.
[84] APHA, Standard methods for the examination of water and wastewater, American Public Health Association (APHA): Washington, DC, USA, (2005).
[85] K. Schulze-Schweifing, A. Banerjee, W.G. Wade, Comparison of bacterial culture and 16S rRNA community profiling by clonal analysis and pyrosequencing for the characterization of the dentine caries-associated microbiome, Frontiers in cellular and infection microbiology, 4 (2014) 164.
[86] R.M. Maier, I.L. Pepper, Bacterial growth, in: Environ. Microbiol., Elsevier, 2015, pp. 37-56.
[87] H. Liu, S. Cheng, B.E. Logan, Production of electricity from acetate or butyrate using a single-chamber microbial fuel cell, Environmental science & technology, 39 (2005) 658-662.
[88] Y.L. Oon, S.A. Ong, L.N. Ho, Y.S. Wong, Y.S. Oon, H.K. Lehl, W.E. Thung, Hybrid system up-flow constructed wetland integrated with microbial fuel cell for simultaneous wastewater treatment and electricity generation, Bioresour Technol, 186 (2015) 270-275.

[89] P. Srivastava, A.K. Yadav, R. Abbassi, V. Garaniya, T. Lewis, Denitrification in a low carbon environment of a constructed wetland incorporating a microbial electrolysis cell, Journal of Environmental Chemical Engineering, 6 (2018) 5602-5607.
[90] S. Sevda, X. Dominguez-Benetton, H. De Wever, K. Vanbroekhoven, T.R. Sreekrishnan, D. Pant, Evaluation and enhanced operational performance of microbial fuel cells under alternating anodic open circuit and closed circuit modes with different substrates, Biochem. Eng. J., 90 (2014) 294-300.
[91] P. Srivastava, A.K. Yadav, B.K. Mishra, The effects of microbial fuel cell integration into constructed wetland on the performance of constructed wetland, Bioresour. Technol., 195 (2015) 223-230.
[92] B. Qu, B. Fan, S. Zhu, Y. Zheng, Anaerobic ammonium oxidation with an anode as the electron acceptor, Environ Microbiol Rep, 6 (2014) 100-105.
[93] Y.L. Oon, S.A. Ong, L.N. Ho, Y.S. Wong, Y.S. Oon, H.K. Lehl, W.E. Thung, Hybrid system up-flow constructed wetland integrated with microbial fuel cell for simultaneous wastewater treatment and electricity generation, Bioresour. Technol., 186 (2015) 270-275.
[94] F. Liu, L. Sun, J. Wan, A. Tang, M. Deng, R. Wu, Organic matter and ammonia removal by a novel integrated process of constructed wetland and microbial fuel cells, RSC Adv., 9 (2019) 5384-5393.
[95] X. Shen, J. Zhang, D. Liu, Z. Hu, H. Liu, Enhance performance of microbial fuel cell coupled surface flow constructed wetland by using submerged plants and enclosed anodes, Chem. Eng. J., 351 (2018) 312-318.
[96] S. Liu, H. Song, S. Wei, F. Yang, X. Li, Bio-cathode materials evaluation and configuration optimization for power output of vertical subsurface flow constructed wetland - microbial fuel cell systems, Bioresour. Technol., 166 (2014) 575-583.
[97] S.N. Mohamed, P.A. Hiraman, K. Muthukumar, T. Jayabalan, Bioelectricity production from kitchen wastewater using microbial fuel cell with photosynthetic algal cathode, Bioresour. Technol., 295 (2020) 122226.
[98] P. Srivastava, S. Gupta, V. Garaniya, R. Abbassi, A.K. Yadav, Up to 399 mV bioelectricity generated by a rice paddy-planted microbial fuel cell assisted with a blue-green algal cathode, Environmental Chemistry Letters, (2018).
[99] B.E. Logan, Microbial fuel cells, John Wiley & Sons, 2008.
[100] C. Corbella, M. Garfi, J. Puigagut, Long-term assessment of best cathode position to maximise microbial fuel cell performance in horizontal subsurface flow constructed wetlands, Sci. Total Environ., 563-564 (2016) 448-455.

[101] R.A. Timmers, M. Rothballer, D.P. Strik, M. Engel, S. Schulz, M. Schloter, A. Hartmann, B. Hamelers, C. Buisman, Microbial community structure elucidates performance of Glyceria maxima plant microbial fuel cell, Appl. Microbiol. Biotechnol., 94 (2012) 537-548.
[102] L. Lu, D. Xing, Z.J. Ren, Microbial community structure accompanied with electricity production in a constructed wetland plant microbial fuel cell, Bioresour. Technol., 195 (2015) 115-121.
[103] P. Yilmaz, P. Yarza, J.Z. Rapp, F.O. Glöckner, Expanding the world of marine bacterial and archaeal clades, Frontiers in microbiology, 6 (2016) 1524.
[104] K. Waites, Medically Relevant Mycoplasmas and Ureaplasmas, (2016).
[105] P. Aelterman, S. Freguia, J. Keller, W. Verstraete, K. Rabaey, The anode potential regulates bacterial activity in microbial fuel cells, Appl. Microbiol. Biotechnol., 78 (2008) 409-418.
[106] K. Rabaey, N. Boon, S.D. Siciliano, M. Verhaege, W. Verstraete, Biofuel cells select for microbial consortia that self-mediate electron transfer, Appl. Environ. Microbiol., 70 (2004) 5373-5382.
[107] M. Hassan, H. Wei, H. Qiu, Y. Su, S.W.H. Jaafry, L. Zhan, B. Xie, Power generation and pollutants removal from landfill leachate in microbial fuel cell: Variation and influence of anodic microbiomes, Bioresour Technol, 247 (2018) 434-442.
[108] J. Zhai, M.H. Rahaman, X. Chen, H. Xiao, K. Liao, X. Li, C. Duan, B. Zhang, G. Tao, Y. John, New nitrogen removal pathways in a full-scale hybrid constructed wetland proposed from high-throughput sequencing and isotopic tracing results, Ecol. Eng., 97 (2016) 434-443.
[109] F. Xu, F.-q. Cao, Q. Kong, L.-l. Zhou, Q. Yuan, Y.-j. Zhu, Q. Wang, Electricity production and evolution of microbial community in the constructed wetland-microbial fuel cell, Chemical Engineering Journal, 339 (2018) 479-486.
[110] F. Xu, D.-l. Ouyang, E.R. Rene, H.Y. Ng, L.-l. Guo, Y.-j. Zhu, L.-l. Zhou, Q. Yuan, M.-s. Miao, Q. Wang, Electricity production enhancement in a constructed wetland-microbial fuel cell system for treating saline wastewater, Bioresour. Technol., 288 (2019) 121462.
[111] J. Villasenor, P. Capilla, M.A. Rodrigo, P. Canizares, F.J. Fernandez, Operation of a horizontal subsurface flow constructed wetland--microbial fuel cell treating wastewater under different organic loading rates, Water Res., 47 (2013) 6731-6738.
[112] M. Maine, N. Sune, H. Hadad, G. Sánchez, C. Bonetto, Nutrient and metal removal in a constructed wetland for wastewater treatment from a metallurgic industry, Ecol. Eng., 26 (2006) 341-347.

[113] A. Sheoran, V. Sheoran, Heavy metal removal mechanism of acid mine drainage in wetlands: a critical review, Miner. Eng., 19 (2006) 105-116.
[114] A. Sochacki, A.K. Yadav, P. Srivastava, N. Kumar, M.W. Fitch, A. Mohanty, Constructed Wetlands for Metals: Removal Mechanism and Analytical Challenges, in: Constructed Wetlands for Industrial Wastewater Treatment, Wiley, 2018, pp. 223-247.
[115] M. Li, S. Zhou, Y. Xu, Z. Liu, F. Ma, L. Zhi, X. Zhou, Simultaneous Cr (VI) reduction and bioelectricity generation in a dual chamber microbial fuel cell, Chem. Eng. J., 334 (2018) 1621-1629.
[116] E. Dermou, Velissariou, A., Xenos, D., & Vayenas, D. V. , Biological chromium (VI) reduction using a trickling filter, J. Hazard. Mater., 126 (2005) 78-85.
[117] M. Asri, El Ghachtouli, N., Elabed, S., Koraichi, S. I., Elabed, A., Silva, B., & Tavares, T., Wicherhamomyces anomalus biofilm supported on wood husk for chromium wastewater treatment, J. Hazard. Mater., 359 (2018) 554-562.
[118] EPA, National Primary Drinking Water Regulations, in, EPA United States Environmental Protection Agency, www.epa.gov, 2018.
[119] F. Vendruscolo, G.L. da Rocha Ferreira, N.R. Antoniosi Filho, Biosorption of hexavalent chromium by microorganisms, International Biodeterioration & Biodegradation, 119 (2017) 87-95.
[120] A. Demir, & Arisoy, M., Biological and chemical removal of Cr (VI) from waste water: cost and benefit analysis, J. Hazard. Mater., 147 (2007) 275-280.
[121] Y. Li, Z. Jin, T. Li, Z. Xiu, One-step synthesis and characterization of core–shell Fe@ SiO2 nanocomposite for Cr (VI) reduction, Sci. Total Environ., 421 (2012) 260-266.
[122] N. Xafenias, Y. Zhang, C.J. Banks, Evaluating hexavalent chromium reduction and electricity production in microbial fuel cells with alkaline cathodes, International Journal of Environmental Science and Technology, 12 (2014) 2435-2446.
[123] G. Wang, L. Huang, Y. Zhang, Cathodic reduction of hexavalent chromium [Cr (VI)] coupled with electricity generation in microbial fuel cells, Biotechnol. Lett, 30 (2008) 1959.
[124] A.C. Sophia, S. Sai, Modified microbial fuel cell for Cr(VI) reduction and simultaneous bio-electricity production, Journal of Environmental Chemical Engineering, 4 (2016) 2402-2409.
[125] X. Wu, X. Zhu, T. Song, L. Zhang, H. Jia, P. Wei, Effect of acclimatization on hexavalent chromium reduction in a biocathode microbial fuel cell, Bioresour. Technol., 180 (2015) 185-191.

[126] Z. Lu, D. Chang, J. Ma, G. Huang, L. Cai, L. Zhang, Behavior of metal ions in bioelectrochemical systems: A review, J. Power Sources, 275 (2015) 243-260.
[127] P. Srivastava, S. Dwivedi, N. Kumar, R. Abbassi, V. Garaniya, A.K. Yadav, Performance assessment of aeration and radial oxygen loss assisted cathode based integrated constructed wetland-microbial fuel cell systems, Bioresour. Technol., 244 (2017) 1178-1182.
[128] C. Ramírez-Vargas, A. Prado, C. Arias, P. Carvalho, A. Esteve-Núñez, H. Brix, Microbial Electrochemical Technologies for Wastewater Treatment: Principles and Evolution from Microbial Fuel Cells to Bioelectrochemical-Based Constructed Wetlands, Water, 10 (2018).
[129] K.K. Onchoke, S.A. Sasu, Determination of Hexavalent Chromium (Cr (VI)) concentrations via ion chromatography and UV-Vis spectrophotometry in samples collected from nacogdoches wastewater treatment plant, East Texas (USA), Advances in Environmental Chemistry, 2016 (2016).
[130] K. Suvardhan, S. Ramanaiah, K.S. Kumar, D. Rekha, U. Bhagan, G. Naidu, G.K. Naidu, B. Sastry, P. Chiranjeevi, Spectrophotometric determination of chromium in water, and pharmaceutical samples using 1-naphthol, E-Journal of Chemistry, 2 (2005) 6-14.
[131] P. Srivastava, A.K. Yadav, V. Garaniya, T. Lewis, R. Abbassi, S.J. Khan, Electrode dependent anaerobic ammonium oxidation in microbial fuel cell integrated hybrid constructed wetlands: A new process, Sci. Total Environ., 698 (2020) 134248.
[132] L. Huang, X. Chai, S. Cheng, G. Chen, Evaluation of carbon-based materials in tubular biocathode microbial fuel cells in terms of hexavalent chromium reduction and electricity generation, Chem. Eng. J., 166 (2011) 652-661.
[133] H.S.J. Tandukar madan, Onodera takashi , Pavlostathis spyros G. , Biological Chromium(VI) Reduction in the Cathode of a Microbial Fuel Cell, Environ. Sci. Technol., 43 (2009).
[134] K. Rajeshwar, J.G. Ibanez, Environmental electrochemistry: Fundamentals and applications in pollution sensors and abatement, Elsevier, 1997.
[135] D. Rajkumar, K. Palanivelu, Electrochemical treatment of industrial wastewater, J. Hazard. Mater., 113 (2004) 123-129.
[136] R. Bhatnagar, H. Joshi, I.D. Mall, V.C. Srivastava, Electrochemical oxidation of textile industry wastewater by graphite electrodes, Journal of Environmental Science and Health, Part A, 49 (2014) 955-966.
[137] Z. Li, X. Zhang, L. Lei, Electricity production during the treatment of real electroplating wastewater containing Cr6+ using microbial fuel cell, Process Biochem., 43 (2008) 1352-1358.

[138] M. Martins, M.L. Faleiro, S. Chaves, R. Tenreiro, E. Santos, M.C. Costa, Anaerobic bio-removal of uranium (VI) and chromium (VI): comparison of microbial community structure, J. Hazard. Mater., 176 (2010) 1065-1072.
[139] M.A.A. Sierra, Integrating microbial electrochemical systems in constructed wetlands, a new paradigm for treating wastewater in samll communities, in, Universidad de Alcalá, 2017.
[140] J.M. Chen, O.J. Hao, Microbial chromium (VI) reduction, Critical Reviews in Environmental Science and Technology, 28 (1998) 219-251.
[141] B. Chardin, A. Dolla, F. Chaspoul, M. Fardeau, P. Gallice, M. Bruschi, Bioremediation of chromate: thermodynamic analysis of the effects of Cr (VI) on sulfate-reducing bacteria, Appl. Microbiol. Biotechnol., 60 (2002) 352-360.
[142] J. Wang, X. Song, Y. Wang, B. Abayneh, Y. Li, D. Yan, J. Bai, Nitrate removal and bioenergy production in constructed wetland coupled with microbial fuel cell: Establishment of electrochemically active bacteria community on anode, Bioresour. Technol., 221 (2016) 358-365.
[143] L. Doherty, Y. Zhao, X. Zhao, W. Wang, Nutrient and organics removal from swine slurry with simultaneous electricity generation in an alum sludge-based constructed wetland incorporating microbial fuel cell technology, Chem. Eng., 266 (2015) 74-81.
[144] C. Kim, C.R. Lee, Y.E. Song, J. Heo, S.M. Choi, D.-H. Lim, J. Cho, C. Park, M. Jang, J.R. Kim, Hexavalent chromium as a cathodic electron acceptor in a bipolar membrane microbial fuel cell with the simultaneous treatment of electroplating wastewater, Chem. Eng. J., 328 (2017) 703-707.
[145] S.A. Patil, C. Hägerhäll, L. Gorton, Electron transfer mechanisms between microorganisms and electrodes in bioelectrochemical systems, Bioanalytical reviews, 4 (2012) 159-192.
[146] R.A. Rozendal, H.V. Hamelers, K. Rabaey, J. Keller, C.J. Buisman, Towards practical implementation of bioelectrochemical wastewater treatment, Trends Biotechnol., 26 (2008) 450-459.
[147] U. Schröder, Anodic electron transfer mechanisms in microbial fuel cells and their energy efficiency, PCCP, 9 (2007) 2619-2629.
[148] W.L. Miller, Minireview: regulation of steroidogenesis by electron transfer, Endocrinology, 146 (2005) 2544-2550.
[149] S. Fishilevich, L. Amir, Y. Fridman, A. Aharoni, L. Alfonta, Surface display of redox enzymes in microbial fuel cells, J. Am. Chem. Soc., 131 (2009) 12052-12053.

[150] L. Tang, G.-D. Yang, G.-M. Zeng, Y. Cai, S.-S. Li, Y.-Y. Zhou, Y. Pang, Y.-Y. Liu, Y. Zhang, B. Luna, Synergistic effect of iron doped ordered mesoporous carbon on adsorption-coupled reduction of hexavalent chromium and the relative mechanism study, Chem. Eng. J., 239 (2014) 114-122.
[151] C. Corbella, M. Guivernau, M. Viñas, J. Puigagut, Operational, design and microbial aspects related to power production with microbial fuel cells implemented in constructed wetlands, Water Res., 84 (2015) 232-242.
[152] S. Larsen, L.P. Nielsen, A. Schramm, Cable bacteria associated with long-distance electron transport in N ew E ngland salt marsh sediment, Environmental microbiology reports, 7 (2015) 175-179.
[153] C. Pfeffer, S. Larsen, J. Song, M. Dong, F. Besenbacher, R.L. Meyer, K.U. Kjeldsen, L. Schreiber, Y.A. Gorby, M.Y. El-Naggar, Filamentous bacteria transport electrons over centimetre distances, Nature, 491 (2012) 218.
[154] J.F. Heidelberg, R. Seshadri, S.A. Haveman, C.L. Hemme, I.T. Paulsen, J.F. Kolonay, J.A. Eisen, N. Ward, B. Methe, L.M. Brinkac, The genome sequence of the anaerobic, sulfate-reducing bacterium Desulfovibrio vulgaris Hildenborough, Nat. Biotechnol., 22 (2004) 554.
[155] D. Pradhan, L.B. Sukla, M. Sawyer, P.K.S.M. Rahman, Recent bioreduction of hexavalent chromium in wastewater treatment: A review, Journal of Industrial and Engineering Chemistry, 55 (2017) 1-20.
[156] R. Batool, Hexavalent Chromium Reduction by Bacteria from Tannery Effluent, J. Microbiol. Biotechnol., 22 (2012) 547-554.
[157] W. Guo, Y. Wen, Y. Chen, Q. Zhou, Sulfur cycle as an electron mediator between carbon and nitrate in a constructed wetland microcosm, Front Environ. Sci. Eng., 14 (2020) 1-13.
[158] L.Y. Liu, G.J. Xie, D.F. Xing, B.F. Liu, J. Ding, G.L. Cao, N.Q. Ren, Sulfate dependent ammonium oxidation: A microbial process linked nitrogen with sulfur cycle and potential application, Environ. Res., 192 (2021) 110282.
[159] Y. Zhao, S. Collum, M. Phelan, T. Goodbody, L. Doherty, Y. Hu, Preliminary investigation of constructed wetland incorporating microbial fuel cell: batch and continuous flow trials, Chem. Eng., 229 (2013) 364-370.
[160] L. Xu, W. Yu, N. Graham, Y. Zhao, J. Qu, Application of Integrated Bioelectrochemical-Wetland Systems for Future Sustainable Wastewater Treatment, Environ. Sci. Technol., 53(4) (2019) 1741-1743.

[161] P. Srivastava, R. Abbassi, V. Garaniya, T. Lewis, A.K. Yadav, Performance of pilot-scale horizontal subsurface flow constructed wetland coupled with a microbial fuel cell for treating wastewater, J. Water Process Eng., 33 (2020).
[162] C. Corbella, J. Garcia, J. Puigagut, Microbial fuel cells for clogging assessment in constructed wetlands, Sci. Total Environ., 569-570 (2016) 1060-1063.
[163] D.K. Yeruva, G. Velvizhi, S.V. Mohan, Coupling of aerobic/anoxic and bioelectrogenic processes for treatment of pharmaceutical wastewater associated with bioelectricity generation, Renew. Energy, 98 (2016) 171-177.
[164] S. Gupta, P. Srivastava, S.A. Patil, A.K. Yadav, A comprehensive review on emerging constructed wetland coupled microbial fuel cell technology: potential applications and challenges, Bioresour. Technol., (2020) 124376.
[165] B. Ji, Y. Zhao, J. Vymazal, Ü. Mander, R. Lust, C. Tang, Mapping the field of constructed wetland-microbial fuel cell: A review and bibliometric analysis, Chemosphere, (2020) 128366.
[166] P. Srivastava, R. Abbassi, A.K. Yadav, V. Garaniya, M.A.F. Jahromi, A review on the contribution of an electron in electroactive wetlands: Electricity generation and enhanced wastewater treatment, Chemosphere, (2020) 126926.
[167] T. González, J. Puigagut, G. Vidal, Organic matter removal and nitrogen transformation by a constructed wetland-microbial fuel cell system with simultaneous bioelectricity generation, Sci. Total Environ., 753 (2021) 142075.
[168] S.V. Mohan, G. Velvizhi, K.V. Krishna, M.L. Babu, Microbial catalyzed electrochemical systems: a bio-factory with multi-facet applications, Bioresour. Technol., 165 (2014) 355-364.
[169] J. Jiang, Q. Zhao, L. Wei, K. Wang, Extracellular biological organic matters in microbial fuel cell using sewage sludge as fuel, Water Res., 44 (2010) 2163-2170.
[170] A. Baudler, I. Schmidt, M. Langner, A. Greiner, U. Schröder, Does it have to be carbon? Metal anodes in microbial fuel cells and related bioelectrochemical systems, Energy Environ. Sci., 8 (2015) 2048-2055.
[171] I.C.B. Rodrigues, V.A. Leão, Producing electrical energy in microbial fuel cells based on sulphate reduction: a review, Environmental Science and Pollution Research, (2020) 1-10.
[172] X. Ge, X. Cao, X. Song, Y. Wang, Z. Si, Y. Zhao, W. Wang, A.A. Tesfahunegn, Bioenergy generation and simultaneous nitrate and phosphorus removal in a pyrite-based constructed wetland-microbial fuel cell, Bioresour. Technol., 296 (2020) 122350.
[173] A. Yakar, C. Türe, O.C. Türker, J. Vymazal, Ç. Saz, Impacts of various filtration media on wastewater treatment and bioelectric production in up-flow constructed wetland combined with microbial fuel cell (UCW-MFC), Ecol. Eng., 117 (2018) 120-132.

[174] L. Xu, Y. Zhao, C. Tang, L. Doherty, Influence of glass wool as separator on bioelectricity generation in a constructed wetland-microbial fuel cell, J. Environ. Manage, 207 (2018) 116-123.
[175] Y.-K. Wang, G.-P. Sheng, B.-J. Shi, W.-W. Li, H.-Q. Yu, A novel electrochemical membrane bioreactor as a potential net energy producer for sustainable wastewater treatment, Sci. Rep., 3 (2013) 1-6.
[176] T.-Y. Chou, C.G. Whiteley, D.-J. Lee, Anodic potential on dual-chambered microbial fuel cell with sulphate reducing bacteria biofilm, Int. J. Hydrog. Energy, 39 (2014) 19225-19231.
[177] P. Srivastava, R. Abbassi, A.K. Yadav, V. Garaniya, N. Kumar, S.J. Khan, T. Lewis, Enhanced chromium (VI) treatment in electroactive constructed wetlands: influence of conductive material, J. Hazard. Mater., 387 (2020) 121722.
[178] T. Sandfeld, U. Marzocchi, C. Petro, A. Schramm, N. Risgaard-Petersen, Electrogenic sulfide oxidation mediated by cable bacteria stimulates sulfate reduction in freshwater sediments, ISME J., (2020).
[179] A. Ter Heijne, R. de Rink, D. Liu, J.B.M. Klok, C.J.N. Buisman, Bacteria as an Electron Shuttle for Sulfide Oxidation, Environ. Sci. Technol. Lett., 5 (2018) 495-499.
[180] Q. Dai, S. Zhang, H. Liu, J. Huang, L. Li, Sulfide-mediated azo dye degradation and microbial community analysis in a single-chamber air cathode microbial fuel cell, Bioelectrochemistry, 131 (2020) 107349.
[181] Z. Jing, Y. Hu, Q. Niu, Y. Liu, Y.Y. Li, X.C. Wang, UASB performance and electron competition between methane-producing archaea and sulfate-reducing bacteria in treating sulfate-rich wastewater containing ethanol and acetate, Bioresour. Technol., 137 (2013) 349-357.
[182] V. Agostino, M.A. Rosenbaum, Sulfate-Reducing ElectroAutotrophs and Their Applications in Bioelectrochemical Systems, Frontiers in Energy Research, 6 (2018).
[183] S. Gupta, P. Srivastava, A.K. Yadav, Integration of microbial fuel cell into constructed wetlands: effects, applications, and future outlook, in: Integrated Microbial Fuel Cells for Wastewater Treatment, Elsevier, 2020, pp. 273-293.
[184] A. González del Campo, P. Cañizares, J. Lobato, M. Rodrigo, F.J. Fernandez Morales, Effects of External Resistance on Microbial Fuel Cell's Performance, in: Environment, Energy and Climate Change II, 2014, pp. 175-197.

[185] M. Sun, Z.X. Mu, Y.P. Chen, G.P. Sheng, X.W. Liu, Y.Z. Chen, Y. Zhao, H.L. Wang, H.Q. Yu, L. Wei, F. Ma, Microbe-assisted sulfide oxidation in the anode of a microbial fuel cell, Environ. Sci. Technol., 43 (2009) 3372-3377.
[186] U. Schröder, F. Harnisch, L.T. Angenent, Microbial electrochemistry and technology: terminology and classification, Energy Environ. Sci., 8 (2015) 513-519.
[187] D.J. Lee, X. Liu, H.L. Weng, Sulfate and organic carbon removal by microbial fuel cell with sulfate-reducing bacteria and sulfide-oxidising bacteria anodic biofilm, Bioresour. Technol., 156 (2014) 14-19.
[188] E. Cato, A. Rossi, N.C. Scherrer, E.S. Ferreira, An XPS study into sulphur speciation in blue and green ultramarine, J. Cult. Herit., 29 (2018) 30-35.
[189] S.S. Kumar, S.K. Malyan, S. Basu, N.R. Bishnoi, Syntrophic association and performance of Clostridium, Desulfovibrio, Aeromonas and Tetrathiobacter as anodic biocatalysts for bioelectricity generation in dual chamber microbial fuel cell, Environ. Sci. Pollut. Res., 24 (2017) 16019-16030.
[190] S. Bratkova, Z. Alexieva, A. Angelov, K. Nikolova, P. Genova, R. Ivanov, M. Gerginova, N. Peneva, V. Beschkov, Efficiency of microbial fuel cells based on the sulfate reduction by lactate and glucose, Int. J. Environ. Sci. Technol., 16 (2019) 6145-6156.
[191] H. Ni, K. Wang, S. Lv, X. Wang, L. Zhuo, J. Zhang, Effects of Concentration Variations on the Performance and Microbial Community in Microbial Fuel Cell Using Swine Wastewater, Energies, 13 (2020).
[192] J. Hu, C. Zeng, G. Liu, Y. Lu, R. Zhang, H. Luo, Enhanced sulfate reduction accompanied with electrically-conductive pili production in graphene oxide modified biocathodes, Bioresour. Technol., 282 (2019) 425-432.
[193] T. Fenchel, H. Blackburn, G.M. King, T.H. Blackburn, Bacterial biogeochemistry: the ecophysiology of mineral cycling, Academic press, 2012.
[194] E.-T. Lim, G.-T. Jeong, S.-H. Bhang, S.-H. Park, D.-H. Park, Evaluation of pilot-scale modified A2O processes for the removal of nitrogen compounds from sewage, Bioresour. Technol., 100 (2009) 6149-6154.
[195] A. Lateef, M.N. Chaudhry, S. Ilyas, Biological treatment of dairy wastewater using activated sludge, Science Asia, 39 (2013) 179-185.
[196] A. Barco, M. Borin, Treatment performance and macrophytes growth in a restored hybrid constructed wetland for municipal wastewater treatment, Ecol. Eng., 107 (2017) 160-171.

[197] X. Tan, Y. Yang, Y. Liu, X. Li, X. Fan, Z. Zhou, C. Liu, W. Yin, Enhanced simultaneous organics and nutrients removal in tidal flow constructed wetland using activated alumina as substrate treating domestic wastewater, Bioresour. Technol., 280 (2019) 441-446.
[198] T. Saeed, S. Muntaha, M. Rashid, G. Sun, A. Hasnat, Industrial wastewater treatment in constructed wetlands packed with construction materials and agricultural by-products, Journal of Cleaner Production, 189 (2018) 442-453.
[199] H.T. Nguyen, B.Q. Nguyen, T.T. Duong, A.T. Bui, H.T. Nguyen, H.T. Cao, N.T. Mai, K.M. Nguyen, T.T. Pham, K.-W. Kim, Pilot-scale removal of arsenic and heavy metals from mining wastewater using adsorption combined with constructed wetland, Minerals, 9 (2019) 379.
[200] P. Li, S. Wang, Y. Peng, Y. Liu, J. He, The synergistic effects of dissolved oxygen and pH on N2O production in biological domestic wastewater treatment under nitrifying conditions, Environ. Technol., 36 (2015) 1623-1631.
[201] Q. Lu, H. Shim, Comparison of chloride effect between A2O and SBR processes treating domestic wastewater, Desalination and Water Treatment, 53 (2015) 2549-2554.
[202] J. Wang, K. Chon, X. Ren, Y. Kou, K.J. Chae, Y. Piao, Effects of beneficial microorganisms on nutrient removal and excess sludge production in an anaerobic-anoxic/oxic (A(2)O) process for municipal wastewater treatment, Bioresour. Technol., 281 (2019) 90-98.
[203] M. Visa, Tailoring fly ash activated with bentonite as adsorbent for complex wastewater treatment, Appl. Surf. Sci., 263 (2012) 753-762.
[204] A.R. Mohammadi, N. Mehrdadi, G.N. Bidhendi, A. Torabian, Excess sludge reduction using ultrasonic waves in biological wastewater treatment, Desalination, 275 (2011) 67-73.
[205] Y. Gao, Y. Peng, J. Zhang, S. Wang, J. Guo, L. Ye, Biological sludge reduction and enhanced nutrient removal in a pilot-scale system with 2-step sludge alkaline fermentation and A2O process, Bioresour. Technol., 102 (2011) 4091-4097.
[206] E. Xiao, Y. Zhou, D. Xu, R. Lu, Y. Chen, Q. Zhou, Z. Wu, The physiological response of Arundo donax and characteristics of anodic bacterial community in BE-CW systems: Effects of the applied voltage, Chem. Eng. J., 380 (2020).
[207] L. Xu, B. Wang, X. Liu, W. Yu, Y. Zhao, Maximizing the energy harvest from a microbial fuel cell embedded in a constructed wetland, Appl. Energy, 214 (2018) 83-91.
[208] S. Gupta, A. Nayak, C. Roy, A.K. Yadav, An algal assisted constructed wetland-microbial fuel cell integrated with sand filter for efficient wastewater treatment and electricity production, Chemosphere, (2020) 128132.

[209] E. Bolyen, J.R. Rideout, M.R. Dillon, N.A. Bokulich, C.C. Abnet, G.A. Al-Ghalith, H. Alexander, E.J. Alm, M. Arumugam, F. Asnicar, Reproducible, interactive, scalable and extensible microbiome data science using QIIME 2, Nat. Biotechnol., 37 (2019) 852-857.
[210] B.J. Callahan, P.J. McMurdie, M.J. Rosen, A.W. Han, A.J.A. Johnson, S.P. Holmes, DADA2: high-resolution sample inference from Illumina amplicon data, Nature methods, 13 (2016) 581-583.
[211] N.A. Bokulich, M.R. Dillon, Y. Zhang, J.R. Rideout, E. Bolyen, H. Li, P.S. Albert, J.G. Caporaso, q2-longitudinal: longitudinal and paired-sample analyses of microbiome data, MSystems, 3 (2018).
[212] A. Prado, C.A. Ramirez-Vargas, C.A. Arias, A. Esteve-Nunez, Novel bioelectrochemical strategies for domesticating the electron flow in constructed wetlands, Sci. Total Environ., 735 (2020) 139522.
[213] M. Wei, J. Rakoczy, C. Vogt, F. Harnisch, R. Schumann, H.H. Richnow, Enhancement and monitoring of pollutant removal in a constructed wetland by microbial electrochemical technology, Bioresour. Technol., 196 (2015) 490-499.
[214] X. Xu, G.L. Mills, Do constructed wetlands remove metals or increase metal bioavailability?, Journal of environmental management, 218 (2018) 245-255.
[215] A.W. Schroth, C.D. Giles, P.D. Isles, Y. Xu, Z. Perzan, G.K. Druschel, Dynamic coupling of iron, manganese, and phosphorus behavior in water and sediment of shallow ice-covered eutrophic lakes, Environmental science & technology, 49 (2015) 9758-9767.
[216] J.-H. Huang, S. Paul, S. Mayer, E. Moradpour, R. Hasselbach, R. Gieré, C. Alewell, Metal biogeochemistry in constructed wetlands based on fluviatile sand and zeolite-and clinopyroxene-dominated lava sand, Scientific reports, 7 (2017) 1-11.
[217] M. Li, S. Zhou, Y. Xu, Z. Liu, F. Ma, L. Zhi, X. Zhou, Simultaneous Cr(VI) reduction and bioelectricity generation in a dual chamber microbial fuel cell, Chem. Eng. J., 334 (2018) 1621-1629.
[218] I.-S. Kim, K.I. Ekpeghere, S.-Y. Ha, B.-S. Kim, B. Song, J.-T. Kim, H.-G. Kim, S.-C. Koh, Full-scale biological treatment of tannery wastewater using the novel microbial consortium BM-S-1, Journal of Environmental Science and Health, Part A, 49 (2014) 355-364.
[219] J. Zhou, H. Li, X. Chen, D. Wan, W. Mai, C. Sun, Cometabolic degradation of low-strength coking wastewater and the bacterial community revealed by high-throughput sequencing, Bioresour. Technol., 245 (2017) 379-385.

[220] M. Hassan, H. Wei, H. Qiu, Y. Su, S.W.H. Jaafry, L. Zhan, B. Xie, Power generation and pollutants removal from landfill leachate in microbial fuel cell: Variation and influence of anodic microbiomes, Bioresour. Technol., 247 (2018) 434-442.
[221] S. Gupta, P. Srivastava, A.K. Yadav, Simultaneous removal of organic matters and nutrients from high-strength wastewater in constructed wetlands followed by entrapped algal systems, Environ. Sci. Pollut. Res., (2019) 1-6.
[222] T. Yamashita, T. Hayashi, H. Iwasaki, M. Awatsu, H. Yokoyama, Ultra-low-power energy harvester for microbial fuel cells and its application to environmental sensing and long-range wireless data transmission, J. Power Sources, 430 (2019) 1-11.
[223] L. Lu, F.L. Lobo, D. Xing, Z.J. Ren, Active harvesting enhances energy recovery and function of electroactive microbiomes in microbial fuel cells, Applied Energy, 247 (2019) 492-502.
[224] M. Mahmud, F. Ejeian, S. Azadi, M. Myers, B. Pejcic, R. Abbasi, A. Razmjou, M. Asadnia, Recent progress in sensing nitrate, nitrite, phosphate, and ammonium in aquatic environment, Chemosphere, (2020) 127492.
[225] Z. Ge, L. Wu, F. Zhang, Z. He, Energy extraction from a large-scale microbial fuel cell system treating municipal wastewater, J. Power Sources, 297 (2015) 260-264.
[226] F. Ejeian, P. Etedali, H.-A. Mansouri-Tehrani, A. Soozanipour, Z.-X. Low, M. Asadnia, A. Taheri-Kafrani, A.J.B. Razmjou, Bioelectronics, Biosensors for wastewater monitoring: A review, 118 (2018) 66-79.
[227] R. Zuraidah, S. Nur, Y. Norilhamiah, S.A. Aida, M. Amelia, F.M. Muhammad, Microbial fuel cell for conversion of chemical energy to electrical energy from food industry wastewater, J. Environ. Science and Technol., 9 (2016) 481-485.
[228] R. Abbassi, A.K. Yadav, Introduction to microbial fuel cells: challenges and opportunities, in: Integrated Microbial Fuel Cells for Wastewater Treatment, Elsevier, 2020, pp. 3-27.
[229] X.A. Walter, J. You, J. Winfield, U. Bajarunas, J. Greenman, I.A. Ieropoulos, From the lab to the field: Self-stratifying microbial fuel cells stacks directly powering lights, Applied Energy, 277 (2020).
[230] H. Wang, Z.J. Ren, A comprehensive review of microbial electrochemical systems as a platform technology, Biotechnol. Adv., 31 (2013) 1796-1807.
[231] L. Xu, Y. Zhao, L. Doherty, Y. Hu, X. Hao, The integrated processes for wastewater treatment based on the principle of microbial fuel cells: A review, Crit. Rev. Environ. Sci. Technol., 46 (2015) 60-91.

[232] P. Srivastava, R. Abbassi, A.K. Yadav, V. Garaniya, F. Khan, Microbial fuel cell–integrated wastewater treatment systems, in: Integrated Microbial Fuel Cells for Wastewater Treatment, Elsevier, 2020, pp. 29-46.
[233] L. Doherty, X. Zhao, Y. Zhao, W. Wang, The effects of electrode spacing and flow direction on the performance of microbial fuel cell-constructed wetland, Ecol. Eng., 79 (2015) 8-14.
[234] Z. Fang, H.-l. Song, N. Cang, X.-n. Li, Electricity production from Azo dye wastewater using a microbial fuel cell coupled constructed wetland operating under different operating conditions, Biosens. Bioelectron., 68 (2015) 135-141.
[235] M. Alaraj, Z.J. Ren, J.-D. Park, Microbial fuel cell energy harvesting using synchronous flyback converter, J. Power Sources, 247 (2014) 636-642.
[236] P. Tamta, N. Rani, A.K. Yadav, Enhanced wastewater treatment and electricity generation using stacked constructed wetland–microbial fuel cells, Environ. Chem. Lett., (2020).
[237] S. Liu, H. Song, S. Wei, F. Yang, X. Li, Bio-cathode materials evaluation and configuration optimization for power output of vertical subsurface flow constructed wetland—Microbial fuel cell systems, Bioresour. Technol., 166 (2014) 575-583.
[238] Y.L. Oon, S.A. Ong, L.N. Ho, Y.S. Wong, F.A. Dahalan, Y.S. Oon, H.K. Lehl, W.E. Thung, N. Nordin, Up-flow constructed wetland-microbial fuel cell for azo dye, saline, nitrate remediation and bioelectricity generation: From waste to energy approach, Bioresour. Technol., 266 (2018) 97-108.
[239] C.L. Nguyen, B. Tartakovsky, L. Woodward, Harvesting Energy from Multiple Microbial Fuel Cells with a High-Conversion Efficiency Power Management System, ACS Omega, 4 (2019) 18978-18986.
[240] D. Zhang, F. Yang, T. Shimotori, K.-C. Wang, Y. Huang, Performance evaluation of power management systems in microbial fuel cell-based energy harvesting applications for driving small electronic devices, J. Power Sources, 217 (2012) 65-71.
[241] L. Xu, W. Yu, N. Graham, Y. Zhao, Revisiting the Bioelectrochemical System Based Biosensor for Organic Sensing and the Prospect on Constructed Wetland-Microbial Fuel Cell, Chemosphere, (2020) 128532.
[242] C. Corbella, M. Hartl, M. Fernandez-gatell, J. Puigagut, MFC-based biosensor for domestic wastewater COD assessment in constructed wetlands, Sci. Total Environ., 660 (2019) 218-226.

[243] T. Kim, J. Yeo, Y. Yang, S. Kang, Y. Paek, J.K. Kwon, J.K. Jang, Boosting voltage without electrochemical degradation using energy-harvesting circuits and power management system-coupled multiple microbial fuel cells, J. Power Sources, 410 (2019) 171-178.
[244] Y.L. Oon, S.A. Ong, L.N. Ho, Y.S. Wong, F.A. Dahalan, Y.S. Oon, H.K. Lehl, W.E. Thung, N. Nordin, Role of macrophyte and effect of supplementary aeration in up-flow constructed wetland-microbial fuel cell for simultaneous wastewater treatment and energy recovery, Bioresour. Technol., 224 (2017) 265-275.
[245] T.-P. Teoh, S.-A. Ong, L.-N. Ho, Y.-S. Wong, Y.-L. Oon, Y.-S. Oon, S.-M. Tan, W.-E. Thung, Up-flow constructed wetland-microbial fuel cell: Influence of floating plant, aeration and circuit connection on wastewater treatment performance and bioelectricity generation, J. Water Process Eng., 36 (2020) 101371.
[246] S. Wu, T. Lv, Q. Lu, Z. Ajmal, R. Dong, Treatment of anaerobic digestate supernatant in microbial fuel cell coupled constructed wetlands: Evaluation of nitrogen removal, electricity generation, and bacterial community response, Sci. Total Environ., 580 (2017) 339-346.
[247] EMEVB8500 EVALUATION BOARD, in.
[248] https://www.analog.com/en/products/ltc3108, in: LTC3108 Datasheet and Product Info, 2020.
[249] J. Vondrak, M. Schmidt, A. Proto, M. Penhaker, J. Jargus, L. Peter, Using Miniature Thermoelectric Generators for Wearable Energy Harvesting, in: 2019 4th International Conference on Smart and Sustainable Technologies (SpliTech), IEEE, 2019, pp. 1-6.
[250] T. Kim, J. Yeo, Y. Yang, S. Kang, Y. Paek, J.K. Kwon, J.K. Jang, Boosting voltage without electrochemical degradation using energy-harvesting circuits and power management system-coupled multiple microbial fuel cells, J. Power Sources, 410-411 (2019) 171-178.
[251] A. Razmjou, M. Asadnia, E. Hosseini, A.H. Korayem, V. Chen, Design principles of ion selective nanostructured membranes for the extraction of lithium ions, Nature Communications, 10 (2019) 1-15.
[252] H. Liu, Z. Hu, J. Zhang, H.H. Ngo, W. Guo, S. Liang, J. Fan, S. Lu, H. Wu, Optimizations on supply and distribution of dissolved oxygen in constructed wetlands: a review, Bioresour. Technol., 214 (2016) 797-805.
[253] G.-C. Gil, I.-S. Chang, B.H. Kim, M. Kim, J.-K. Jang, H.S. Park, H.J. Kim, Operational parameters affecting the performannce of a mediator-less microbial fuel cell, Biosens. Bioelectron., 18 (2003) 327-334.

[254] S. Wu, D. Zhang, D. Austin, R. Dong, C. Pang, Evaluation of a lab-scale tidal flow constructed wetland performance: oxygen transfer capacity, organic matter and ammonium removal, Ecol.l Eng., 37 (2011) 1789-1795.
[255] H. Brix, Do macrophytes play a role in constructed treatment wetlands?, Water Sci. Technol., 35 (1997) 11-17.
[256] F. Xu, Y.-j. Zhu, Y.-q. Wang, H.-y. Chen, Y.-l. Zhang, D. Hao, X.-y. Qi, B. Wang, Q. Wang, C.-c. Zhao, Coupling iron pretreatment with a constructed wetland-microbial fuel cell to improve wastewater purification and bioelectricity generation, Journal of Cleaner Production, 276 (2020) 123301.
[257] J. Wang, X. Song, Y. Wang, Z. Zhao, B. Wang, D. Yan, Effects of electrode material and substrate concentration on the bioenergy output and wastewater treatment in air-cathode microbial fuel cell integrating with constructed wetland, Ecol. Eng., 99 (2017) 191-198.
[258] X. Wang, Y. Tian, H. Liu, X. Zhao, S. Peng, Optimizing the performance of organics and nutrient removal in constructed wetland–microbial fuel cell systems, Sci. Total Environ., 653 (2019) 860-871.
[259] P. Srivastava, A.K. Yadav, V. Garaniya, T. Lewis, R. Abbassi, S. Khan, Electrode dependent anaerobic ammonium oxidation in microbial fuel cell integrated hybrid constructed wetlands: A new process, Sci. Total Environ., (2019) 134248.
[260] P. Srivastava, R. Abbassi, A.K. Yadav, V. Garaniya, N. Kumar, S.J. Khan, T. Lewis, Enhanced Chromium (VI) Treatment in Electroactive Constructed Wetlands: Influence of Conductive Material, J. Hazard. Mater., (2019) 121722.
[261] M. Asadnia, M. Myers, N.D. Akhavan, K. O'Donnell, G.A. Umana-Membreno, U. Mishra, B. Nener, M. Baker, G.J.A.c.a. Parish, Mercury (II) selective sensors based on AlGaN/GaN transistors, 943 (2016) 1-7.
[262] L. Guo, K. He, S. Wu, H. Sun, Y. Wang, X. Huang, R. Dong, Optimization of high-rate TN removal in a novel constructed wetland integrated with microelectrolysis system treating high-strength digestate supernatant, Journal of environmental management, 178 (2016) 42-51.

Appendix 1

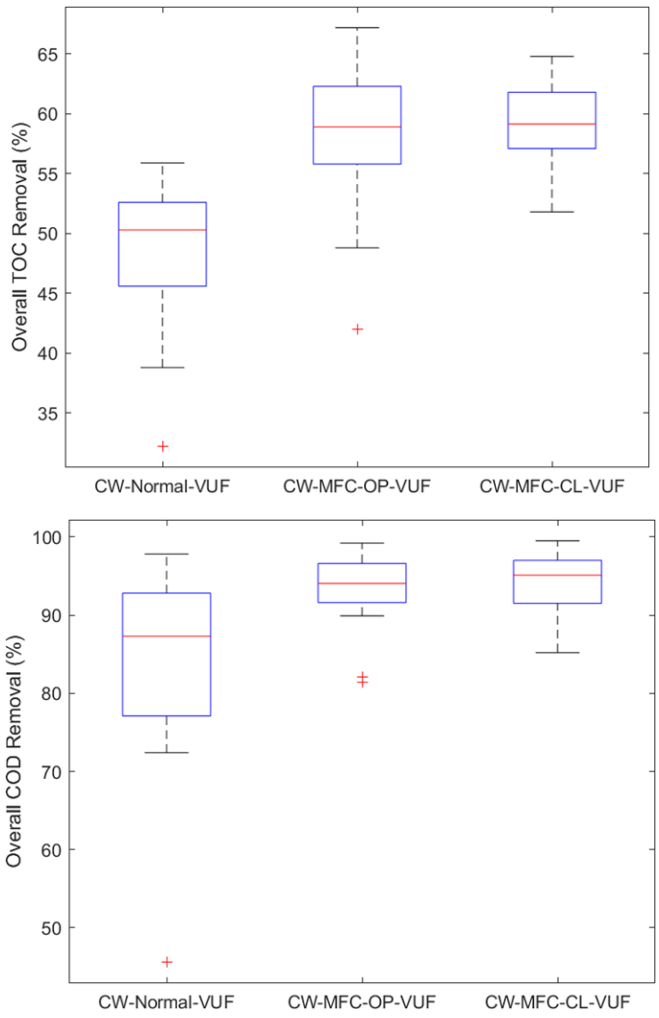

Figure A 1. Percentage removal in the various microcosms of the CW-MFC-CL, CW-MFC-OP and CW-Normal systems. A) Overall TOC removal B) Overall COD removal.

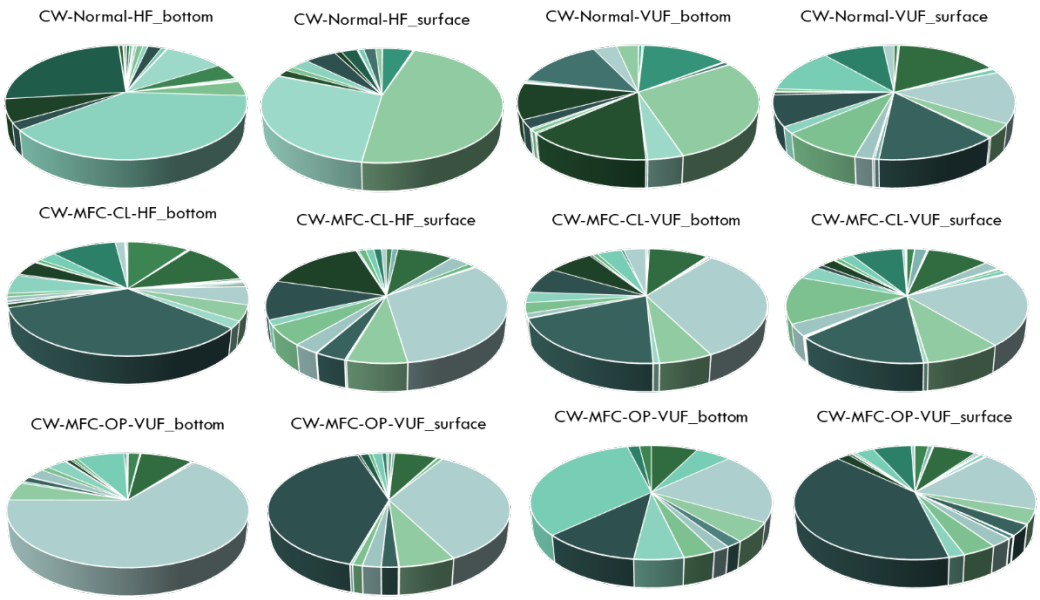

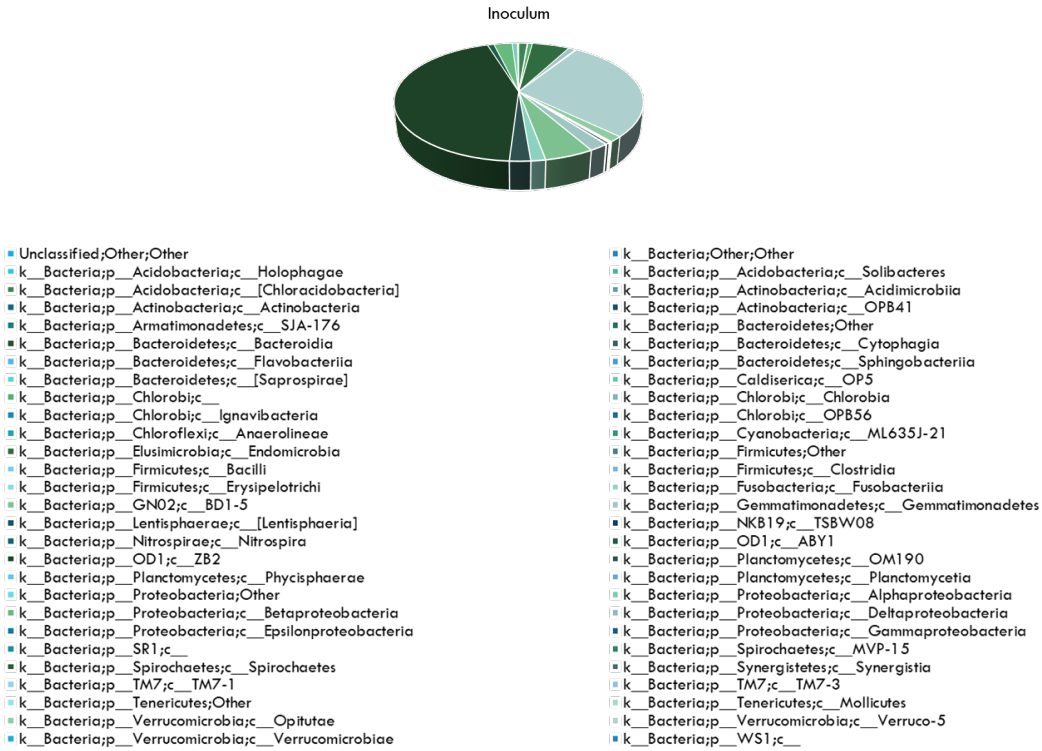

Figure A 2. Microbiological analysis based on Class at surface and bottom: A) CW-MFC-OP, HF and VUF; B) CW-MFC-CL, HF and VUF; C) CW-Normal, HF and VUF; D) Sludge.

Appendix 2

Table A 1. The $E_{emf,}$ cathode and anode potential of CW-MFC-replete and CW-MFC-deplete during experimental period.

Time (days)	*CW-MFC-replete*				*CW-MFC-deplete*			
	OCV (mV)	$E_{cathode}$ (mV)	E_{anode} (mV)	E_{emf} (mV)	OCV (mV)	$E_{cathode}$ (mV)	E_{anode} (mV)	E_{emf} (mV)
7	65.0	285.2	-213.8	499.0	24.0	69.2	-114.8	184.0
21	72.0	250.5	-34.8	85.3	30.0	147.8	-267.8	120.0
49	78.0	232.2	-39.8	272.0	32.1	223.2	-129.8	353.0
70	85.2	221.0	-75.6	296.6	65.3	190.8	-123.8	314.6
91	55.4	177.2	-106.2	71.0	28.3	98.6	-56.8	155.4
112	59.0	177.3	-76.8	254.1	22.9	266.1	-103.1	369.2
140	61.6	203.7	-164.8	368.5	18.5	206.4	-111.8	318.2
168	60.8	221.2	-33.8	255.0	31.8	203.2	-56.8	260.0

A

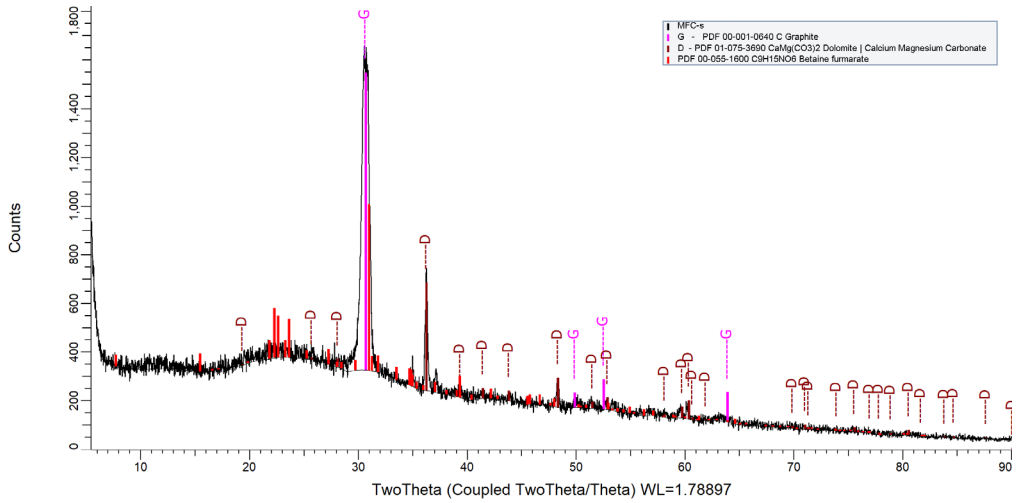

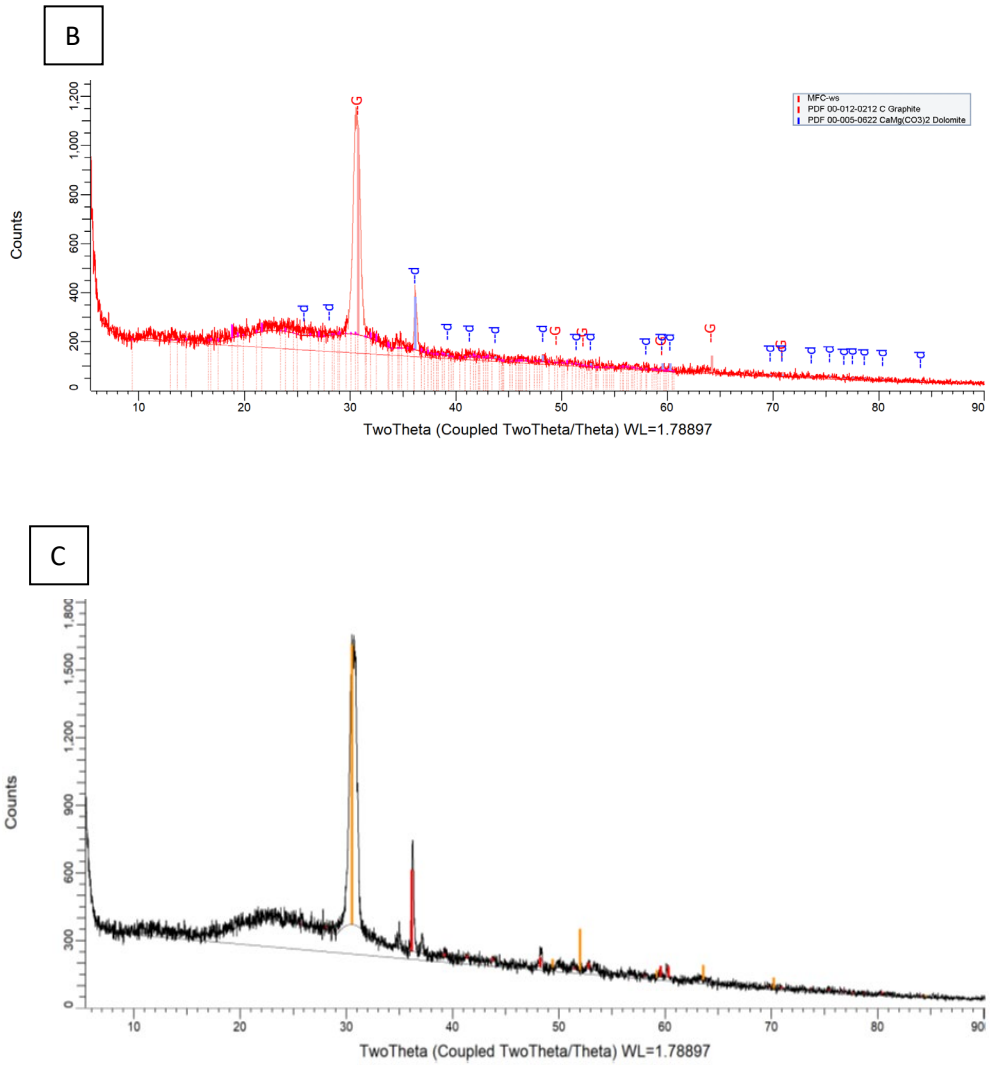

Figure A 3. XRD of A. CW-MFC-replete, B. CW-MFC-deplete, and C. CW-replete.

Table A 2. Detailed XRD chemical analysis of precipitate in CW-MFC-deplete, CW-MFC-replete, and CW-replete.

Sample	Major Crystalline phases, formula	Minor crystalline phase	Other (minor) possible phases	Crystallinity
CW-MFC-deplete	Graphite, C	Dolomite, CaMg (CO3)2	Organic	Low, amorphous (30-45%)
CW-MFC-replete	Graphite, C	Dolomite, CaMg (CO3)2	Organic (betaine Furmarate), Antimony Sulphide	Amorphous (30-45%)
CW-replete		Dolomite, CaMg (CO3)2	Berlinite, Sanidine, Anhydrite, Amorphous silica	Low, amorph. >70%

Curriculum Vitae

List of Publications:

1. **Srivastava, P.**, Abbassi, R., Yadav, A. K., Garaniya, V., Lewis, T., Zhao, Y., & Aminabhavi, T. (2021). Interrelation between sulphur and conductive materials and its impact on ammonium and organic pollutants removal in constructed wetlands-microbial fuel cells. Journal of Hazardous Materials, 126417. **(Impact Factor = 9.0)**
2. **Srivastava, P.**, Abbassi, R., Yadav, A., Garaniya, V., Asadnia, M., Lewis, T., & Khan, S. J. (2021). Influence of applied potential on treatment performance and clogging behaviour of hybrid constructed wetland-microbial electrochemical technologies. Chemosphere, 131296. (**Impact Factor = 5.8**)
3. **Srivastava, P.**, Belford, A., Abbassi, R., Asadnia, M., Garaniya, V., Yadav, A. K. (2021). Low-power energy harvester from constructed wetland-microbial fuel cells for initiating a self-sustainable treatment process. Sustainable Energy Technologies and Assessments, 46, 101282. **(Impact factor = 3.4)**
4. **Srivastava, P.**, Abbassi, R., Yadav, A. K., Garaniya, V., Kumar, N., Khan, S. J., & Lewis, T. (2020). Enhanced chromium (VI) treatment in electroactive constructed wetlands: Influence of conductive material. Journal of Hazardous Materials, 121722. **Impact factor = 9.0**.
5. Gupta, S., **Srivastava, P.**, Patil, S. A., & Yadav, A. K. (2020). A comprehensive review on emerging constructed wetland coupled microbial fuel cell technology: Potential applications and challenges. Bioresource Technology, 124376. **Impact factor = 7.5.**
6. **Srivastava, P.**, Yadav, A. K., Garaniya, V., Lewis, T., Abbassi, R., & Khan, S. J. (2020). Electrode dependent anaerobic ammonium oxidation in microbial fuel cell integrated hybrid constructed wetlands: A new process. Science of the Total Environment, 698, 134248. **Impact factor = 6.5**.
7. **Srivastava, P.**, Abbassi, R., Yadav, A. K., Garaniya, V., Jahromi, M. A. F (2020). A review on electrochemistry of electroactive wetlands: Electricity generation and enhanced wastewater treatment. Chemosphere. **Impact factor = 5.8**.
8. Mittal, Y., **Srivastava, P.**, Kumar, N., Yadav, A. K. (2020). Remediation of fluoride contaminated water using encapsulated active growing blue-green algae, Phormidium sp. Environmental Technology & Innovation. **Impact factor = 3.3**.
9. Gupta, S., **Srivastava, P.**, & Yadav, A. K. (2020). Simultaneous removal of organic matters and nutrients from high-strength wastewater in constructed wetlands followed by entrapped

algal systems. Environmental Science and Pollution Research, 27(1), 1112-1117. **Impact factor = 3.0**.

10. **Srivastava, P.**, Abbassi, R., Garaniya, V., Lewis, T., Yadav, A. K. (2019). Performance of pilot-scale horizontal subsurface flow constructed wetland coupled with a microbial fuel cell for treating wastewater. Journal of Water Process Engineering. **Impact factor = 3.4**.
11. **Srivastava, P**., Gupta, S., Garaniya, V., Abbassi, R., & Yadav, A. K. (2019). Up to 399 mV bioelectricity generated by a rice paddy-planted microbial fuel cell assisted with a blue-green algal cathode. Environmental Chemistry Letters, 17(2), 1045-1051. **Impact factor = 5.9**.
12. **Srivastava, P.**, Yadav, A. K., Abbassi, R., Garaniya, V., & Lewis, T. (2018). Denitrification in a low carbon environment of a constructed wetland incorporating a microbial electrolysis cell. Journal of Environmental Chemical Engineering, 6(4), 5602-5607. **Impact factor = 4.3**.
13. **Srivastava, P.**, Dwivedi, S., Kumar, N., Abbassi, R., Garaniya, V., & Yadav, A. K. (2017). Performance assessment of aeration and radial oxygen loss assisted cathode based integrated constructed wetland-microbial fuel cell systems. Bioresource Technology, 244, 1178-1182. **Impact factor = 7.5**.
14. **Srivastava, P.**, Yadav, A. K., & Mishra, B. K. (2015). The effects of microbial fuel cell integration into constructed wetland on the performance of constructed wetland. Bioresource technology, 195, 223-230. **Impact factor = 7.5.**

Book chapters:

1. **Srivastava, P.**, Abbassi, R., Yadav, A. K., Garaniya, V., & Khan, F. (2020). Microbial fuel cell–integrated wastewater treatment systems. In Integrated Microbial Fuel Cells for Wastewater Treatment (pp. 29-46). Butterworth-Heinemann.
2. Gupta, S., **Srivastava, P.**, & Yadav, A. K. (2020). Integration of microbial fuel cell into constructed wetlands: effects, applications, and future outlook. In Integrated Microbial Fuel Cells for Wastewater Treatment (pp. 273-293). Butterworth-Heinemann.
3. Gupta, S., Mittal, Y., Tamta, P., **Srivastava, P.**, & Yadav, A. K. (2020). Textile wastewater treatment using microbial fuel cell and coupled technology: a green approach for detoxification and bioelectricity generation. In Integrated Microbial Fuel Cells for Wastewater Treatment (pp. 73-92). Butterworth-Heinemann.
4. **Srivastava, P.**, Yadav, A. K., Garaniya, V., & Abbassi, R. (2019). Constructed wetland coupled microbial fuel cell technology: development and potential applications. In Microbial Electrochemical Technology (pp. 1021-1036). Elsevier.

5. Yadav, A. K., **Srivastava, P.**, Kumar, N., Abbassi, R., & Mishra, B. K. (2018). Constructed Wetland-Microbial Fuel Cell: An Emerging Integrated Technology for Potential Industrial Wastewater Treatment and Bio-Electricity Generation. Constructed wetlands for industrial wastewater treatment, 493-510. John Wiley & Sons, Ltd.
6. Sochacki, A., Yadav, A. K., **Srivastava, P.**, Kumar, N., Fitch, M. W., & Mohanty, A. (2018). Constructed Wetlands for Metals: Removal Mechanism and Analytical Challenges. Constructed Wetlands for Industrial Wastewater Treatment, 223-247. John Wiley & Sons, Ltd.

Conference paper:

1. **Pratiksha Srivastava**, R Abbassi, V Garaniya, T Lewis, A Yadav (2019). Exploration of higher total nitrogen removal in hybrid constructed wetland incorporated with microbial fuel cell. 8th International Symposium on Wetlands Pollutant Dynamics and Control, WETPOL, Aarhus, Denmark.
2. **Pratiksha Srivastava**, R Abbassi, V Garaniya, T Lewis, A Yadav (2018). Degradation of azo dye in constructed wetland coupled with a microbial electrolysis cell. 16th IWA International Conference on Wetland Systems for Water Pollution Control Programme, ICWS 2018, Valencia, Spain.
3. **Pratiksha Srivastava** (2016) Microbial electrolysis: Possibility of de-nitrification in Constructed Wetland" has been accepted for AN ORAL PRESENTATION in Specialist Conference on Wetland Systems for Water Pollution Control - ICWS 2016, Gdansk, Poland.
4. **Pratiksha Srivastava**, Asheesh K Yadav (2015) Design and development of high performing constructed wetland using the concept of microbial fuel cell for wastewater treatment. in "WETPOL 2015 International Symposium on Wetland Pollutant Dynamics and Control and the Annual Conference of the Constructed Wetland Association, which will be held in York, UK, 13-18th September 2015. (**Grant winning paper**)
5. **Pratiksha Srivastava**, Asheesh K Yadav (2015) Passive aeration opportunity through photosynthesis of entrapped algae, in conference 23rd International Conference on Bioencapsulation which will be held in Delft, The Netherlands, 2nd-4th September 2015. (**Grant winning paper**).

Graduates & Undergraduates Co-Supervision:

1. **Parth Ambalal Patel** (Master's student, 2019-2020) - Experimental analysis of pitting corrosion in offshore structures

2. **Kai Foong Voon** (Undergraduate student, 2019) - Conceptual development of Biosensors using Constructed Wetland – Microbial Fuel Cell (CW-MFC) technology
3. **Hong Yaog Wong** (Undergraduate student, 2018) - Two Chambered-Microbial Fuel Cell for Resource Recovery and Wastewater Treatment in Coastal Areas
4. **Dean Bong** (Undergraduate student, 2018) - Decolourisation of Methylene Blue by Using Low Cost Adsorbent